

**Bio-fabrication and Characterisation of Silver Nanoparticles from
Trema orientalis (L.) Blume**

A Dissertation for

Course code and Course Title: Bot-651 Discipline Specific Dissertation

Credits:16

Submitted in partial fulfilment of Master's Degree

M.Sc. in Botany

by

Ms. RIDA YASSIN MAMLEKAR

Seat number: 22P0480023

ABC ID: 925-012-618-057

PRN: 201900846

under the supervision of

PROF. S. KRISHNAN

School of Biological Sciences and Biotechnology

Botany Discipline



GOA UNIVERSITY

April 2024



Seal of the School

Examined by:

[Handwritten signatures]
Sankar Varmad
Sankar
Sankar
Sankar

DECLARATION BY STUDENT

I hereby declare that the data presented in this Dissertation report entitled, "**Bio-fabrication and Characterisation of Silver Nanoparticles from *Trema orientalis* (L.) Blume**" is based on the results of investigations carried out by me in the Botany discipline at the School of Biological Sciences and Biotechnology, Goa University, under the supervision of Prof. S. Krishnan and the same has not been submitted elsewhere for the award of a degree/or by me. Further, I understand that Goa University or its authorities will not be responsible for the correctness of observations/experimental or other findings given the dissertation.

I hereby authorize the University authorities to upload this dissertation on the dissertation repository or anywhere else as the UGC regulations demand and make it available to any one as needed.

Date: 08/04/24

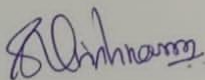
Place: Goa University

R.Mam
8/4/24
Rida.Yassin. Mamlekar

Seat No: 22P0480023

COMPLETION CERTIFICATE

This is to certify that the dissertation report, "**Bio-fabrication and Characterisation of Silver Nanoparticles from *Trema orientalis* (L.) Blume**" is a bonafide work carried out by Ms. Rida Yassin Mamlekar under my supervision in partial fulfilment of the requirements for the award of the degree of Masters of Science in the Discipline Botany at the School of Biological Sciences and Biotechnology, Goa University.

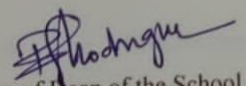


Signature and Name of Supervising Teacher
(Prof. S. Krishnan)

Date: 08.04.2024



School Stamp


Signature of Dean of the School

Date: 8-4-2024

Place: Goa University

CONTENTS

Chapter	Particulars	Page numbers
	Preface	iv
	Acknowledgements	v
	Tables, Figures and Plates	vi- xiv
	Abstract	xv
1.	Introduction	1-22
2.	Review of Literature	23-36
3.	Materials and Methods	37-48
4.	Results and Discussion	49-116
5.	Conclusions	117-119
8.	References	120-133

Preface

The chemistry of the earth is impossibly complicated, owing to a magnificent tangled network of interdependencies between living and non-living components, which includes a wide, diversified, and global array of naturally occurring nanomaterials. Green synthesis methods are more environmentally friendly and safer than other physical and chemical approaches. This study deals with green synthesis of novel silver nanoparticles from the plant *Trema orientalis* (L) Blume. and its evaluation on the biological activities.

AKNOWLEDGEMENTS

I want to acknowledge first of all the silent guardianship and blessing of the God. I owe him deep gratitude for helping me to complete this Dissertation successfully.

I express my sincere thanks to my guide Prof. S. Krishnan, for guiding me throughout and helping in successful completion of the Dissertation. I thank all the other faculty members of the School of Biological Sciences and Biotechnology, Botany discipline; Prof. B. F. Rodrigues (Dean), Prof. Vijaya Kerkar, Dr. Rupali Bhandari, Dr. Siddhi Jalmi and Dr. Aditi Naik for their support during my dissertation work.

I am grateful to Ms. Jyothi Yarram, Technical Assistant from Central Sophisticated Instrumentation Facility (CSIF) BITS PILANI KK Birla Goa Campus for her guidance during my work.

I would also express my gratitude to the non- teaching staff of Botany discipline for their help during my work.

My sincere thanks to research scholar Mrs. Annie Princy Nadar for all her support, encouragement, and helpful advice during my dissertation.

Special thanks to my classmates Mr. Rupesh Velip, Mr. Fedrick Vas and Ms. Saiksha Kuttiker for their constant help in my dissertation work.

My sincere appreciation goes to my family and friends for their unwavering support and encouragement.

(Ms. Rida Yassin Mamlekar)

TABLES

Table no.	Description
4.1	Qualitative phytochemical test of <i>Trema orientalis</i> leaf and bark water extract.
4.2	Total Phenolic Content (TPC) in <i>Trema orientalis</i> leaf water extract and bark water extract.
4.3	Total Tannin Content (TTC) in <i>Trema orientalis</i> leaf water extract and bark water extract.
4.4	Total Flavonoid Content (TFC) in <i>Trema orientalis</i> leaf water extract and bark water extract.
4.5	Total Alkaloid Content (TAC) in <i>Trema orientalis</i> leaf water extract and bark water extract.
4.6	Total phenolic content (TPC), Total Flavonoids content (TFC), Total Tannins content (TTC) and Total Alkaloid content of (TAC) <i>Trema orientalis</i> Leaf extract and Bark extract.
4.7	FTIR data showing wave number at characteristic functional group for <i>Trema orientalis</i> leaf extract.
4.8	FTIR data showing wave number at characteristic functional group for <i>Trema orientalis</i> leaf extract synthesized silver nanoparticles.

4.9	FTIR data showing wave number at characteristic functional group for <i>Trema orientalis</i> bark extract.
4.10	FTIR data showing wave number at characteristic functional group for bark extract synthesized silver nanoparticles.
4.11	2 θ value, FWHM and Crystalline size of silver nanoparticles synthesized from <i>Trema orientalis</i> leaf extract.
4.12	2 θ value, FWHM and Crystalline size of silver nanoparticles synthesized from <i>Trema orientalis</i> bark extract.
4.13	DPPH free radical scavenging assay: % scavenging activity of DPPH by Ascorbic acid and water extract of leaf and bark of <i>Trema orientalis</i> and silver nanoparticles synthesized from respective extracts.
4.14	IC ₅₀ values for DPPH free radical scavenging activity.
4.15	Starch-iodine assay for Acarbose.
4.16	Starch-iodine assay for <i>Trema orientalis</i> Leaf extract.
4.17	Starch-iodine assay for silver nanoparticles synthesized from <i>Trema orientalis</i> leaf extract.
4.18	Starch-iodine assay for <i>Trema orientalis</i> bark extract.
4.19	Starch-iodine assay for silver nanoparticles synthesized from <i>Trema orientalis</i> bark extract.

4.20	Protein Denaturation assay using egg albumin: % inhibition of egg albumin denaturation by Diclofenac sodium, <i>Trema orientalis</i> leaf and bark extract and silver nanoparticles extracted from respective extracts.
4.21	IC ₅₀ values for Anti-inflammatory assay.

FIGURES

Figure no.	Description
4.1	Calibration curve for Total Phenolic content.
4.2	Calibration curve for Total Flavonoid content.
4.3	Calibration curve for Total Tannin content.
4.4	Calibration curve for Total Alkaloids content.
4.5	UV-Visible Absorption spectrum for a) Silver nitrate b) <i>Trema orientalis</i> Leaf extract and c) <i>Trema orientalis</i> Bark extract.
4.6	UV-visible spectrum for silver nanoparticles synthesised from leaf extract of <i>Trema orientalis</i> a) 1 hour of incubation b) 2 hours of incubation.
4.7	UV-visible spectrum for silver nanoparticles synthesised from leaf extract of <i>Trema orientalis</i> c) 3 hours of incubation d) 4 hours of incubation.
4.8	UV-visible spectrum for silver nanoparticles synthesised from Bark extract of <i>Trema orientalis</i> a) 1 hour of incubation b) 2 hours of incubation.
4.9	UV-visible spectrum for silver nanoparticles synthesised from Bark extract of <i>Trema orientalis</i> c) 3 hours of incubation d) 4 hours of incubation.

4.10	UV-visible spectrum for silver nanoparticles at different hours of incubation (1 hour to 4 hour) a) From <i>Trema orientalis</i> Leaf extract and b) <i>Trema orientalis</i> Bark extract.
4.11	FTIR graph for <i>Trema orientalis</i> a) Leaf extract b) Bark extract.
4.12	FTIR graph for silver nanoparticles synthesised from <i>Trema orientalis</i> a) Leaf extract b) Bark extract.
4.13	Particles size distribution for silver nanoparticles synthesised from <i>Trema orientalis</i> a) Leaf extract b) Bark extract.
4.14	EDS data for silver nanoparticles synthesised from <i>Trema orientalis</i> a) leaf extract b) Bark extract.
4.15	XRD Graph for Silver nanoparticles synthesised from <i>Trema orientalis</i> a) Leaf extract b) Bark extract.
4.16	DLS data for silver nanoparticles synthesised from <i>Trema orientalis</i> a) Leaf extract and b) Bark extract.
4.17	Zeta potential data for silver nanoparticles synthesised from <i>Trema orientalis</i> a) Leaf extract, b) Bark extract.
4.18	Antioxidant activity: DPPH radical scavenging activity by a) Ascorbic acid b) <i>Trema orientalis</i> Leaf extract c) <i>Trema orientalis</i> Bark extract.
4.19	Antioxidant activity: DPPH radical scavenging activity by silver nanoparticles synthesised from <i>Trema orientalis</i> d) Leaf extract

	e) Bark extract f) Comparative graph.
4.20	Antidiabetic activity: Starch iodine assay for a) Acarbose b) <i>Trema orientalis</i> Leaf extract and c) <i>Trema orientalis</i> Bark extract.
4.21	Antidiabetic activity: Starch iodine assay for silver nanoparticles synthesised from <i>Trema orientalis</i> d) Leaf extract and e) Bark extract.
4.22	Anti-inflammatory activity: Protein denaturation inhibition activity by a) Diclofenac sodium b) <i>Trema orientalis</i> Leaf extract c) <i>Trema orientalis</i> Bark extract.
4.23	Anti-inflammatory activity: Protein denaturation inhibition activity by silver nanoparticles extracted from <i>Trema orientalis</i> d) Leaf extract and e) Bark extract f) Comparative graph.

PLATES

Plate no.	Description
4.1	<i>Trema orientalis</i> a) Habit b) Twig c) leaf abaxial side and adaxial side d) bark.
4.2	<i>Trema orientalis</i> a) leaf b) bark kept for drying c) leaf powder d) bark powder e) leaf and bark extract respectively f) leaf extract after hot maceration g) bark extract after maceration.
4.3	Qualitative Phytochemicals test screening of <i>Trema orientalis</i> leaf extract. a: Test for Alkaloids; b: Test for Carbohydrates; c: Test for Glycosides; d: Test for saponins, e: test for Proteins; f test for Phytosterols, h: test for Phenols and Tannins, I: test for Gums and Mucilage.
4.4	Qualitative Phytochemicals test screening of <i>Trema orientalis</i> bark extract. a: Test for Alkaloids; b: Test for Carbohydrates; c: Test for Glycosides; d: Test for saponins; e: test for Proteins; f: test for Phytosterols; h: test for Phenols and Tannins; I: Test for Gums and Mucilage.
4.5	Quantitative estimation of phenols in <i>Trema orientalis</i> leaf and bark extract a) Standard series for calibration b) bark extract c) Leaf extract.
4.6	Quantitative estimation of tannins in <i>Trema orientalis</i> leaf and bark extract a) Standard series for calibration b) Leaf extract and c) Bark extract.
4.7	Quantitative estimation of flavonoids in <i>Trema orientalis</i> leaf and bark extract a) Standard series for calibration b) bark extract and c) Leaf extract.
4.8	Quantitative estimation of alkaloids in <i>Trema orientalis</i> leaf and bark extract.

	a) Standard series for calibration b) bark extract and Leaf extract respectively.
4.9	a) silver nitrate solution, b) <i>Trema orientalis</i> leaf extract c) <i>Trema orientalis</i> bark extract.
4.10	Represents the colour change during the silver nanoparticles synthesis from <i>Trema orientalis</i> leaf extract: a) Before incubation b) 1 hour incubation, c) 2 hours of incubation d) 3 hours of incubation e) 4 hours of incubation.
4.11	Represents the colour change during the silver nanoparticles synthesis from <i>Trema orientalis</i> bark extract: a) Before incubation b) 1 hour incubation, c) 2 hours of incubation, d) 3 hours of incubation e) 4 hours of incubation.
4.12	a) Synthesised silver nanoparticles from <i>Trema orientalis</i> leaf extract before drying b) Synthesised silver nanoparticles from <i>Trema orientalis</i> bark extract before drying c) Synthesised silver nanoparticles from <i>Trema orientalis</i> leaf extract after drying. d) Synthesised silver nanoparticles from <i>Trema orientalis</i> bark extract after drying.
4.13	FESEM images of silver nanoparticles synthesised from <i>Trema orientalis</i> leaf extract a) at 500 nm scale (inset image enlarge view) b) 1 μ m scale.
4.14	FESEM images of silver nanoparticles synthesised from <i>Trema orientalis</i> bark extract a) at 500 nm (inset image) scale b) 1 μ m scale.
4.15	DPPH Scavenging activity by a) Ascorbic acid, b) <i>Trema orientalis</i> leaf extract, c) <i>Trema orientalis</i> Bark extract.
4.16	DPPH Scavenging activity by d) Silver nanoparticles synthesised from <i>Trema orientalis</i> leaf extract, e) Silver nanoparticles synthesised from <i>Trema orientalis</i> Bark extract.

4.17	Antidiabetic activity a) by Acarbose b) by <i>Trema orientalis</i> Leaf extract c) by <i>Trema orientalis</i> Bark extract.
4.18	Antidiabetic activity by d) Silver nanoparticles synthesised from <i>Trema orientalis</i> leaf extract, e) silver nanoparticles synthesised from <i>Trema orientalis</i> bark extract.
4.19	Anti-inflammatory activity by a) Diclofenac sodium b) <i>Trema orientalis</i> Leaf extract, b) <i>Trema orientalis</i> Bark extract.
4.20	Anti-inflammatory activity by d) Silver nanoparticles synthesised from <i>Trema orientalis</i> leaf extract, e) Silver nanoparticles synthesised from <i>Trema orientalis</i> bark extract.

ABSTRACT

This study deals with the synthesis of silver nanoparticles from *Trema orientalis* (L) Blume leaf and bark water extract, the current study aimed at first screening the plant extracts phytochemistry and quantifying it and then characterisation of synthesised nanoparticles using UV-vis spectroscopy, FTIR, XRD, FESEM-EDS, DLS and Zeta potential analysis, which confirmed that the synthesised silver nanoparticles are spherical, moderately stable, has high crystalline nature and are of 20-23nm in diameter. The evaluation of synthesised nanoparticles was performed to study its antioxidant, antidiabetic, and anti-inflammatory activities. The antioxidant study using DPPH free radical scavenging activity was conducted on both aqueous plant extract and silver nanoparticles. The IC₅₀ value of the standard (Ascorbic acid) was found to be 47.9 µg/ml, whereas, the IC₅₀ values for the leaf and bark extract were found to be 436µg/ml and 423.2µl/ml. The IC₅₀ value for silver nanoparticles synthesised from the leaf extract was found to be 1212.07 µg/ml and that for silver nanoparticles synthesised from bark extract was found to be 522µg/ml.

The study also aimed to evaluate the antidiabetic activity of silver nanoparticles in comparison to the plant extract. The starch iodine colour assay was conducted which revealed that as the concentration of the plant extract and silver nanoparticle increased the absorbance also increased indicating that the starch is not broken down as the enzyme alpha amylase is inhibited by the extract and nanoparticles, the results were compared in accordance to the standard antidiabetic drug acarbose.

The anti-inflammatory study was conducted on synthesised nanoparticles using egg albumin denaturation method and were compared with that of the plant extract. The IC₅₀ value for Diclofenac sodium which was used as the standard drug was found to be 53 µg/ml. The IC₅₀ value for leaf extract was found to be 130 µg/ml and for bark extract it was found to be 129 µg/ml. The IC₅₀ value for silver nanoparticles synthesised from leaf extract was found

to be 106 $\mu\text{g/ml}$ and for silver nanoparticles synthesised from bark extract was found to be 57.6 $\mu\text{g/ml}$. From the study we concluded that the green synthesis of silver nanoparticles was successfully carried out using *Trema orientalis* leaf and bark aqueous extracts, and the synthesised nanoparticles showed potential antioxidant, antidiabetic and anti-inflammatory activities which can be further helpful in pharmacological and biomedical field.

CHAPTER 1: INTRODUCTION

1. INTRODUCTION

Nanotechnology, stemming from the Greek "nano" for "dwarf," delves into the intricate exploration and precise manipulation of matter at scales typically ranging from one to hundreds of nanometres. This discipline not only investigates the fundamental properties of materials at these dimensions but also harnesses them for practical applications. At the atomic, molecular, and even supramolecular levels, nanotechnology enables the design, fabrication, and utilization of materials with tailored properties, paving the way for innovations across various sectors including electronics, medicine, energy, and environmental remediation. The seminal work by Raliya *et al.*, (2013) underscores the pivotal role of nanotechnology in advancing industrial processes and catalysing technological breakthroughs.

Nanotechnology has the potential to produce unique materials and devices with a wide range of uses, including nanomedicine, nanoelectronics, biomaterials, energy production, and consumer goods. Many nanotechnology applications involve new materials with significant different properties and effects than larger-scale materials. This is due to nanoparticles having a very high surface to volume ratio when compared to larger particles, as well as effects that show at that small scale but are not visible at higher scales (Bhushan *et al.*, 2017). Nanotechnology is already being employed in industrial sectors such as information and communications, but it is also being applied in food technology, energy technology, and some medicinal products and treatment (Gabriel *et al.*, 2004). For applications in medicine and physiology, these materials and devices can be developed to interact with tissues and cells at a molecular level with a high degree of functional specificity, enabling for a novel combination of technology and biological systems. Nanotechnology is not itself an emergent scientific discipline, but rather a meeting of traditional sciences such as

chemistry, physics, material science, and biology to bring together the requisite collective skills needed to produce these revolutionary technologies (Gabriel *et al.*, 2004).

The core of nanoscience and nanotechnology are illustrated on the bases that the chemical, physical and biological properties of materials at the nanoscale may be very different from those of a bulk material (Hu *et al.*, 1999). When the dimensions of a material are diminished below 100 nm substantial alterations may occur in their properties. Materials therefore might be nanostructured to provide a certain performance or to provide novel properties to a material along with the changes linked specifically to size and structure. Such particles made of a few counts of molecules, at sizes of 1–50 nm, possess distinct physicochemical properties. In comparison with bulk materials, nanoparticles (NPs) showcase properties of gassed up performance when they are used for similar applications (Nasrollahzadeh *et al.*, 2019).

1.1. Classification of nanomaterials based on dimension:

- 1) **One dimensional nanomaterial** - The term Nano featured the number 10^{-9} , which represents the one billionth of any unit that results in the production of one-dimension nanomaterials such as thin films. These nanoparticles are used in a variety of fields, including chemistry, pharmaceuticals, electronics, and engineering. The monolayers or thin films range in size from 1 to 100 nm. These nanomaterials are very important in research and are utilized in the fabrication of electronics, storage systems, nanoscale LEDs, optoelectronics, chemical and biosensing, magneto optics, fibre optic systems, and optical devices. One-dimensional nanomaterials have a role in the development of significant nanoscale materials such as nanotubes, nanobelts, nanowires, nanoribbons, and hierarchical nanostructures (Ijaz *et al.*, 2020).

- 2) **Two-dimension 2D nanostructures-** have two dimensions that are larger than nanometric, as well as a unique shape, and they are employed as building blocks for important components of nanodevices. Two-dimensional nanomaterials are used in nanocontainers, sensor photocatalysts, nanoreactors, and as 2D structural templates. Carbon nanotubes are a type of two-dimensional nanoparticle (Jibowu *et al.*, 2016).
- 3) **Three-dimensional nanomaterial-** the behaviour of nanomaterials is determined by their shape, size dimension, and morphology, which are fundamental parameters for nanostructure application and performance. Three-dimensional nanomaterials have been increasingly popular in medical science and research during the last decade. These nanoparticles have a wide range of uses, including catalysis, batteries, and magnetic materials for reactant and product transport. Examples of three-dimensional nanoparticles include fullerenes, dendrimers, and quantum dots (Ijaz *et al.*, 2020).

1.2. Nanoparticles

Nanoparticles can be defined as objects ranging in size from 1 and 100 nanometers (nm). Nanotechnology refers to an emerging field of science that includes synthesis and development of various nanomaterials (Hasan *et al.*, 2015). The rationale for scientist's current obsession with nanoparticles is that nanoparticles can have distinct properties and functions than bulk materials (Raffi *et al.*, 2008). The most significant feature that makes it possible to produce nanostructures with the appropriate size, shape, and properties and makes them useful in a variety of sectors is the decrease in the impacts of classical physics and the activation of quantum physics. Additional causes of the varying behaviour of nanoparticles in terms of their physical, chemical, optical, electrical, and magnetic characteristics include the restricted capacity of load carriers, electronic structures that are reliant on size (Raffi *et al.*, 2008).

Metallic nanoparticles are very desirable in material science and chemical engineering due to their key attributes, which are mostly associated with the following qualities: high surface area to volume ratio; presence of surface plasmon resonance effect; this aspect is basically important for optical applications; different physical properties with respect to the bulk metal. Easy surface functionalization makes them very attractive in nanomedicine for a selective drug transport in target organs and tissues (Ahmed *et al.*, 2016).

Nanotechnology examines the relationship between nano-biosynthesis and nanomaterials and it also expresses how the different parameters like structure, chemical properties and origin can alter the functionality of the nanomachinery of cells (Ahmed *et al.*, 2016). The entire nanoparticle characteristics depend on various parameters such as the nature, size and shape of nanoparticles and their surroundings (Longoria *et al.*, 2011).

1.2.1. Types of nanoparticles

Nanoparticles (NPs) are particles found in natural, accidental, or produced materials (Jeevannandam *et al.*, 2018). Nanoparticles can be divided into two types: (i) Inorganic and (ii) Organic.

i) Inorganic nanoparticles- Inorganic NPs have the advantages of a higher surface area to volume ratio. They have a wide and easily modified surface conjugation chemistry and facile preparation (Liu *et al.*, 2020). Semiconductor nanoparticles (such as ZnO, ZnS, and CdS), metallic nanoparticles (such as Au, Ag, Cu, and Al), and magnetic nanoparticles (such as Co, Fe, and Ni) are examples of inorganic nanoparticles (Mathur *et al.*, 2018).

ii) Organic nanoparticles - Organic NPs have been widely explored for decades and contain many types of materials. Liposome, the first nano-scale drug approved for clinical application (Liu *et al.*, 2020), carbon nanoparticles (such as fullerenes, quantum dots, and carbon nano tubes) are examples of organic nanoparticles (Mathur *et al.*, 2018).

1.2.2. Applications of Nanoparticles

In recent years, metallic nanoparticles have attracted considerable interest because of their physicochemical properties, small size and their high monodispersity (Manosalva *et al.*, 2017). Metallic nanoparticles are used in the biomedical field for purposes such as protection from harmful microorganisms, bio-imaging, drug transport, cancer treatment, medical diagnosis, and sensor construction because of their unique properties such as being insulator, optics, antimicrobial, antioxidant, anti-metastasis, biocompatibility, stability, and manipulability. Metallic nanoparticles, which can be used in the industrial field due to their catalytic activity, are of great importance nowadays (Nadargolu *et al.*, 2017).

Gold nanoparticles are widely used in the medical industry. Au NPs have high surface compatibility and can adsorb a variety of biomolecules, which could provide a greater efficacy for clinical medicine. For example, Au NPs are used as a carrier of bioactive molecules such as anticancer agents, which is of great help to the treatment of diseases particularly cancer (Ying *et al.*, 2022). The palladium nanoparticles are used in modifying glass carbon electrode, which could be applied to electrocatalytic reduction of hydrogen peroxide. Zinc nanoparticles are used in sunscreens (Robert *et al.*, 2007) as well as starting material for UV protection film, electronic appliances, and chemical sensors (Meulenkamp *et al.*, 1998).

Infections in living species, including humans, are caused by a variety of microbes such as fungus, bacteria, and molds. Various antibacterial and antibiotic substances have been identified to combat these illnesses (Komolafe *et al.*, 2004). However, there is a need to develop alternate methods, as over a while these microorganisms have started exhibiting resistance against most antibiotics. Nanoparticles can be considered an excellent alternative to overcome antibiotic resistance and simultaneously be cost-effective (Kim *et al.*, 2011).

Antibacterial drugs and DNA sequencing are two significant biological applications of silver nanoparticles, about antibacterial uses, silver has demonstrated significant toxicity to a variety of microbes. The destructive effects of silver ions on bacteria are well-known to scientists; these ions are released from nanoparticles when they undergo oxidation. Almost anything that aims to prevent the spread of germs uses silver nanoparticles, such as food containers, socks, cosmetics, detergents, sprays, and a host of other items (Abbasi *et al.*, 2016).

1.3. Silver nanoparticles

Humankind has been using metals such as silver for ages due to their antimicrobial characteristics, and at present, their applications are being explored in consumer products such as textiles, shampoo, and hygiene products (Dawadi *et al.*, 2021). Among the all-noble metal nanoparticles, silver nanoparticle is an arch product from the field of nanotechnology which has received a lot of interests because of their unique properties such as chemical stability, good conductivity, catalytic activity, and importantly antibacterial, anti-viral, antifungal activities (Mukherjee *et al.*, 2003). Silver functions as an antiseptic and showcase a broad biocidal effect against microorganisms through the disruption of their unicellular membrane thus disturbing their enzymatic activities (Ahmed *et al.*, 2016).

Due to the surface plasmon resonance properties, silver nanoparticles find application in the sensors like colorimetric sensors, surface-enhanced Raman spectrometry sensors, fluorescence sensors, and chemiluminescence sensors (Jouyban *et al.*, 2020). Likewise treating diseases like cancer is prolonged because of the late identification of the illness; silver nanoparticles have helped in early identification (Hernández *et al.*, 2017). Moreover, silver nanoparticles can be applied for pollution remediation as their high surface-to-volume ratio makes the silver nanoparticles a better catalytic agent for the degradation of pollutants like nitroarenes and organic dyes (Dawadi *et al.*, 2021).

1.3.1. Methods of silver nanoparticles synthesis

Several distinct techniques can synthesise silver nanoparticles. The methods are broadly classified as physical, chemical, biological, or green synthesis. Generally, two approaches are concerned with forming silver nanoparticles; the “bottom to top” approach and the “top to bottom” approach. In the “bottom to top” approach, the nanoparticles are formed by assembling smaller atoms or molecules. In the “top to bottom” approach, the nanoparticles are synthesised by breaking down the bulk material into the minute, fine sized particles using several lithographic techniques like milling, thermal/laser ablation, grinding and sputtering (Ahmed *et al.*, 2016).

1.3.1.1. Physical method

Numerous techniques involved in physical method of silver nanoparticle synthesis are thermal evaporation, vapour condensation method, lithographic techniques, ultrathin films, diffusion flame synthesis, ball milling and plasma arching (Parveen *et al.*, 2016). The most important physical approaches are Evaporation-condensation and laser ablation. The advantage of physical method is the absence of solvent contamination in the prepared thin films and the uniformity of nanoparticles distribution. However, there are many disadvantages like high energy requirement, high maintenance, and time consuming (Iravani *et al.*, 2014).

1.3.1.2. Chemical method

One of the most method used to synthesise silver nanoparticles is the chemical method. This method reduces the silver ion, stabilising the nanoparticles using various chemicals and reagent (Dawadi *et al.*, 2021). These include methods like the chemical reduction method, catalytic route, micro emulsion method, polyol process, sol gel process, chemical solution deposition, wet chemical method, Tollen’s method, Langmuir-Blodgett method (Parveen *et al.*, 2016). Physically and chemically synthesized silver nanoparticles

although are very popular but they offer toxic substances and high-temperature settings, which are rather environmentally unsafe and costly (Yousaf *et al.*, 2020).

1.3.1.3. Biological method/Green synthesis

The Biological method enables an environmentally acceptable choice to synthesize nanoparticles and is presented as an alternative to chemical and physical methods (Nadaroglu *et al.*, 2017). The biological method follows the principle of green chemistry, using various natural products like phytochemicals, enzymes, and biodegradable polymerase reducing and capping agents to replace potentially hazardous chemicals like sodium borohydride during the synthesis of silver nanoparticles, and using water as a solvent (Adil *et al.*, 2015; Dawadi *et al.*, 2021). Green synthesis in plants involves using only the extracts of plant and the aqueous solution of silver the silver ion. Reducing agents for synthesis can be acquired by extracting various parts of the plants (roots, leaf, and flower), microorganisms (extracellular and intracellular enzymes, metabolites), and biodegradable polymers (Dawadi *et al.*, 2021). Green synthesis also provides an advantage over other methods since they are simple, one-step, cost-effective, environment friendly, and relatively reproducible, often resulting in more stable materials (Ahmed *et al.*, 2016).

Biological synthesis of silver nanoparticles using plant extracts

The utilisation of plants in the production assembly of silver nanoparticles has generated interest due to its rapid, environmentally sustainable, non-pathogenic, cost-effective procedure and ability to facilitate biosynthetic processes in a single step (Ahmed *et al.*, 2016). Silver ion reduction and stabilization using biomolecules, including proteins, amino acids, enzymes, polysaccharides, alkaloids, tannins, phenolics, saponins, terpenoids, and vitamins, which are known to be present in plant extracts with medicinal properties and that are both environmentally friendly while chemically complex (Kulkarni *et al.*, 2014).

Plant extracts contain antioxidants such as polyphenols, triterpenoids, alkaloids, steroids, and tannins (Jadhav *et al.*, 2018; Hemlata *et al.*, 2020). It has been hypothesized that polyphenols in plant extracts, such as polysaccharides and alkaloids, may be what reduce silver nitrate to Ag-NPs (Oluwafemi *et al.*, 2019). The average size of Ag NPs can be adjusted by adjusting the extract concentration (extract: salt solution ratio), temperature, and pH of the reaction mixture.

A low concentration of extract can reduce silver ions but cannot protect quasispheroidal NPs from agglomeration due to a lack of biomolecules that act as capping agents. At greater concentrations, the biomolecules function as both reducing and capping agents, and symmetrical Ag NPs are formed (Dawadi *et al.*, 2021). Furthermore, raising the mixture's temperature can quicken Ag NPs' sluggish rate of decrease at room temperature (Prathna *et al.*, 2011). By changing the pH of the reaction mixture, biosynthesized Ag NPs' size and form may be changed. The reduction/capping properties of biomolecules and the consequent growth of Ag NPs are directly impacted by pH, which makes it easier to alter the electrical charges of biomolecules. As a result, the Ag NPs' size and shape are changed by the combined action of reducing and capping agents brought on by pH fluctuations. Particle size is often greater in an acidic media than in an alkaline one (Khalil *et al.*, 2019).

1.4. Applications of Silver nanoparticles

Due to their special physical, chemical, and electrical properties, silver nanoparticles have many applications in a variety of industries, including the food industry, optics, medications, and water treatment. According to recent investigations, cryogenic superconducting materials, composite fibres, and electronic components can all incorporate silver nanoparticles (Xu *et al.*, 2020). Silver nanoparticles are used extensively in pharmaceuticals

and medicines due to their low toxicity and stability at different temperatures (Mathur *et al.*, 2018).

1.4.1. Antimicrobial agents

Silver nanoparticles are efficient against both gram-positive and gram-negative bacteria and have the potential to overcome antibiotic resistance (Dawadi *et al.*, 2021). Colloidal state, shape, size, surface charge and concentration are a few physico-chemical parameters that affect their antimicrobial properties, which depend on the nanoparticle synthesis method (Burdusel *et al.*, 2018). The mechanism for bringing about cell death is such that the silver nanoparticles can penetrate the cell wall of the bacteria and cause extreme disturbances in the functioning of the cell (Yan *et al.*, 2018). It has been reported that 0.06mg/ml or more silver nanoparticle concentration was effectively against *Escherichia coli* (Raffi *et al.*, 2018). In *Escherichia coli*, the nanoparticles attach to the bacterial cell wall, forming holes in the membrane responsible for cell death. Large particles were less potent than smaller particles (Sondi *et al.*, 2004).

1.4.2. Anticancer agent

The use of silver nanoparticles as anticancer agents is because the toxicity of silver nanoparticles is more towards the cancerous cells than bulk materials. It is inferred from recent studies that the silver nanoparticles suppress tumour cell progression and thus act as an antitumour agent. Silver nanoparticles have inhibitory action in numerous signalling cascades needed for cancer development and pathogenesis (Gomathi *et al.*, 2019). Different human cancer cell lines like the endothelial cells, U251 glioblastoma cells, MCF-7 breast cancer cells are tested with silver nanoparticles to investigate their anticancer effects (Thapa *et al.*, 2016; Rajeshkumar *et al.*, 2016). Silver nanoparticles have been reported to suppress the growth of the tumour by blocking the process of angiogenesis (El-Naggar *et al.*, 2017).

1.4.3. Wound healing

Antiseptics, enzyme treatment, herbal therapeutics, granulation tissue suppressing agents, tropical antibiotics, and other tropical agents are conventional drugs used in wound healing. These drugs have limitations like allergies, skin irritation, cytotoxicity on body cells and narrow antimicrobial spectrum. Due to properties like low toxicity to the system and effectiveness against multi drug resistance pathogens, silver nanoparticles can be used as an alternative to conventional methods (Gunasekaran *et al.*, 2012).

1.4.4. Drug delivery system

The silver nanoparticles can easily penetrate the tissue and bring about effective drug delivery due to their nano-size (Patra *et al.*, 2018). Using conventional methods in drug delivery may lead to the death of healthy and normal cells and tumour cells (Ivanova *et al.*, 2019). The silver nanoparticles are used in drug delivery system as they effectively deliver anticancer drugs to the tumour cells and tissue.

1.4.5. Antidiabetic

Type 2 diabetes mellitus (T2DM) is a growing global health concern, directly linked to the obesity epidemic. Individuals with T2DM are at increased risk for both microvascular consequences (retinopathy, nephropathy, and neuropathy) and macrovascular issues (such as cardiovascular comorbidities), which are caused by hyperglycaemia and individual components of the insulin resistance (metabolic) syndrome. Environmental variables, such as obesity, a poor diet, and physical inactivity and hereditary factors all play a role in the many pathophysiological disturbances that cause impaired glucose homeostasis in type 2 diabetes. Insulin resistance and decreased insulin secretion remain the primary problems in type 2 diabetes, although at least six other pathophysiological disorders contribute to the dysregulation of glucose metabolism (DeFronzo *et al.*, 2015). AgNPs were discovered to

have outstanding potential antidiabetic action against the major enzymes of diabetes, making them an ideal nanomedicine for nano biomedical applications (Balan *et al.*, 2016).

1.5. *Trema orientalis* (L.) Blume

Classification

Kingdom: Plantae

Phylum: Tracheophyta

Class: Magnoliopsida

Order: Rosales

Family: Cannabaceae

Genus: *Trema*

Species: *Trema orientalis* (L.) Bl.

Description

Dioecious trees, to 15 m high, bark 0.6 cm, thin, greyish or bluish-green, rough, lenticellate; blaze creamy-yellow, streaked; branchlets scabrous to adpressed pubescent. Leaves simple, alternate; stipules lateral, cauducous; petiole 5-10 mm, slender, tomentose, grooved above; lamina 7.5-15 x 2.5-6 cm, ovate-lanceolate, ovate, or oblong-lanceolate, base obliquely cordate, apex acuminate, margin serrulate, scabrid above, tomentose beneath, chartaceous, 3-5-ribbed from base, prominent, lateral nerves 3-4 pairs, pinnate, prominent, intercostae reticulate, prominent. Flowers unisexual, 3-4 mm across, greenish, in axillary fascicles or cymes; male flowers usually sessile; tepals 4 or 5, equal, 2 mm long, curved, ciliate; stamens 5; pistillode oblong; female flowers: tepals unequal, ciliate; ovary superior,

sessile, 1-celled, ovate; style bifid, villous; stigma plumose. Fruit a drupe, 4 x 3 mm, globose, black; stylar tip persistent; seed globose (India Biodiversity portal).

For their medical needs, most people in developing nations rely on herbalists. As a result, most people, particularly the impoverished resort to herbal therapy due to its acceptability, cost, and ease of usage (Nwauzoma *et al.*, 2013). The application of medical health care in developing nations will continue to be significantly influenced by the treatment and control of diseases using local medicinal plants (Nwauzoma *et al.*, 2013). Medicinal plants play an important part in traditional medicine, drug development, and discovery. They are also regarded as the primary source of chemical components with therapeutic importance and many pharmacological activities. *Trema orientalis* is a significant medicinal plant that traditional healers use to cure a variety of illnesses (Zabin *et al.*, 2022).

The plant is known to be used traditionally to cure intestinal sickness, loose stools, diabetes, respiratory and pyrogenic ailments, and solid pain. It also possesses potential pharmacological properties (Parvez *et al.*, 2019). Infusions made from the fruits and flowers are used to treat children with bronchitis, pneumonia, and pleurisy (Adinortey 2013). The plant's root is used to cure diarrhea, asthma, and blood in urine, while the bark is used as a poultice for muscle pain. The roots, bark, and leaves are also used to treat epilepsy (Uddin *et al.*, 2008). Traditional medicine includes the use of fruits, leaves, bark, stems, twigs, and seeds. The leaves are used to heal coughs and sore throats, while the bark is made into cough syrups. Reported uses include treating bronchitis, gonorrhoea, malaria, yellow fever, toothaches, and intestinal worms (Uddin *et al.*, 2008).

The therapeutic use of plants is based on phytochemistry. Knowing the chemical composition of plants allows you to better grasp their potential medical usefulness. The vast and diversified pharmacological effects of medicinal plants are mostly dependent on their

phytochemical ingredients (Seigler 2012). In general, these phytochemicals are divided into two categories: primary and secondary metabolites. Primary metabolites are engaged in basic biological functions, while secondary metabolites are created by other pathways, such as the Shikimic acid pathway (Hussein *et al.*, 2019).

In the search for new medications, the therapeutic actions of plants are becoming more focused on secondary metabolites. Secondary metabolites have been found to have a vital role in the treatment of a variety of disorders in traditional medicine and folk remedies. They have a variety of biological roles, which explains why they are used in science and traditional medicine by many ancient communities. Based on their chemical structure, they are categorized into numerous classes such as phenolics, alkaloids, saponins, and terpenes (Hussein *et al.*, 2019).

1.6. Antioxidant study

In food and medicinal items, antioxidants help prevent oxidative stress-induced pathogenic processes and deterioration of the product. Oxygen is needed for numerous enzyme activities in the intricate systems that make up living organisms (Wickens *et al.*, 2001). Therefore, a key element of metabolism is molecular oxygen. However, it can also exist in the form of hydroxyl radical, hydrogen peroxide, and ROS. Cell harm may result from these chemicals (Wickens *et al.*, 2001). To mitigate these harms, living things have evolved diverse antioxidant defence mechanisms. Nevertheless, as they age, these defences become less effective, and the build-up of reactive oxygen species can lead to the onset of different ailments (Baillie *et al.*, 2009).

Free radicles are the substances produce from physiological reactions, or environmental changes such as exposure to smoking, tobacco or radiations, free radicles can damage cells and can cause diseases like cancer, heart failure and other diseases. The substances that protect cells from this free radicle are antioxidants (Baillie *et al.*, 2009). In a

study conducted by Salprima *et al.* (2011), methanol extracts of the leaves of *T. orientalis* resulted to show potential free-radical scavenging activity whereas aqueous extract showed very little free-radical scavenging activity. The methanol fraction extracted from *T. orientalis* leaves has been shown to show an anti-radical activity that is almost same as to that of ascorbic acid (Angasa *et al.*, 2011).

The antioxidant activity can be screened by different methods viz., ABTS scavenging, DPPH radical scavenging, Ferric reducing power antioxidant assay (FRAP), Cupric ion reducing power assay, FCR assay, Peroxyl radical, Superoxide radical, Anion, hydrogen peroxide scavenging assay, hydroxyl radical scavenging assay, singlet oxygen scavenging assay and Chemiluminescence assay (Alam *et al.*, 2013). Among these, the DPPH based is probably the most popular due to its simplicity, speed and low cost (Alam *et al.*, 2013). DPPH is a stable free radical which can be reduced by transferring hydrogen from another compound. Antioxidant can react with DPPH by providing an electron or hydrogen atom, thus reducing it to DPPH, characterized by the pale-yellow colour that could be easily monitored with a spectrophotometer (Njoya *et al.*, 2021).

1.7. Antidiabetic study

Diabetes mellitus is a metabolic disorder characterised by chronic hyperglycaemia or an increase in blood glucose levels that disturbs carbohydrates, fat and protein metabolism resulting from absolute or relative lack of insulin secretion (Sudha *et al.*, 2011). This disorders frequency is rising to a tremendous level globally. The primary threat to human health is type 2 diabetes due to its increasing prevalence, chronic course, and disabling complications, many diverse therapeutic strategies for treating Type 2 diabetes are in use. The available conventional therapies for diabetes include endogenous insulin secretion stimulation, oral hypoglycaemic agents, such as biguanides and sulfonylureas, and the

inhibition of the degradation of dietary starch by glycosidases such as alpha amylase and alpha glucosidase (Sudha *et al.*, 2011).

The two most significant enzymes involved in the metabolism of carbohydrates are glucosidase and alpha amylase. Alpha amylase degrades complex dietary carbohydrates to oligosaccharides and disaccharides and alpha glucosidase converts complex dietary carbohydrates into monosaccharides. Glucose which is liberated, is absorbed by the gut, resulting in postprandial hyperglycaemia. Inhibiting intestinal alpha glycosidases and alpha amylase limits postprandial hyperglycaemia levels by delaying the process of carbohydrate hydrolysis and absorption, making it helpful in managing type 2 diabetes. Plant sources and microorganisms shows an excellent ability to inhibition of these enzymes. For example, acarbose, 4-1 deoxy nojirimycin and genistein have all been isolated from natural resources (Shinde *et al.*, 2008). Aqueous bark extract of *T. orientalis* has been shown to possess hypoglycemic effects in induced diabetic rats via mechanism different from that of sulfonylurea drugs; these results provide pharmacological evidence that the usage of this plant in herbal treatment is significant in diabetic patients (Dimo 2008).

The starch-iodine method has received considerable attention because it can be used to screen many potential candidates α -amylase inhibitors in a short time frame. This is largely due to its sensitivity and requirement of low-cost reagents and less rigorous protocol (Oliveira *et al.*, 2019). The DNSA method, on the other hand, is very sensitive and stable, but suffers from a relatively high cost of the reagents required and a more rigorous protocol.

1.8. Anti-inflammatory study

Inflammation and inflammatory illnesses are widespread in today's world. Inflammation occurs when the body's immune system reacts to an irritant (Chen *et al.*, 2018). Inflammation can be acute or persistent. Pathogenic infection, allergic reaction, burn trauma/injury, wounds, and other factors could be to blame. Chronic inflammation can cause rheumatoid arthritis, cardiovascular disease, dermatitis, and other conditions. Inflammation symptoms include redness, heat, swelling, discomfort, and/or functional loss. Inflammatory reactions serve primarily to protect the body from microbial infection; nevertheless, in rare situations, they can be uncomfortable, leading to specific medical problems. Cellular inflammation may result in cell death or organ damage. Chronic inflammation can cause circulatory/digestive system abnormalities, potentially resulting in tissue damage or disease (Chen *et al.*, 2018). Thus, lowering inflammation is a therapeutic technique for combating inflammation-related disorders. Anti-inflammatory medications can interfere with the mechanism of inflammation, aiming to reduce tissue damage and improve patient comfort (Nunes *et al.*, 2020). As a result, anti-inflammatory techniques are being investigated at many levels to treat these disorders. For years, man-made steroids (glucosteroids and corticosteroids) have been widely utilized in therapy to decrease inflammation (Nunes *et al.*, 2020).

Although these treatments are helpful and give relief from the condition, they can have dangerous short- or long-term repercussions. Furthermore, they might be expensive or scarce in all regions (Yatoo *et al.*, 2018; Buchman, 2001). NSAIDs (non-steroidal anti-inflammatory medications) are a very successful method of contemporary medicine to the efficient treatment of pain, fever, and inflammation, but they have also been shown to have some major adverse effects (Haley *et al.*, 2019; Vonkeman *et al.*, 2010). To overcome this and develop effective anti-inflammatory pharmaceuticals, scientists are currently focusing on medicinal components and extracts, as well as researching natural and traditional applications

for medicines. Furthermore, medicinal plants are known to generate bioactive chemicals that have anti-inflammatory and analgesic properties. Secondary metabolites of medicinal plants, such as polyphenols, flavonoids, terpenoids, alkaloids, and others, are key sources for generating these medications (Kumar *et al.*, 2013). The leave extracts of *T. orientalis* have noticeable ability to reduce pain in mice in acetic acid induced writhing test, and in rats by the hot plate model. The leaves extract also show anti-arthritis effects in acute and chronic models in mice (Barbera *et al.*, 1992).

Protein denaturation occurs through an unpredictable mechanism that includes changes in electrostatic hydrogen, hydrophobic, and disulfide bonds. Protein denaturation produces autoantigens in inflammatory disorders such as rheumatoid arthritis, cancer, and diabetes. Thus, by inhibiting protein denaturation, inflammatory activity can be reduced (Modak *et al.*, 2017). In the protein denaturation test, heat treatment was used to promote denaturation of egg albumin. When denatured, most biological proteins lose their integrity and function. Heat exposure breaks or changes the functional three-dimensional structure. Conventional NSAIDs can prevent heat-induced protein denaturation. The plant extracts and the silver nanoparticles are been study to check similar protein denaturation inhibition activity to overcome the side effects of NSAID drugs (Modak *et al.*, 2017).

Principle of egg albumin denaturation method: Inflammation and protein denaturation are related. A substance's potential anti-inflammatory properties are demonstrated by its capacity to prevent protein denaturation. The in-vitro egg albumin denaturation method is used to screen for anti-inflammatory activities using a fresh hen's egg. Ovoinhibitor, ovotransferin, ovalbumin, clusterin, and prostaglandin D2 synthase are all found in egg whites. Diclofenac sodium, an NSAID, is used in this approach to assess the ability to suppress the denaturation of the egg protein (albumin). The plant extracts and silver nanoparticle's ability to reduce inflammation is also measured and it is presumed to be an

NSAID. Protein denaturation through heating is used to screen for prostaglandin activity decrease. The percentage inhibition of egg albumin denaturation indicates this. The anti-inflammatory capacity increases with the percentage of denaturation inhibition (Samaraweera *et al.*, 2023).

1.9. Scope of the current study

In this study, silver nanoparticles were synthesized using the green synthesis method from *Trema orientalis* leaf and bark. Among the various biological methods of silver nanoparticle synthesis, microbe-mediated synthesis is not industrially feasible due to the requirements for highly aseptic conditions and their maintenance. As a result, the employment of plant extracts for this purpose is possibly preferable over microorganisms due to the simplicity of improvement, less biohazard, and complicated procedure of sustaining cell cultures. It is the finest platform for nanoparticle synthesis since it is devoid of harmful chemicals and contains natural capping agents that stabilize silver nanoparticles. Furthermore, using plant extracts lowers the cost of microorganism separation and culture medium (Ahmed *et al.*, 2015).

Plant extracts may be used as both reducing and capping agents in nanoparticle production. The bio reduction of metal nanoparticles using biomolecules contained in plant extract is ecologically friendly (Siavash *et al.*, 2011). The study sought to identify the phytochemicals contained in leaf extract and bark extract that are responsible for the synthesis of silver nanoparticles, as well as to quantify the quantity of tannins, phenols, flavonoids, and alkaloids. The green synthesis is performed using 5mM silver nitrate, and the nanoparticles are then characterized to validate the size, morphology, and shape stability of silver nanoparticles.

The nanoparticles are next examined for their activity, as significant research has previously demonstrated the high antibacterial activity of silver nanoparticles. The current study aims to assess the possible antioxidant, antidiabetic, and anti-inflammatory activity of synthesised silver nanoparticles derived from leaf extract and bark extract, and the following activity of silver nanoparticles will be compared to the corresponding leaf extract and bark extract.

The biosynthesis of nanoparticles (NPs) from *T. orientalis* is a topic with limited available reports, creating an opportunity for future studies to expand our understanding. Considering the ethnobotanical value of the plant, biosynthesis appears to be a promising avenue for producing nanoparticles that exhibit robust biological activity. Further research in this area has the potential to uncover novel insights and applications for nanoparticles derived from *T. orientalis*, contributing to both scientific knowledge and the exploration of the plant's medicinal property.

Specific objectives proposed for the study:

- 1) Collection of plant material (*Trema orientalis*) from the Goa University campus.
- 2) Qualitative and quantitative phytochemical analysis of leaf and bark aqueous extracts.
- 3) Bio-fabrication of silver nanoparticles from the aqueous extract of *Trema orientalis* using silver nitrate as precursor salt.
- 4) Characterisation of silver nanoparticles using UV-vis spectroscopy, FTIR, XRD, FESEM-EDS, DLS and Zeta potential techniques.
- 5) Evaluation of the bio-fabricated silver nanoparticles for biological activities such as antioxidant, antidiabetic, and anti-inflammatory activities.

CHAPTER 2: REVIEW OF LITERATURE

2. REVIEW OF LITERATURE

The relevant literature on the present study has been briefly reviewed to understand the different parameters of the study done on the mentioned objectives. In the study carried out by Uddin *et al.* (2008) the methanol and aqueous extracts of the plant *T. orientalis* leaves were tested for antioxidant and antibacterial properties. The medicinal curiosity of this plant, combined with its traditional use (antidiarrheal, antiseptic, analgesic, etc.), spurred tests for antioxidant and antibacterial properties. The antioxidant capability of the methanolic extract was examined using the scavenging activity of the stable 1,1-diphenyl-2-picryl hydrazyl free radical. The methanol extract of *T. orientalis* exhibited high antioxidant activity, with an IC₅₀ of 110.25 µg/ml. However, the aqueous extract demonstrated moderate antioxidant activity. In the antibacterial activities test, the extract's efficiency against both Gram-positive and Gram-negative bacteria was determined using the agar diffusion method. The crude methanol and aqueous extract produced zones of inhibition against a few sensitive organisms, which were quantified and compared to those of the conventional antibiotic Gentamycin. Both extracts clearly have antibacterial activity at low doses. The findings support the use of this plant in traditional medicine and encourage additional research.

In the study conducted by Uddin (2009), test for anti-inflammatory, antinociceptive, and diuretic properties of charcoal tree was revealed. The carrageenin-induced rat paw edema model and the cotton pellet implantation method in mice were used to examine the potential anti-inflammatory properties of the crude methanolic leaves extract of *T. orientalis*. Next, the extract's antinociceptive properties were examined using a mouse model that elicited writhing in response to acetic acid. Both models showed that the extract, at 200 and 400 mg/kg body weight of mice, exhibited considerable anti-inflammatory effect. In mice given 200 and 400

mg/kg body weight of acetic acid, the extract also considerably decreased the amount of acetic acid-induced belly constriction. Additionally, albino mice treated with the extract exhibited good diuretic action.

In the study conducted by David (2014), Silver nanoparticles (AgNPs) was produced in extracellular matrix utilising fruit extracts from elder berries (*Sambucus nigra*, Adoxaceae family) and its anti-inflammatory activity was evaluated., The diameters of the synthesized nanoparticles ranged from 20 to 80 nm, and they showed the typical absorbance peak at 426nm for AgNPs. AgNPs' anti-inflammatory qualities were evaluated on UVB-exposed HaCaT cells *in vitro*, on an acute inflammation model *in vivo*, and on psoriasis lesions in patients.

their findings *in vitro* showed that functionalized AgNPs have anti-inflammatory effects by reducing of the generation of cytokines brought on by UVB exposure. *In vivo*, shortly after inflammation was induced, pre-administration of AgNPs decreased the levels of cytokines and edema in the paw tissues. The current study also showed that synthetic AgNPs might be used to treat psoriasis lesions.

Logeswari (2015), reported the synthesis of silver nanoparticles with plant extract and evaluated for their antibacterial capabilities, plant extracts from *Ocimum tenuiflorum*, *Solanum tricobatum*, *Syzygium cumini*, *Centella asiatica*, and *Citrus sinensis* were utilized to create silver nanoparticles (Ag NPs). Atomic force microscopy (AFM), scanning electron microscopy (SEM), X-ray diffractometer (XRD), and UV–vis spectrophotometer was used to characterize Ag NPs. Via UV–vis spectrophotometer examination, the reduced silver nanoparticles production and stability in the colloidal solution were observed. For silver nanoparticles, the mean particle diameter was determined Utilizing Scherrer's equation, the XRD pattern is determined by the plane's line width and refraction peak. AFM revealed the development of silver nanoparticles, which had an average size of 26.5 and 28 nm. The

corresponding wavelengths for *O. tenuiflorum*, *S. cumini*, *C. sinensis*, *S. tricobatum*, and *C. asiatica* are 65 nm, 22.3 nm, and 28.4 nm, respectively. The brown colour stable samples SEM analysis revealed the presence of silver nanoparticles, while the samples treated with silver nitrate had evenly distributed nanoparticles. The antimicrobial activity of the silver bio-nanoparticles was assessed using the well-diffusion method against *Klebsiella pneumoniae*, *Pseudomonas aeruginosa*, *Escherichia coli*, and *Staphylococcus aureus*. When silver nanoparticles made from extracts of *S. aureus* (30 mm) and *E. coli* (30 mm) were tested, they showed the greatest antibacterial efficacy. Effective antibacterial activity against pathogenic bacteria is exhibited by the Ag NPs produced in this technique. The fields of nanotechnology and nanomedicine are mostly reliant on silver nanoparticles among these.

In the study conducted by Ahmed (2015), aqueous leaf extract from *Azadirachta indica*, silver nanoparticles were synthesised. In this study, an easy-to-use, quick method was used to create silver nanoparticles from *Azadirachta indica* aqueous leaf extract. The plant extract serves as a capping and reducing agent in tandem. The functional groups found in plant extract were examined using FTIR to pinpoint the substances causing the decrease of silver ions. DLS, photoluminescence, TEM, and UV-visible spectrophotometer are among the methods used to characterize produced nanoparticles. The absorbance peak was found in the 436–446 nm region using a UV-Visible spectrophotometer. The antibacterial properties of the silver nanoparticles were demonstrated against *Escherichia coli* and *Staphylococcus aureus*. Studies on the synthesized silver nanoparticles using photoluminescence were also assessed. The methodology was verified by the results to be easy to follow, quick, one-step, safe for the environment, non-toxic, and a substitute for traditional physical/chemical methods. At room temperature, silver ions were converted into silver nanoparticles in about 15 minutes without the need of any dangerous chemicals.

In the study carried out by Punchal (2015), the macro and microscopical characteristics of *Trema orientalis* leaves were assessed through pharmacognostic standardization, physic-chemical evaluation, and the determination of certain insoluble ash and sulphated ash values, as well as alcohol-and water-soluble extractive values for phytochemical analyses. Additionally, a preliminary phytochemical screening was carried out to identify various, phytoconstituents. Under a microscope, leaf revealed calcium oxalate crystals, stomata, midrib regions, lamina, and trichomes. Powder microscopy revealed the following: the mesophyll area; numerous xylem vessels with annular thickenings; unicellular, multiseriate covering trichomes and glandular trichomes; calcium oxalate crystals in the shapes of rosettes and prisms; and anomocytic stomata. Total ash was around twice as high as water soluble extractives and four times higher than acid insoluble extractives, respectively. Ethanol soluble extractives were roughly twice as high as water soluble extractives. Petroleum ether and ethanol extract subjected to TLC revealed four spots using chloroform: ethyl acetate (5:4) and five spots using hexane: ethyl acetate (12:4). The root showed phytosterols, flavonoids, tannins, and phenolic substances phytochemically.

In the study reported by Kharat (2016) the green synthesis of silver nanoparticles was produced using an extract from the leaves of the medicinal plant *Elephantopus scaber* L. UV-vis spectroscopy, nanoparticle tracking analysis (NTA), transmission electron microscopy (TEM), X-ray diffraction (XRD), and Fourier transform infrared (FTIR) analysis were used to characterise the synthesised silver nanoparticles (AgNPs). The UV spectra reveal a maximum absorbance of 435 nm, the NTA analysis reveals an average size of 78 nm for the nanoparticles, and the TEM study reveals a spherical form with an average diameter of 50 nm for the nanoparticles. The metallic silver structure is indicated by the reflection planes (111), (200), (220), and (311) that correlate to the XRD peaks in 2θ range of 30–80°. Phenolic group surface capping is revealed by FTIR analysis. The presence of aromatic rings

in the leaf extract is indicated by the appearance of peaks in the 1611–1400 cm^{-1} range. The presence of OH groups is responsible for the peak at 1109 cm^{-1} . Using the DPPH assay, the antioxidant activity of the synthesised nanoparticles was assessed, and it was found that the photosynthesised nanoparticle also has antioxidant potential. As a result, it has the potential to be a free radical scavenger. Applications for silver particles in medicine and diagnostics are enormous. The surface coating of plant metabolite components presents significant potential in this regard. To evaluate and access the antioxidant activities of the AgNPs, the current effort has been conducted to synthesise them utilising the leaf extract of the medicinal plant *E. scaber*.

As reported by Balan in (2016), the aqueous leaf extract of *Lonicera japonica* was used in the green synthesis of silver nanoparticles (AgNPs). During the synthesis process, a pale yellow to brown colour shift was noticed. The surface plasmon resonance of the AgNPs is responsible for the absorption band observed at 435 nm in ultraviolet-visible (UV-vis) experiments. The stability and average size of the AgNPs, as measured by a zeta sizer, were found to be 53 nm and -35.6 mV, respectively. The face-centered cubic crystalline structure and spherical, hexagonal shape of metallic silver were verified by X-ray diffraction (XRD) and high-resolution transmission electron microscopy (HR-TEM). Fourier transform infrared spectra (FTIR) were used to characterise the functional group of biomolecules contained in the AgNPs. AgNPs that were synthesised shown potent antioxidant action. AgNPs demonstrated their antidiabetic potential by effectively inhibiting enzymes that break down carbohydrates, including α -amylase and α -glucosidase, with IC_{50} values of 54.56 and 37.86 $\mu\text{g mL}^{-1}$, respectively. Using Dixon and LB plots, the inhibition of the kinetic mechanism was examined. α -amylase and α -glucosidase, two important diabetes-related enzymes, showed K_i values of 25.9 and 24.6 μg for AgNPs, which were found to be reversible non-competitive inhibitors. We draw the conclusion that the data indicate that AgNPs have a

remarkable potential for antidiabetic activity against the major diabetes-related enzymes and are a suitable nanomedicine for use in nano- biomedical applications.

In the study conducted by Akin (2016), the active phytochemicals of the *Trema orientalis* plant leaves and stalk were examined. Three different solvents were used in the extraction process: methanol, ethyl acetate, and hexane. It was discovered that there were bioactive substances present, including alkaloids, volatile oils, terpenoids, flavonoids, saponins, phenols and glycosides. Using the well diffusion method, the antibacterial activity of *Trema orientalis* extracts was also investigated. The extracts were evaluated against the following clinical isolates: yeast extract from *Candida albicans*, *Escherichia coli*, *Klebsiella pneumonia*, *Pseudomonas aeruginosa*, and *Staphylococcus aureus*. Based on concentration, the results indicated that the stalk's methanol extract was more effective against all microorganisms than the matching extracts of the two plant sections that were studied in ethyl acetate and hexane.

In the study conducted by Trouno (2016), assessment of the total phenolic content and α -amylase inhibitory and antioxidant activity of *T. orientalis* bark extracts in water and methanol (80:20 v/v) by *in-vitro* studies were done. To determine the bioactive components, a preliminary phytochemical profile was carried out. The lethality assay for brine shrimp was also used to determine toxicity screening. Using GC-MS to identify some phytoconstituents, phytochemical screening indicated the presence of a variety of chemical compounds. With IC_{50} values of 48.40 $\mu\text{g/ml}$ and 127.56 $\mu\text{g/ml}$, respectively, the data showed that the methanol extract had high DPPH scavenging ability and α -amylase inhibitory activity.

Additionally, it was shown that the methanol extract had a larger total phenolic content than the aqueous extract. The findings imply that the bioactivity may emerge from the active substances' synergistic effects, with phenolic components: phenols, flavonoids, and tannins having the most impact. There was also evidence of a little cytotoxicity of the

methanol fraction towards brine shrimp. Nonetheless, the decoction-prepared aqueous extract turned out to be non-toxic, confirming the safety of the conventional method. The combination of *T. orientalis* bark extract's antioxidant and α -amylase inhibitory properties may suggest the plant has promising anti-diabetic properties.

In the study conducted by Singh (2017), showed how to synthesize silver nanoparticles (P-AgNPs) and gold nanoparticles (P-AuNPs) from fresh fruit extract of *P. serrulata*. Gold and silver nanoparticles were produced quickly, effectively, and easily in 50 minutes and 30 seconds, at 80°C, respectively. FT-IR, XRD, DLS, elemental mapping, UV-Vis, FE-TEM, EDX, and visual observation were used to characterize the nanoparticles, and the results verified the development of monodispersed, crystalline, and stable nanoscale fragments. They further investigated the potential of these nanoparticles to block NF- κ B activation downstream in macrophages (RAW264.7) to have anti-inflammatory effects. In lipopolysaccharide, there was a decreased production of inflammatory mediators such nitric oxide (NO), prostaglandin E2 (PEG2), inducible nitric oxide synthase (iNOS), and cyclooxygenase-2 (COX-2). All things considered, the findings imply that *P. serrulata* fresh fruit extract is a sustainable resource for the environmentally friendly synthesis of P-AgNPs and P-AuNPs.

In the study conducted by Majid (2019), root extract from *Astragalus tribuloides Delile* was used as a bio-reduction and capping agent at room temperature to create silver nanoparticles (AgNPs) in a simple, economical, and environmentally friendly manner. The examination of the chemical processes was done using UV-vis spectroscopy. X-ray diffraction spectroscopy (XRD), transmission electron microscopy (TEM), and Fourier-transform infrared spectroscopy (FTIR) studies were used to characterize the greenly produced AgNPs. Furthermore, assessed were the antioxidant, antibacterial, and anti-inflammatory properties, as well as the total phenolic and flavonoid contents, of the A.

tribuloides root extract and the greenly generated AgNPs. The AgNPs spherical form and crystalline structure were revealed by the results, and their average size was 34.2 ± 8.0 nm. The overall phenolic and flavonoid contents of the greenly produced AgNPs were lower than those of the *A. tribuloides* root extract. The resultant AgNPs exhibited more antioxidant activity (64%) than the *A. tribuloides* root extract (47%). The findings of the antibacterial test showed that the generated AgNPs exhibited more bactericidal activity against both Gram-positive and Gram-negative bacteria when compared to the *A.tribuloides* root extract. In terms of anti-inflammatory activity, the root extract of *A.tribuloides* was less effective than the greenly produced AgNPs (82% versus 69% at 500 $\mu\text{g/mL}$). All things considered, the AgNPs generated from *A.tribuloides* root extract shown appropriate antibacterial, antioxidant, and anti-inflammatory activities, making them a good choice for a variety of biomedical applications.

In the study conducted by Adjileye (2019), the phytochemical analysis of *Dialium guineense* and *Trema orientalis* antioxidant activity was examined. Standard operating protocols were followed in the phytochemical screening. Folin-Ciocalteu and aluminium chloride reagent were used to measure the amounts of flavonoids and phenolic compounds. Superoxide anion, ferric reducing capacity, 2,2-diphenyl-1-picryl-hydrazyl, and Ferric reducing power, peroxide and superoxide reducing power assay was also carried on. The most antioxidant activity was resulted through ferric reducing power assay *Tremas orientalis* with 6007.8 ± 175.57 $\mu\text{mol AAE g}^{-1}$. The range of hydrogen peroxide and superoxide anion scavenging activities was $88.52 \pm 0.68\%$ to $91.33 \pm 4.01\%$. The activity of DPPH scavenging was dose-dependent. With an inhibitory percentage of $96.06 \pm 0.34 \%$, which was close to ascorbic acid ($99.46 \pm 0.37 \%$), *Dialium guineense* was the most active.

In the study conducted by Rajput (2020), green synthesis of silver nanoparticles (AgNPs) from the aqueous leaf extract of the medicinal herb *A. acuminata* was carried out,

which is critically threatened. AgNPs was produced when 1 mM silver nitrate was added to aqueous leaf extract and the mixture was heated to 60°C for 30 minutes at pH 7. UV-vis spectroscopy revealed an absorption band at 428 nm, which confirmed the production of AgNPs. AgNPs crystalline nature was demonstrated by XRD patterns, and TEM examination indicated that most of the nanoparticles had a spherical form. AgNPs zeta potential was determined to be -33.5 mV, confirming their remarkable stability. Different functional groups involved in the reduction and capping of AgNPs were confirmed by FT-IR experiments. Effective DPPH (IC₅₀-16.08 µg/mL), H₂O₂ (IC₅₀-25.40µg/mL), and superoxide (IC₅₀-21.12 µg/mL) radical scavenging activities were demonstrated by the synthesized AgNPs. The anti-proteinase activity (IC₅₀-18.401 µg/mL) and albumin denaturation (IC₅₀-12.98 µg/mL) were significantly inhibited by these plant-AgNPs. Additionally, it was discovered that biosynthesized AgNPs exhibited strong inhibitory effects against a cervical cancer (HeLa) cell line (IC₅₀-5.418 µg/mL) and larvicidal activity against *Anopheles stephensi* (LC₅₀-18.9 ppm, LC₉₀-40.18 ppm), *Aedes aegypti* (LC₅₀-12.395 ppm, LC₉₀-36.34 ppm), and *Culex quinquefasciatus* (LC₅₀-17.76 ppm, LC₉₀-30.82 ppm) and were shown to be non-toxic to a non-target organism (*Meso-cyclops thermocyclopoidea*) as well as a normal cell line (HEK 293). This is the first study on AgNPs production utilizing *A. acuminata* leaf extract in aqueous form confirming their significant therapeutic potential.

In the study conducted by Saleh (2020), phytochemical screening revealed the presence of saponins, tannins, steroids, cardiac glycosides, alkaloids, triterpenes, flavonoids, and phenolic compounds in *Trema orientalis*. Total phenolic contents were found to be 260.96±2.31 mg GAE/g and 134.08±0.56 mg GAE/g in the ethanol and aqueous extracts respectively. Similarly, total flavonoid contents were between 32.71±0.89 and 4.70±0.23 mg GAE/g. The radical scavenging effect was observed in ethanol extract with IC₅₀ of 9.27

$\mu\text{g/mL}$. The abundance of polyphenolic compounds and antioxidant activities of the *T. orientalis* could confirm their good therapeutic potentials in ethnobotany.

In the study conducted by Parabakaran (2019), presented an empirical analysis on the use of aqueous extract of *Eichhornia crassipes* to produce silver nanoparticles (AgNPs) from silver nitrate. The *Eichhornia crassipes* leaf extract, AgNPs and Diclofenac sodium at different concentrations was incubated with egg and Bovine serum albumin in controlled experimental conditions and subjected to determination of absorbance to assess the anti-inflammatory property. Diclofenac sodium was used as the reference drug. The present findings exhibited a concentration dependent inhibition of protein denaturation by *Eichhornia crassipes* extract and AgNPs. The effect of AgNPs was found to be high when compared with the *Eichhornia crassipes* extract and near to the diclofenac sodium. From the present study it can be concluded that AgNPs possessed marked in vitro anti-inflammatory effect against the denaturation of protein.

In the study conducted by Yousaf (2020), the silver nanoparticles were synthesised using green synthesis method from extracts from *Achillea millefolium L.* and its antibacterial and antioxidant properties were examined. A colour shift and UV-vis spectroscopy was used to track the SNPs during their synthesis process, which involved extracts of *A. millefolium* in aqueous, ethanolic, and methanolic forms. X-ray diffraction was used to evaluate the phase of the nanoparticles and scanning electron microscopy was used to analyse the size and shape of the particles. The SNPs were found to be generated from aqueous, ethanol, and methanol extract, respectively, and had an average diameter of 20.77nm, 18.53nm, and 14.27 nm with spherical, rectangular, and cubical geometries. Fourier transform infrared spectroscopy was used to examine the response of biomolecules found in plant extract during the production of SNPs. The results indicated that alcohol, proteins, carboxylic acid, and polyphenols are all involved in the formation of SNPs. Following that, the antibacterial potential of the plant

extracts and SNPs was investigated against common human pathogens, including gram-positive (*Staphylococcus aureus* and *Bacillus subtilis*) and gram-negative (*Salmonella enterica*, *Escherichia coli*, and *Pseudomonas aeruginosa*) bacteria. Both extract and SNPs showed very good activity against all the bacteria. The Methanol-SNPs demonstrate a higher level of DPPH radical inhibition, with an IC_{50} of $7.03 \pm 0.31 \mu\text{g/mL}$. This environmentally friendly synthesis technique of SNPs would facilitate the synthesis of SNPs with greatly increased antioxidant and antibacterial capabilities as well as dramatically improved therapeutic efficacy.

In the study conducted by Purkait (2020), described the green synthesis of Titanium dioxide nanoparticles (TiO_2 NPs) using *Trema Orientalis* (L) aqueous leaf extract and their efficiency in the photodegradation of zoxamide under UV light ($\lambda_{\text{max}} > 250 \text{ nm}$). The reducing agent is leaf extract, while the precursor is titanium (IV) iso-propoxide. The synthesised TiO_2 NPs are verified by powder X-ray diffraction (XRD) analysis, and the crystalline size was determined using the Williaman-Hall (W-H) equation (59 nm) and Scherrer's formula (52 nm). The synthesised TiO_2 NPs are verified by powder X-ray diffraction (XRD) analysis, and the crystalline size was determined using the Williaman-Hall (W-H) equation (59 nm) and Scherrer's formula (52 nm). The synthesized TiO_2 NPs' stability and roughly 88–94 nm particle size is revealed by the Dynamic Light Scattering (DLS) investigation. A functional group analysis using Fourier Transform Infrared Spectroscopy (FTIR) verifies that the synthesized NPs contain different functional groups. The computed energy band gap is determined to be 3.27eV, which is the UV absorption wavelength measured at the peak of 351 nm. Scanning electron microscopy (SEM) is used to determine the surface morphology of the produced TiO_2 NPs. In an acetonitrile/water solvent mixture, zoxamide photodegraded at a rate that followed pseudo first-order kinetics, with predicted half-lives between 2.33 and 10.46 hours. One photoproduct was identified and isolated from

this investigation using X-ray crystallography, mass spectrum data, and column chromatography. 3,5-dichloro-4 methyl benzoic acid was discovered as the isolated photoproduct. A probable molecular pathway for the photoproduct's synthesis is also illustrated. A Langmuir–Hinshelwood (L–H) kinetic model was put out to explain the rate equation of photodegradation of zoxamide in the presence of TiO₂ nanoparticles under ultraviolet light.

Purkait (2023), reported the green synthesis of zinc oxide nanoparticles (ZnO NPs) utilizing *Trema orientalis* (L) aqueous leaf extract. Zinc nitrate hexahydrate served as the precursor for the synthesis of the ZnO NPs, while leaf extract served as the reducing and capping agent. The average crystalline size was determined by powder X-ray diffraction (XRD) analysis, which validated the production of ZnO NPs. Williamson-Hall (W-H) equation (26 nm) and Scherrer's formula (24 nm). The investigation of Dynamic Light Scattering (DLS) revealed the stability and the synthesized ZnO NPs approximate 65–67 nm particle size. Infrared Spectroscopy with Fourier Transform (FTIR) Analysis verified that the synthesized NPs contained a variety of functional groups. 370 nm is the wavelength at which UV absorption is measured, and 3.13 eV is the predicted direct band gap. Scanning electron microscopy (SEM) was used to determine the synthesised ZnO NPs surface morphology and crystalline form. Under UV irradiation ($\lambda_{\text{max}} \geq 250$ nm), the efficacy of ZnO NPs on photocatalytic degradation of doxamide, a benzamide type of fungicide, was evaluated. The half-lives of zoxamide photodegradation in an acetonitrile/water solvent combination were determined to be between 4.09 and 10.46 hours. Additionally, the impact of pH, the starting concentration of zoxamide, and the dose of ZnO NPs for photocatalysis were investigated. When the starting concentration of zoxamide was increased from 120 to 260 mg/L, the reaction rate constant (k_{obs}) fell from 0.1695 to 0.1511 h⁻¹. The Langmuir–Hinshelwood (L–

H) kinetic model was put forth to solve the rate equation of the UV-induced zoxamide degradation in the presence of ZnO NPs.

CHAPTER 3: MATERIALS AND METHODS

3.MATERIALS AND METHODS

3.1. Collection of plant material (*Trema orientalis*) from the Goa University campus.

The plant materials i.e. the leaf and bark of *Trema orientalis* was collected from the Goa university campus in the month of August 2023, the plant material was confirmed using authentic flora available. The plant materials were washed with tap water and rinsed with double distilled water; the materials were then kept for drying at room temperature (25±1°C) for 14 days. The dried materials were ground in to a fine powder and stored in air tight container for further use.

3.2. Qualitative and quantitative phytochemical analysis of leaf and bark aqueous extracts.

3.2.1. Preparation of aqueous plant extract

The aqueous plant extract of *Trema orientalis* leaf powder and bark powder was prepared by hot maceration method. 5g of powder was dissolved in 100 mL of double distilled water and boiled for 30 minutes, the boiled extract was filtered with strainer and centrifuged at 7000rpm for 20 minutes at 25°C, the supernatant was collected and poured in the petriplate and dried completely in oven at 50°C, the dried extract was than scrapped and weighed, the percentage yield of the powder was calculated.

Percentage (%) yield = (weight of the extract/ total weight of sample) ×100

3.2.2. Preliminary phytochemical screening

Preliminary qualitative phytochemical screening was carried out according to the methods described by (Raaman 2006). Each test was performed in triplicates.

3.2.2.1. Qualitative phytochemical analysis

1) Detection of Alkaloids: 50mg of plant extract stirred with 1 ml of hydrochloric acid and filtered.

Wagner's test

To a few mL of the filtered extract, few drops of Wagner's reagent was added by the sides of the test tube. A reddish- brown precipitate confirmed the test as positive.

Wagner's reagent: Iodine (1 .27 g) and potassium iodide (2 g) were dissolved in 5 mL of water and made up to 100 mL with distilled water

2) Detection of Carbohydrates: 100mg of plant extract dissolved in 5 ml of water and filtered

Benedict's test

To a few drops of filtered extract, 0.5 mL of Benedict's reagent was added. The mixture was heated on boiling water bath for 2 min. A characteristic-coloured precipitate indicated the presence of sugars.

Benedict's reagent: Sodium citrate (173 g) and sodium carbonate (100 g) was dissolved in 800 mL of distilled water and boiled to make it clear. Copper sulphate (17.3 g) was dissolved in distilled water and was added to it.

3) For detection of glycosides: 50mg of plant extract hydrolysed with concentrated hydrochloric acid for two hours on water bath and filtered this is known as hydrolysate

Borntrager's test

3ml of chloroform was added to 2ml of hydrolysate and shaken, chloroform layer was separated and to it 10 % of ammonia solution was added to it. Pink colour indicated the presence of glycosides

4) Detection of Saponins: 50mg of plant extract was diluted with 20ml of distilled water and filtered. The filtered extract was shaken in a graduated cylinder for 15 min. A two cm layer of foam indicated the presence of saponins.

5) Detection of Proteins and Amino acids: 100mg of extract was dissolved in 10ml of distilled water and filtered.

Biuret test

The 2ml of filtered extract was treated with one drop of 2% copper sulphate solution. To this, 1 mL of ethanol (95%) was added, followed by excess of potassium hydroxide pellets. Pink colour in the ethanolic layer indicated the presence of proteins.

6) Detection of Phytosterols

Libermann-Burchard's test: 50mg of plant extract were dissolved in 2 mL Acetic anhydride. To this, one or two drops of concentrated sulphuric acid was added slowly along the sides of the test tube. An array of colour changes showed the presence of phytosterols.

7) Test for fixed oils and fats**Saponification test**

To a small quantity of plant extract few drops of 0.5 N Alcoholic potassium hydroxide was added and a drop of phenolphthalein was added to it, the mixture was then heated in water bath for 2 hours., the soap formation indicates the test positive.

8) Detection of Phenolic compounds and Tannins**Ferric chloride test**

50mg of plant extract was dissolved in 5ml of distilled water, to it a few drops of 5% Ferric chloride solution were added to. A coloured compound indicated the presence of phenolic compounds.

9) Test for gums and mucilage

100mg of extract dissolved in 10ml of distilled water and 25 ml of absolute alcohol and constantly stirred. White colour precipitate indicates the presence of gums and mucilage.

3.2.2.2. Quantitative phytochemical analysis

Preparation of plant extract: 10mg of dried plant extract was dissolved in 10 ml of distilled water and series of 20, 40, 60,80 and 100 ml was made.

Determination of total flavonoids by $AlCl_3$ colorimetric method (Chang *et al.*, 2002)

Plant extract of 0.5 ml was mixed with 15 ml of methanol 0.1 ml of 10% $AlCl_3$,0.1 ml of 1 M potassium acetate and 2.8 ml of distilled water and kept at room temperature for 30 minutes. The absorbance of the reaction mixture was measured at 415 nm. The calibration curve was prepared using quercetin in methanol and results are expressed as amount of flavonoid content.

Determination of total tannins (Amorim *et al.*, 2008)

The extract of 1ml was added with 0.5 ml of Folin's reagent in 7.5 ml of demineralised water 35% sodium carbonate 1 ml solution was added to mixture solution and shaken well. The solution was incubated for 30 minutes at room temperature. The absorbance was read at 725 nm and the concentration of total tannin was calculated as mg tannic acid equivalent of extract using tannic acid calibration curve.

Determination of total phenols (Dewanto *et al.*, 2008)

The calibration curve was plotted by mixing 100 μ L aliquots of 20, 40, 60, 80, and 100 μ L gallic acid solution and 100 μ L. The final volume was made to 500 μ L with distilled water.150 μ L of Folin's reagent was added and vortexed. The mixture was left at room temperature for 10minutes.500 μ L of 7.5 % sodium carbonate was added and test tubes were incubated in the dark for 1 hour followed by measurement of absorbance 650 nm and 760nm.

Determination of Total Alkaloids (Sreevidya and Mehrotra 2003)

The experiment was performed in serial dilution 1ml, 2ml, 3ml, 4ml, 5ml, 6ml, 7ml, 8ml, and 9ml, of plant extract.

Solutions

(a) **Draggondroff reagent**- Prepared by mixing solution of 0.8g bismuth nitrate pentahydrate in 40 mL distilled water and 10 mL glacial acetic acid, and solution of 8.0g potassium iodide in 20 mL distilled water.

(b) **Standard bismuth nitrate solution**- Bismuth nitrate stock solution was made by dissolving 10 mg $\text{Bi}(\text{NO}_3)_3 \cdot 5\text{H}_2\text{O}$ in 5 mL concentrated nitric acid and diluting to 100 mL with distilled water.

(c) **Thiourea, 3%**- Prepared by dissolving 3 g in 100 mL distilled water.

(d) **Disodium sulfide (1%)**- Prepared by dissolving 1 g in 100 mL distilled water.

(e) **Stock solutions of alkaloid**- 5ml of the amount of extract was taken and the pH was maintained at 2 to 2.5 with dilute HCl. 2 ml of DR was added to it and the precipitate was centrifuged. The centrifugate decant completely and meticulously. The precipitate was further washed with alcohol. The filtrate was discarded and the residue was then treated with 2 ml disodium sulfide. The residue was dissolved in 2ml concentrated nitric acid with warming. This solution was diluted to 10 ml in a standard flask with distilled water .1ml was then pipetted out and 5 ml thiourea solution was added to it. The absorbance was measured at 435 nm against the blank containing nitric acid and thiourea.

Procedure for Calibration Curve: The calibration curve was obtained with Bismuth nitrate pentahydrate stock solution. Series dilutions of the stock solution were made by pipetting out 1, 2, 3, 4, 5, 6, 7, 8, and 9-mL stock solution into separate 10 mL standard flasks and diluting to volume with distilled water. A 1 mL amount of this solution was taken, and 5 mL thiourea solution was added to it. The absorbance value of the yellow solution was measured at 435 nm against colourless reagent blanks. All the experiments were performed in triplicates.

3.3. Bio-fabrication of silver nanoparticles from the aqueous extract of *Trema orientalis* using silver nitrate as precursor salt.

3.3.1. Preparation of leaf extract

1g of leaf powder and bark powder was dissolved in 40ml double distilled water respectively and boiled at 80°C in water bath for 30 minutes, the extract was then strained and centrifuged at 7000rpm at 25°C for 20 minutes.

3.3.2. Synthesis of silver nanoparticles

An aqueous 5×10^{-3} M solution of silver nitrate was prepared in distilled water at room temperature and stocked in amber coloured glass bottle in cabinet to elude photoactivation of silver nanoparticles at sterile condition. The classic reaction mixture was prepared by adding 14.1 ml of plant extract to 500 ml of 5×10^{-3} M silver nitrate solution and kept for incubation at 64°C for four hours in a water bath. The initial pale-yellow colour of the solution starts turning brown, which is a visual observation representing the synthesis of silver nanoparticles. The synthesised nanoparticles were centrifuged at 8000rpm for 30 minutes at 25°C and the pellets were washed with water for 2 times each for 30 minutes each at 8000rpm at 25°C to ensure the removal of impurities. Isolated silver nanoparticles were transferred into petriplate and kept in oven for drying at 50°C. The isolated nanoparticles were stored in dark container for further use.

3.4. Characterisation of silver nanoparticles using UV-VIS spectroscopy, FTIR, XRD, FESEM-EDS, and DLS and Zeta potential analysis.

Characterisation of the nanoparticles is crucial to understanding and controlling nanoparticle synthesis and applications. The morphology of the synthesised silver nanoparticles was observed and confirmed by using various techniques of characterisation such as:

3.4.1. UV-VIS spectrophotometric analysis

The UV-Vis spectrophotometry analysis was carried out using Shimadzu UV-vis spectrophotometer model: UV-1800, confirms the silver nanoparticle formation by showing

the surface plasmon resonance (Kholoud *et al.*, 2010). The formation of silver nanoparticles and the reduction of Ag^+ ions were monitored using UV-vis spectrophotometer. The UV-Vis spectrum of the synthesis medium comprising the leaf extract and the bark extract with 0.05 M silver nitrate was taken at regular intervals (1h, 2h, 3h, 4h) in the wavelength range between 300nm and 600nm. The UV-Vis readings were recorded. Microsoft excel analysis tools were used to analyse the data. Origin 8.5 version software was used for constructing SPR graphs.

3.4.2. Fourier Transform Infrared Spectroscopy (FTIR) Analysis using (Shimadzu IRSpirit)

The Fourier Transform Infrared Spectroscopy (FTIR) Analysis Of the synthesised silver nanoparticles from *Trema orientalis* was done using Shimadzu IRSpirit. The humidity of the lab was maintain using a POWER PYE dehumidifier. The 100mg of potassium bromide (KBr) pellets were oven-dried at 60°C in the hot air oven for 30 minutes and powdered (Sahayaraj *et al.*, 2012). 1 mg of synthesised silver nanoparticles from each sample were mixed with 100 mg of purified FTIR grade powdered KBr respectively and allowed to dry at 60°C in the hot air oven for 30 minutes and then it was analysed (Sahayaraj *et al.*, 2012). The powder analysis spectrum was done using the software 'LabSolutions' in the range between 400 to 4000 cm^{-1} .

3.4.3. Field Emission Scanning Electron microscopy (FE-SEM) and EDS

The nanoparticles were mounted on the copper stubs, and the images were studied using a scanning electron microscope (SEM) EDS, Quanta FEG 250, with secondary electron detectors at an operating voltage of 30 kV. Specific areas were located from SEM images and the elemental composition was recorded using EDS.

3.4.4. X-Ray diffraction (XRD) analysis

The X-Ray Diffraction (XRD) measurement of synthesised nanoparticles was carried out on a Bruker D8 Advance powder diffractometer. The pattern was recorded by CuK α radiation with k of 1.5406\AA and nickel monochromator filtering the wave at a tube voltage of 40kV and tube current of 30mA the presence crystalline nature, phase variety. The average crystalline size D of the silver nanoparticles have been estimated from the diffractogram by using Debye-Scherrer formula, $D = 0.9\lambda / \beta \cos \theta$, where λ is the wavelength of the X-rays used for diffraction and β is full width at half maximum (FWHM) of a peak. To estimate FWHM, each of the four peaks was fitted with a Gaussian function. The FWHM of the fitted gaussian curve is taken as FWHM of the peak. This could be done in the software origin (Mehta 2017).

3.4.5. DLS (dynamic light scattering) and ZETA Potential analysis

The Dynamic light scattering (DLS) and Zeta potential was determined using with NanoPLUS AT instrument model. The dynamic light scattering (DLS) measures distribution and polydispersity of nanoparticles of dispersed phase. The zeta potential value indicated the nanoparticles degree of electrostatic repulsion between adjacent, similarly charged particles in dispersion. It is useful in understanding state of surface and long-term stability of colloidal dispersion.

3.5. Evaluation of the bio-fabricated silver nanoparticles for biological activities such as antioxidant, antidiabetic, and anti-inflammatory activities.

Preparation of Silver nanoparticles for evaluation for biological activities: The synthesised nanoparticles were added in 10 ml of double distilled water and sonicated in a sonicator at room temperature for 30 minutes.

3.5.1. Antioxidant assay

The antioxidant studies in the selected plant were carried out using the 1,1-diphenyl-2-picrylhydrazyl (DPPH) method (Blois 1958; Madhu *et al.*, 2020).

- A) Preparation of DPPH:** stock solution was prepared by dissolving 24mg of DPPH to 100ml of ethanol in the dark and stored in amber coloured bottle. The working solution was prepared by adding 10ml of the stock solution to 45ml of ethanol.
- B) Preparation of L-Ascorbic acid solution:** 10mg of ascorbic acid was dissolved in 10ml of distilled water. Serial dilution was performed to prepare solutions with different concentrations (12.5µg/ml-200µg/ml). It was used as a standard.
- C) Preparation of test solution:** 10mg of aqueous extract of leaf and bark was dissolved in 10 ml of water and serial dilution was performed to prepare solutions with different concentrations (12.5µg/ml-200µg/ml), similarly sonicated silver nanoparticles serial dilution was performed to prepare solutions with different concentrations (12.5µg/ml-200µg/ml).
- D) Preparation of control:** 3ml DPPH was used as negative control. In the reaction mixture, 3ml of DPPH working solution was added to 250µl of plant extract/silver nanoparticles of different concentration and incubated in the dark for 30 minutes at room temperature. The absorbance was measured at 517nm. The following equation calculated the percent inhibition:

$$\text{Inhibition \%} = (A_0 - A_1) / A_0 * 100$$

Here A_0 is the absorbance of the control and A_1 is the absorbance of the extract.

The antioxidant assay was performed in triplicate, and the mean value was expressed. IC_{50} values were calculated by plotting percentage (%) inhibition against the concentration (µg/ml) of the extract.

3.5.2. Antidiabetic assay

Alpha amylase inhibitory assay: Starch iodine colour assay (Xiao *et al.*, 2006)

Screening of plant extract and silver nanoparticles for alpha amylase inhibitors was carried out based on starch iodine test according to xiao (2006) with slight modification. Test samples (500 μL) of varied concentrations (20 μL , 40 μL , 60 μL , 80 μL , 100 μL) were added to 500 μL of 0.02 M sodium phosphate buffer (pH 6.9 containing 6mM sodium chloride) containing 0.04 units of the α -amylase solution and were incubated at 37°C for 10 min.

Then 500 μL soluble starch (1%, w/v) was added to each reaction well and incubated at 37 °C for 15 min. 1 M HCl (20 μL) was added to stop the enzymatic reaction, followed by the addition of 100 μL of iodine reagent (5 mM I_2 and 5 mM KI). The colour change was noted and absorbance was read at 620nm. The known PPA inhibitor acarbose was used as positive control at concentration series (20, 40, 60, 80 and 100 μl). Without any extract, the control reaction represented 100% enzymatic activity. Starch was recognised by the dark blue colour when it was present and by the brown colour when it was absent. When the extract contains inhibitors, the starch added to the enzyme assay combination is not broken down and produces a dark blue colour complex; in contrast, when the extract is not present, no colour complex is produced, indicating that the starch has been fully hydrolysed by alpha amylase.

3.5.3. Anti-inflammatory assay: Protein denaturation method using egg albumin.

Preparation of the standard concentrations and screening of the egg albumin denaturation method (Samaweera *et al.*, 2023).

Standard concentration series were prepared, and they are 20, 40, 60. 80, 100 $\mu\text{g}/\text{mL}$. Diclofenac sodium was used as a positive control, and all the plant nanoparticles and silver nanoparticles concentration series were made similarly. Phosphate buffer saline (PBS, pH 6.4) was made using 28.80 g of the disodium salt of hydrogen phosphate and 11.45 g of

dipotassium salt of hydrogen phosphate dissolved in 1000 mL of distilled water. For the preparation of determined test samples 2.8 ml of PBS, 0.2 ml egg albumin, and 0.2 ml plant extract/sonicated silver nanoparticles was added. For the reference, drug diclofenac sodium test samples were prepared using 2.8 ml of PBS, 0.2 ml egg albumin, and 0.2 ml diclofenac sodium. A control sample was prepared using 2.8 ml of PBS, 2 ml of distilled water, and 0.2 ml of egg albumin. All prepared samples were incubated at 37°C in the water bath for 15-20 minutes using the laboratory water bath, followed by heating at 70°C, for five minutes. Allowed the samples to cool for 10 minutes at room temperature. Absorbances were taken at 660 nm against a blank, using the Double beam UV- Visible spectrophotometer.

% inhibition of egg albumin denaturation was measured using the bellow equation.

% inhibition of egg albumin denaturation = (Absorbance of the control – Absorbance of the Standard)/ (Absorbance of the control) ×100

(The whole test procedure was done in triplicates for all above assays.)

CHAPTER 4: RESULTS AND DISCUSSION

4.RESULTS AND DISCUSSION

4.1. Collection of plant material (*Trema orientalis*) from Goa University campus

The healthy leaf and bark of *Trema orientalis* was collected from Goa university campus from the month of August 2023 to November 2023 (**Plate 4.1**). The GPS coordinates were recorded using the google earth application with Lat:15.460569° and Long:73.834289°. The plant materials were washed with running tap water and rinsed with double distilled water. The plant materials were shade-dried at room temperature and grounded into powder (**Plate 4.2**). The water extract was prepared using the hot maceration method. Due to its high polarity index, water as a solvent for extracting secondary metabolites has played an important role even in the traditional healthcare systems. Hot maceration method makes sure all the bioactive compounds are dissolved in the solvent (water in this case). Percentage yield determines how much of the plant constituent is been dissolved in the water. Percentage yield calculated was found to be 6% for leaf extract and 5.8 % for bark extract. It was observed that there is no significant difference in both the extract percentage (%) yield obtained using the hot maceration technique.

4.2. Qualitative and quantitative phytochemical analysis of leaf and bark extract

The phytochemicals found in plant extract that are responsible for reducing silver nitrate and synthesising silver nanoparticles were estimated qualitatively and quantitatively. The qualitative phytochemical examination of the leaf and bark extracts (**Table 4.1**) revealed the presence of alkaloids, carbohydrates, glycosides, saponins, phytosterols, phenols, gums, and mucilage (**Plate 4.3, Plate 4.4**).

Adjileye (2019), have reported the presence of similar phytochemicals in the leaf ethanolic extract which were flavonoids, tannins and saponins. The ethanolic extract was extracted by maceration method.



Plate 4.1. *Trema orientalis* a) Habit, b) Twig, c) leaf abaxial side and adaxial side, d) bark.

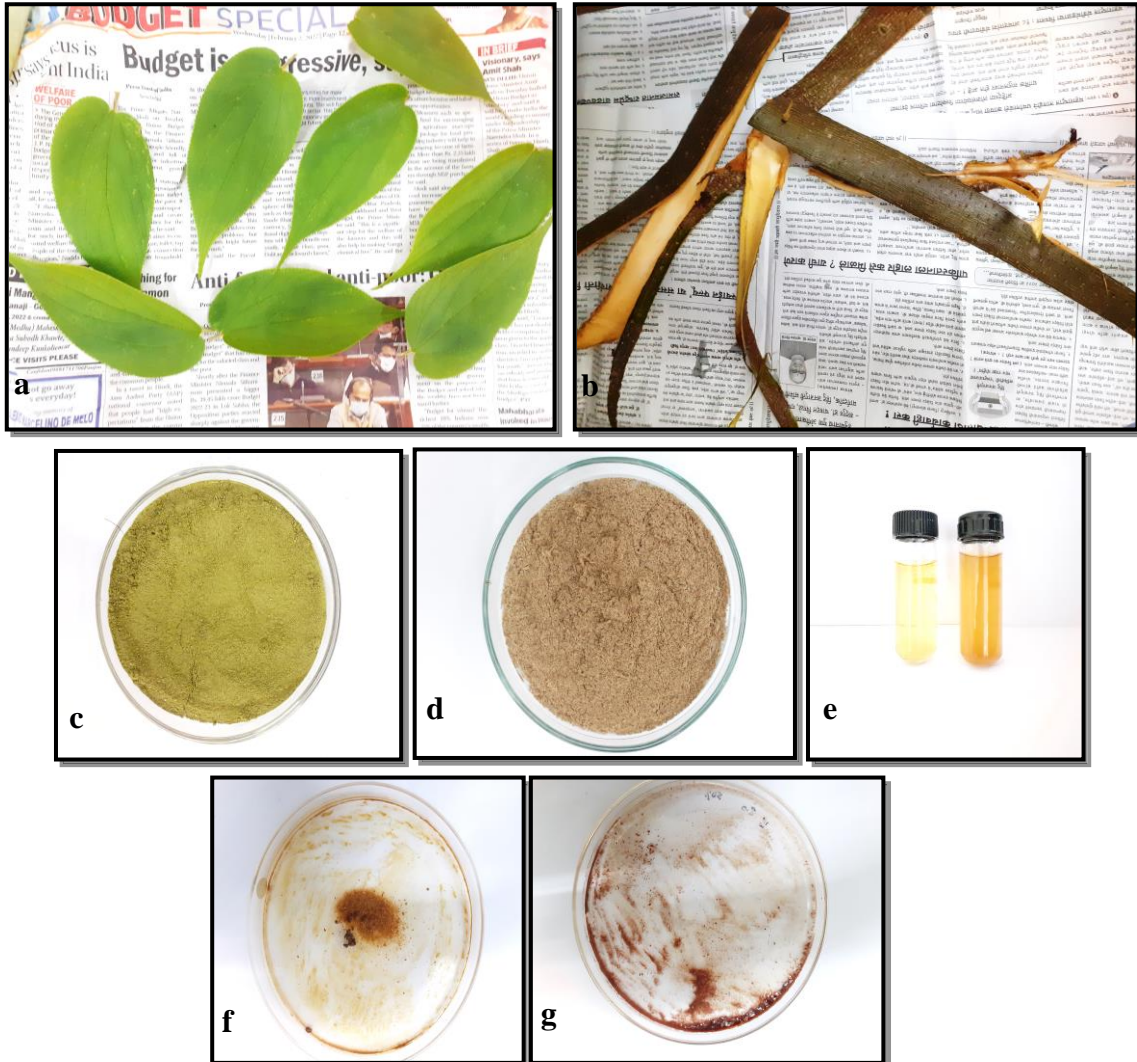


Plate 4.2. *Trema orientalis* a) leaf and b) bark kept for drying c) leaf powder d) bark powder e) leaf and bark extract respectively f) leaf extract after hot maceration g) bark extract after maceration.

In the study reported by Trono (2016), the bark water extract was prepared by maceration method., the presence of phenol, tannins, saponin flavonoids, alkaloids have been revealed which is like the results revealed by us. Saleh (2020), has reported the presence of saponins, tannins, alkaloids, flavonoids, and phenolic compounds in leaf water and ethanolic extract which was extracted maceration method, except the alkaloids which was absent in water extract. As per our results the alkaloids have been found present in water extract of both leaf and bark.

A significant quantity of these secondary metabolites (**Table 4.2, Table 4.3, Table 4.4, Table 4.5**) were found by quantitatively estimating total phenols (**Plate 4.5**), total tannins (**Plate 4.6**), total flavonoids (**Plate 4.7**) and total alkaloids (**Plate 4.8**). For the leaf water extract, the amounts of the total phenol content were 1.92 ± 0.005 mg GAE/g of dry extract, the total tannins content was 3.23 ± 0.11 mg TAE/g of dry extract, the total flavonoid content was 13 ± 0.01 mg QE/g of dry extract, and the total alkaloid content was 5.8 ± 0.002 mg BiNO₃ E/g of dry extract. In the bark water extract, the total phenol content was 4.132 ± 0.007 mg GAE/g of dry extract, the total tannin content was 133 ± 0.18 mg TAE/g of dry extract, the total flavonoid content was 35.3 ± 0.01 mg QE/g of dry extract, and the total alkaloid content was 8.35 ± 0.003 mg BiNO₃ E/g of dry extract.

It was earlier studied by Adjileye (2019), that the total polyphenolic content of leaf ethanolic extract was found to be 13.89 ± 1.01 mg EAG/100g. Saleh (2020) found that Total phenolic content in water extract was found to be 134.08 ± 0.56 mg GAE/g, total flavonoid contents were and 4.70 ± 0.23 mg QE/g, Also in ethanolic extract the total phenol content was found to be 260.96 ± 2.31 mg GAE/g and total flavonoid content to be 40.26 ± 0.47 mg QE/g. In comparison to the study reported by Saleh (2020), total phenolic and flavonoids content was found to be less in our results. In the study reported by Trono (2016), the amount of total phenolic content was found to be 94.12 mg GAE/g which is not like the observation made by

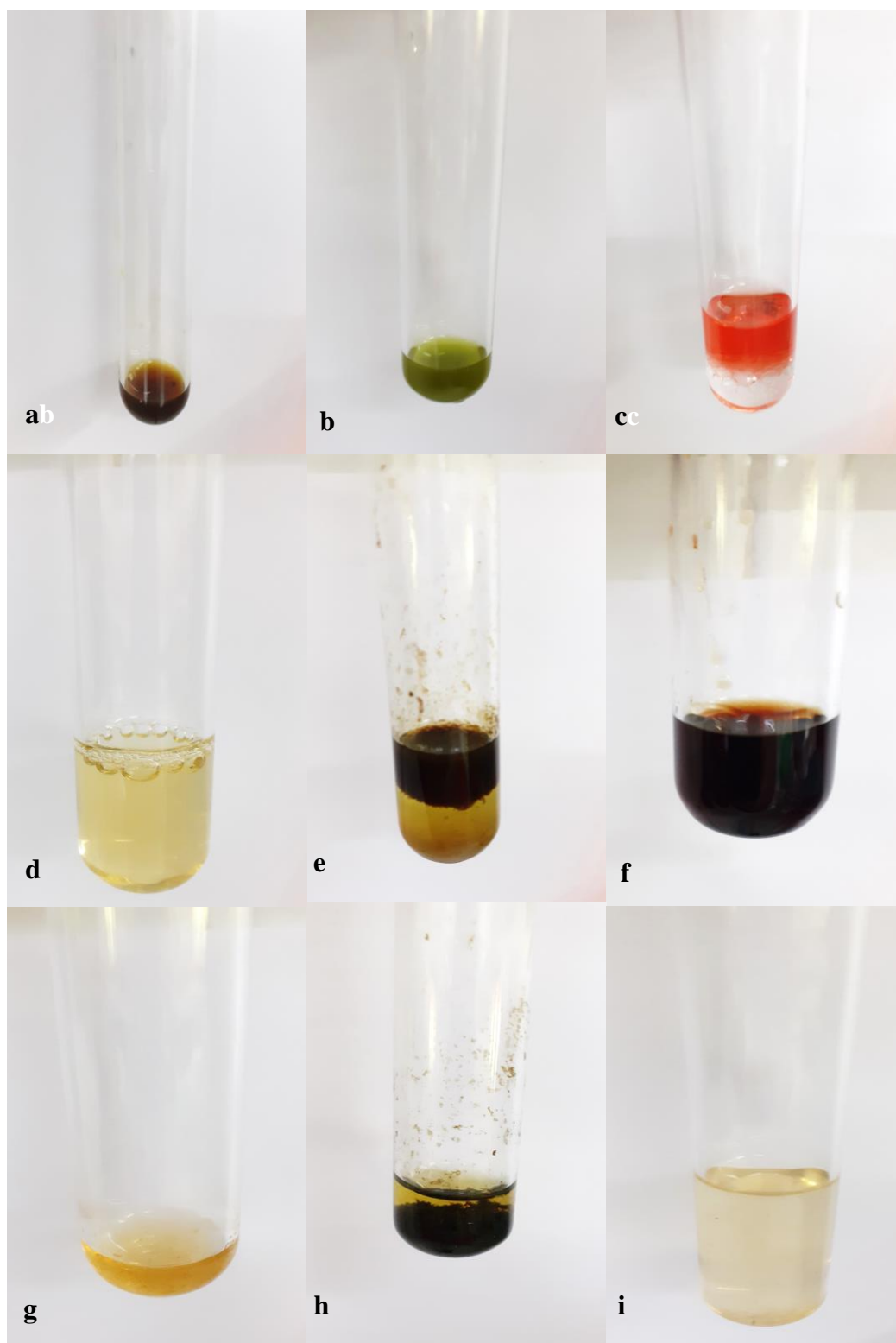


Plate 4.3. Qualitative Phytochemicals test screening of *Trema orientalis* leaf extract.

a: Test for Alkaloids; b: Test for Carbohydrates; c: Test for Glycosides; d: Test for saponins, e: test for Proteins; f test for Phytosterols, h: test for Phenols and Tannins, I: test for Gums and Mucilage.

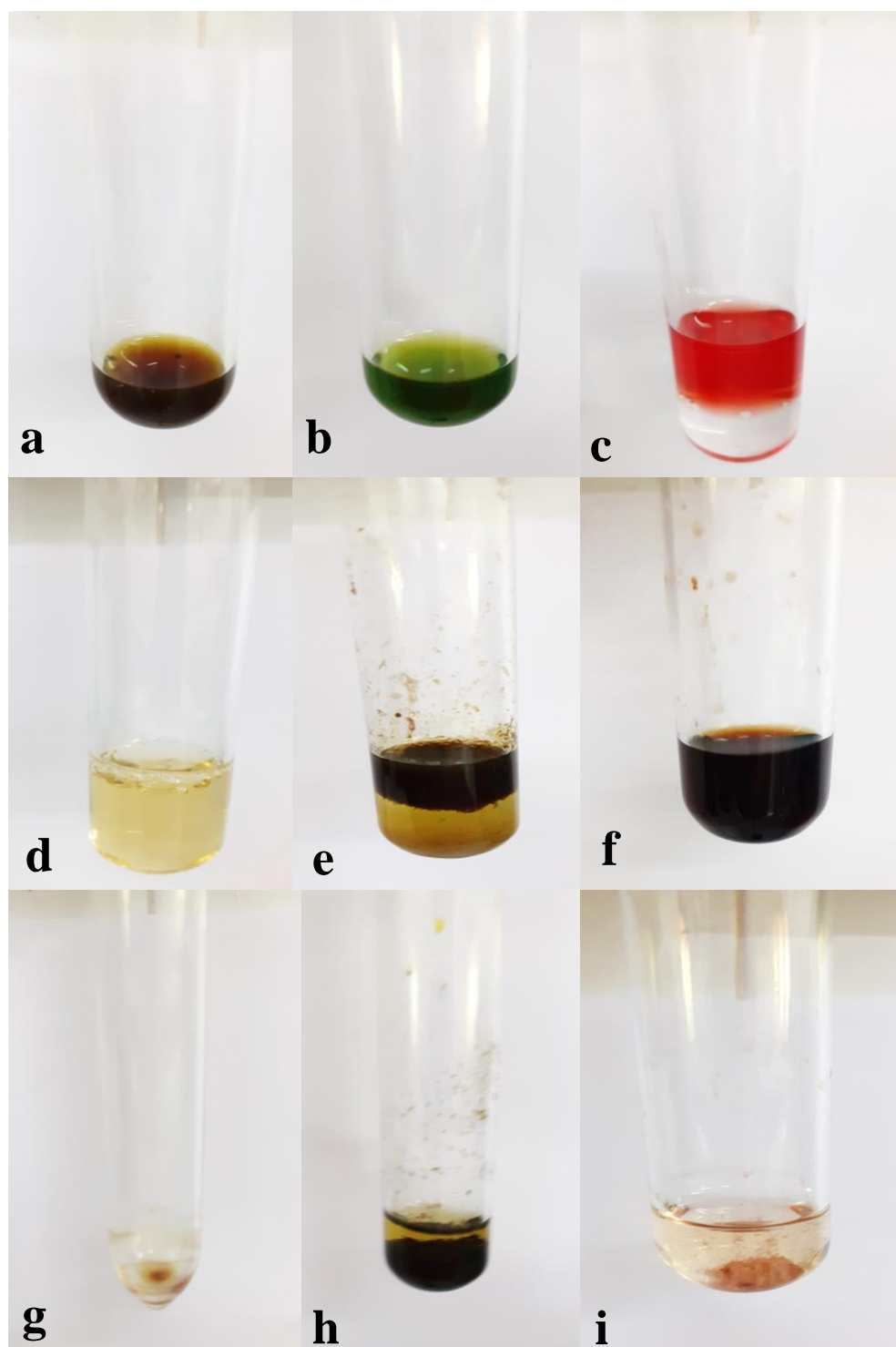


Plate 4.4. Qualitative Phytochemicals test screening of *Trema orientalis* bark extract.

a: Test for Alkaloids; b: Test for Carbohydrates; c: Test for Glycosides; d: Test for saponins; e: test for Proteins; f: test for Phytosterols; h: test for Phenols and Tannins; I: Test for Gums and Mucilage.

Table 4.1. Qualitative phytochemical test of *Trema orientalis* Leaf and Bark water extract.

Sr no.	Phytochemical test	Leaf Extract	Bark extract
1	Alkaloids (Wagner test)	+	+
2	Carbohydrates (Benedict's test)	+	+
3	Glycosides (Borntrager's test)	+	+
4	Saponins (Foam test)	+	+
5	Proteins (Biuret test)	-	-
6	Phytosterols (Liebermann Burchard's test)	+	+
7	Saponification	+	+
8	Phenols (Ferric chloride test)	++	++
9	Gums and mucilage	+	+

Note: + Positive test, - Negative test, ++ Intensively positive test

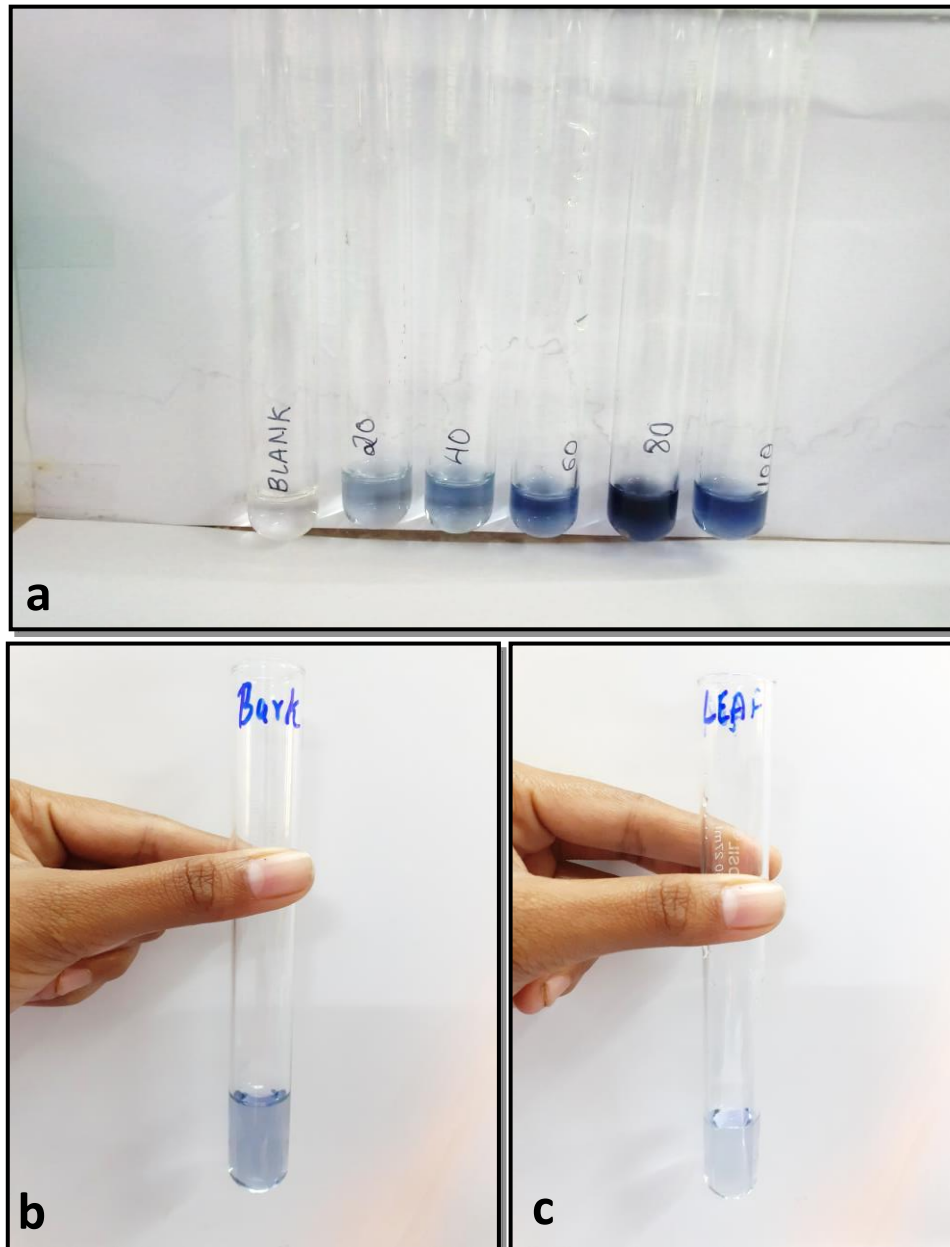


Plate 4.5. Quantitative estimation of phenols in *Trema orientalis* leaf and bark extract a) Standard series for calibration b) bark extract c) Leaf extract.

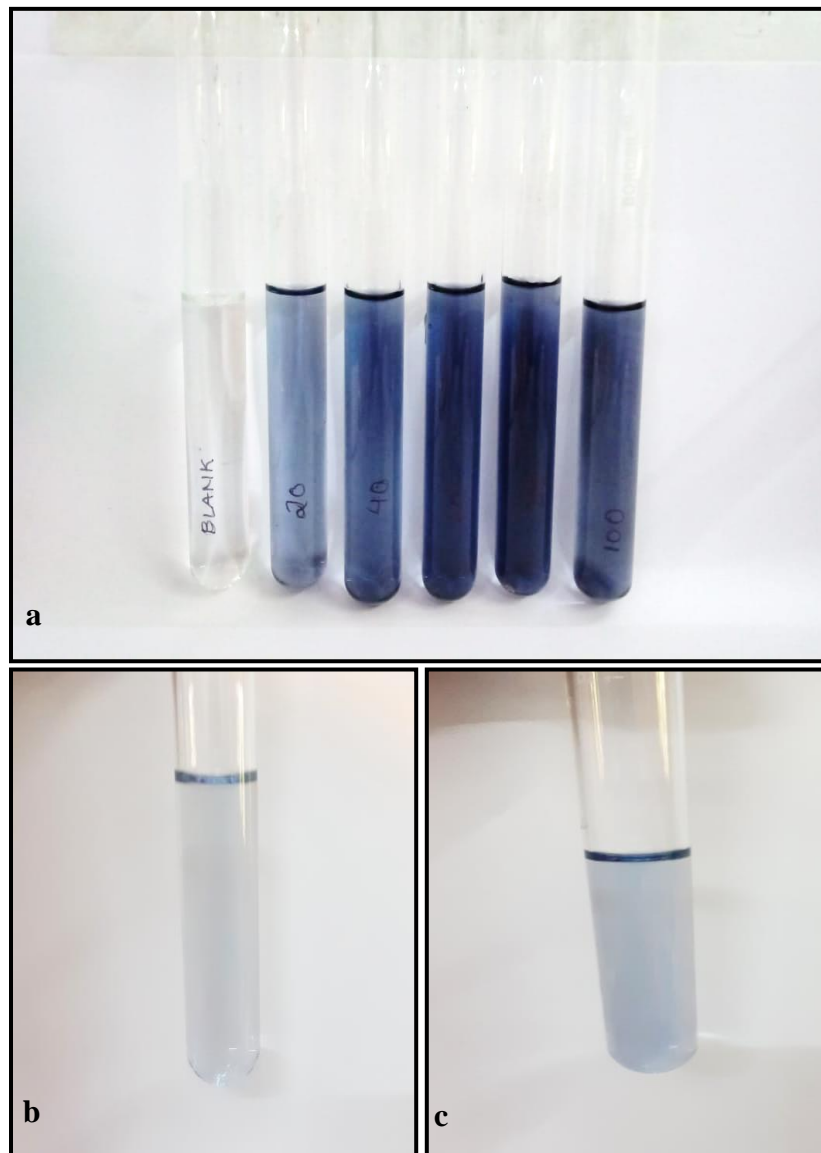


Plate 4.6. Quantitative estimation of tannins in *Trema orientalis* leaf and bark extract a) Standard series for calibration b) Leaf extract and c)Bark extract .

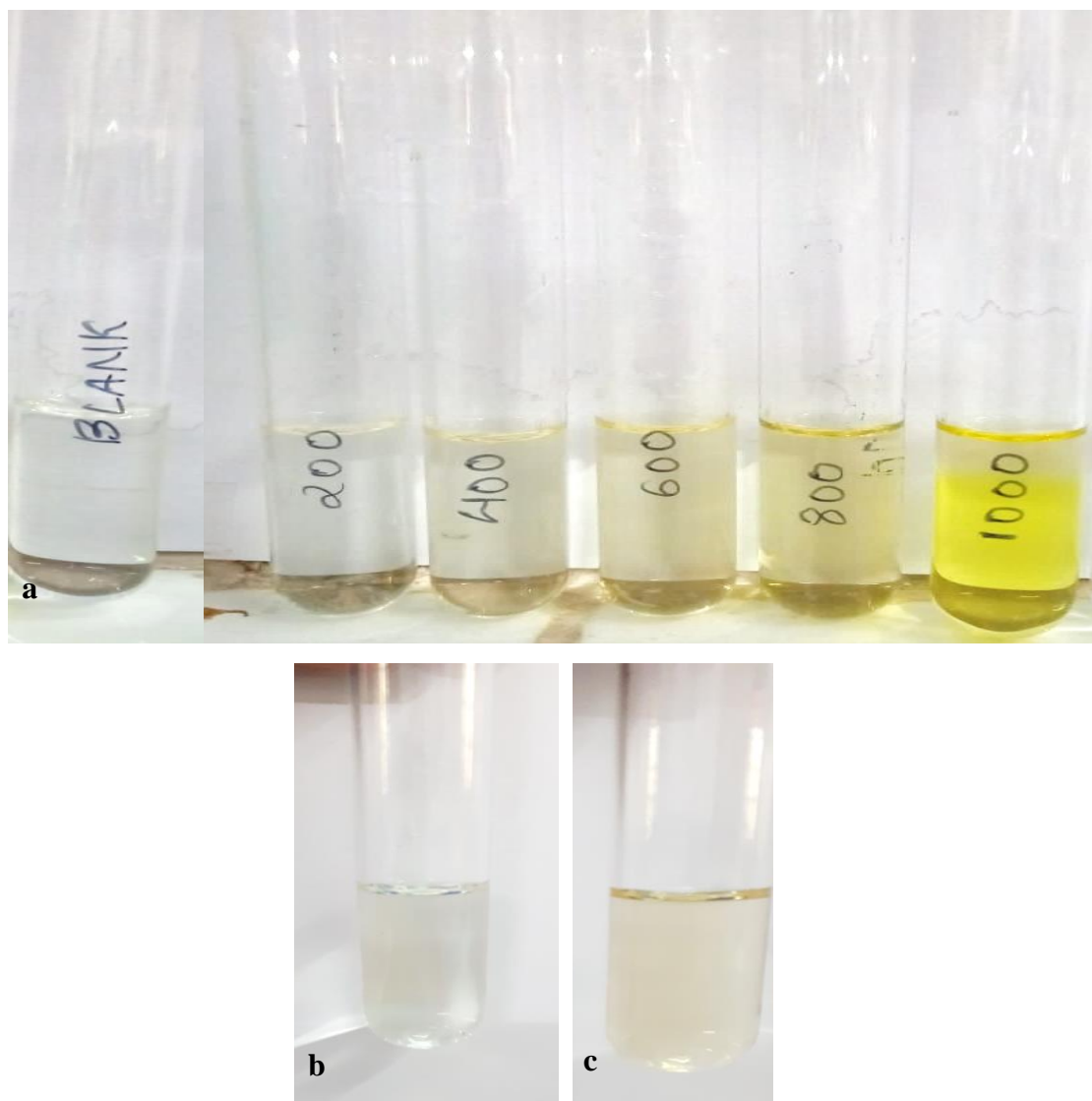


Plate 4.7. Quantitative estimation of flavonoids in *Trema orientalis* leaf and bark extract a) Standard series for calibration b) bark extract and c) Leaf extract.

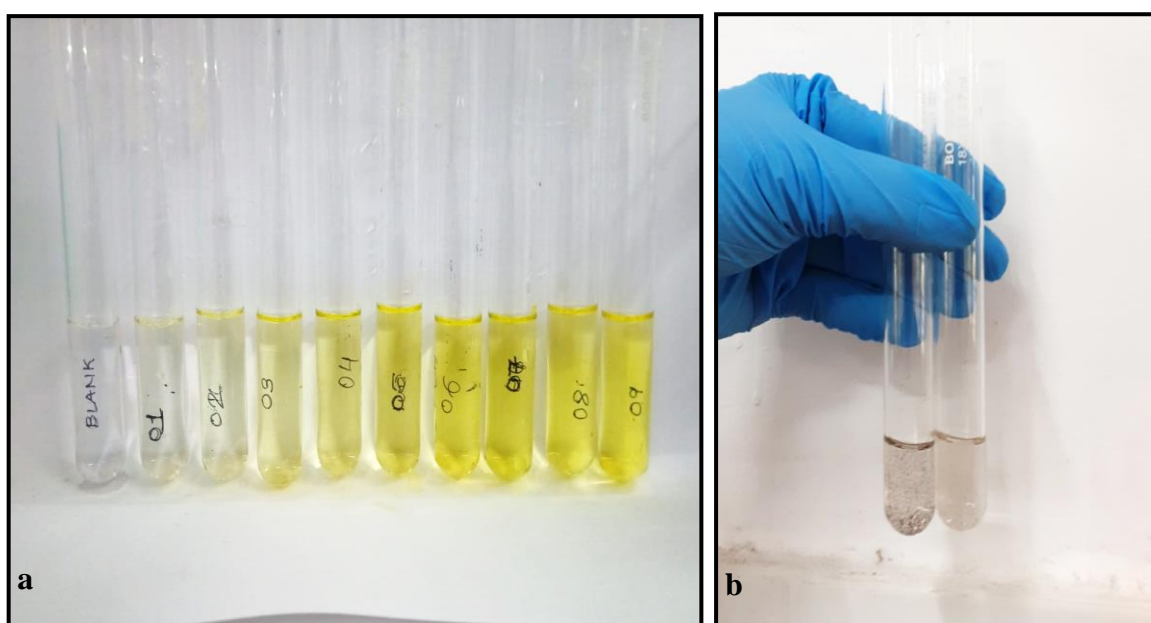


Plate 4.8. Quantitative estimation of alkaloids in *Trema orientalis* leaf and bark extract a) Standard series for calibration B) bark extract and Leaf extract respectively.

Table 4.2. Total Phenolic Content (TPC) in *Trema orientalis* leaf water extract and bark water extract.

Concentration ($\mu\text{g/ml}$)	Absorbance at 760nm			Mean absorbance
	R ₁	R ₂	R ₃	
0	0	0	0	0
20	0.139	0.134	0.134	0.135 \pm 0.002
40	0.301	0.104	0.303	0.236 \pm 0.11
60	0.147	0.393	0.352	0.297 \pm 0.131
80	0.312	0.318	0.395	0.341 \pm 0.046
100	0.277	0.745	0.386	0.469 \pm 0.244
Leaf extract	0.11	0.12	0.11	0.113 \pm 0.005
Bark extract	0.2	0.211	0.213	0.208 \pm 0.007

Note: \pm Standard deviation

Table 4.3. Total Tannin Content (TTC) in *Trema orientalis* leaf water extract and bark water extract.

Concentration ($\mu\text{g/ml}$)	Absorbance at 760nm			Mean Absorbance
	R ₁	R ₂	R ₃	
0	0	0	0	0
20	0.251	0.228	0.228	0.235 \pm 0.013
40	0.417	0.392	0.399	0.402 \pm 0.012
60	0.527	0.54	0.537	0.534 \pm 0.006
80	0.57	0.599	0.584	0.584 \pm 0.014
100	0.509	0.65	0.724	0.602 \pm 0.109
Leaf extract	0.113	0.114	0.112	0.113 \pm 0.001
Bark extract	0.188	0.187	0.187	0.187 \pm 0.000

Note: \pm Standard deviation

Table 4.4. Total Flavonoid Content (TFC) in *Trema orientalis* leaf water extract and bark water extract.

Concentration ($\mu\text{g/ml}$)	Absorbance at 760nm			Mean Absorbance
	R ₁	R ₂	R ₃	
Blank	0	0	0	0
20 μl	0.047	0.044	0.046	0.045 \pm 0.001
40 μl	0.068	0.067	0.065	0.066 \pm 0.001
60 μl	0.075	0.072	0.071	0.072 \pm 0.002
80 μl	0.121	0.121	0.122	0.121 \pm 0.000
100 μl	0.168	0.169	0.167	0.168 \pm 0.001
Leaf extract	0.021	0.021	0.023	0.021 \pm 0.001
Bark extract	0.057	0.055	0.055	0.055 \pm 0.002

Note: \pm Standard deviation

Table 4.5. Total Alkaloid Content (TAC) in *Trema orientalis* leaf water extract and bark water extract.

Concentration ($\mu\text{g/ml}$)	Absorbance at 760nm			Mean Absorbance
	R ₁	R ₂	R ₃	
Blank	0.002	0.002	0.002	0.000
1ml	0.027	0.025	0.027	0.026 \pm 0.001
2ml	0.051	0.055	0.051	0.052 \pm 0.002
3ml	0.076	0.065	0.076	0.072 \pm 0.006
4ml	0.118	0.11	0.115	0.114 \pm 0.004
5ml	0.121	0.126	0.125	0.124 \pm 0.002
6ml	0.144	0.139	0.145	0.142 \pm 0.003
7ml	0.138	0.149	0.15	0.145 \pm 0.006
8ml	0.178	0.168	0.178	0.174 \pm 0.005
9ml	0.192	0.188	0.183	0.187 \pm 0.004
Leaf extract	0.134	0.132	0.129	0.131 \pm 0.002
Bark extract	0.186	0.183	0.18	0.183.003

Note: \pm Standard deviation

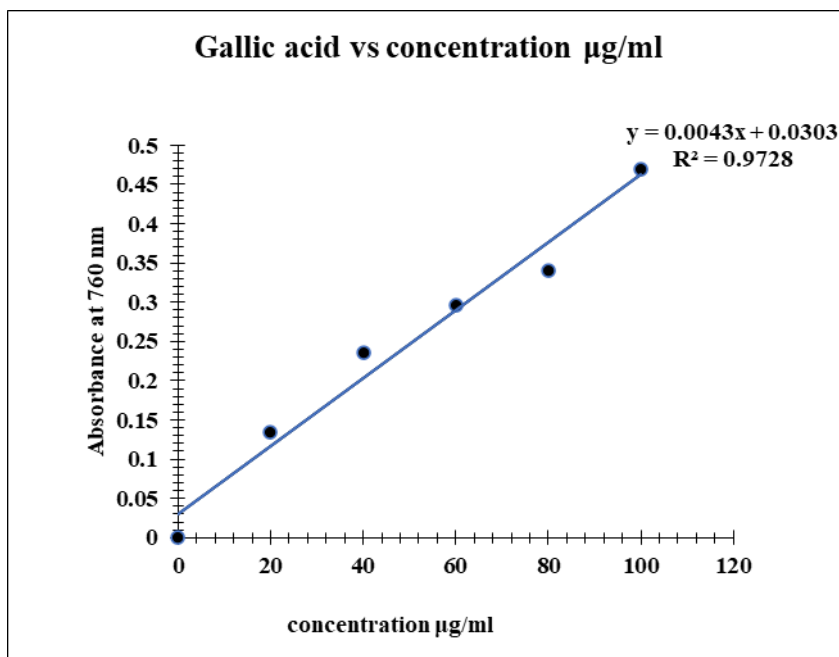


Figure 4.1. Calibration curve for Total Phenolic content

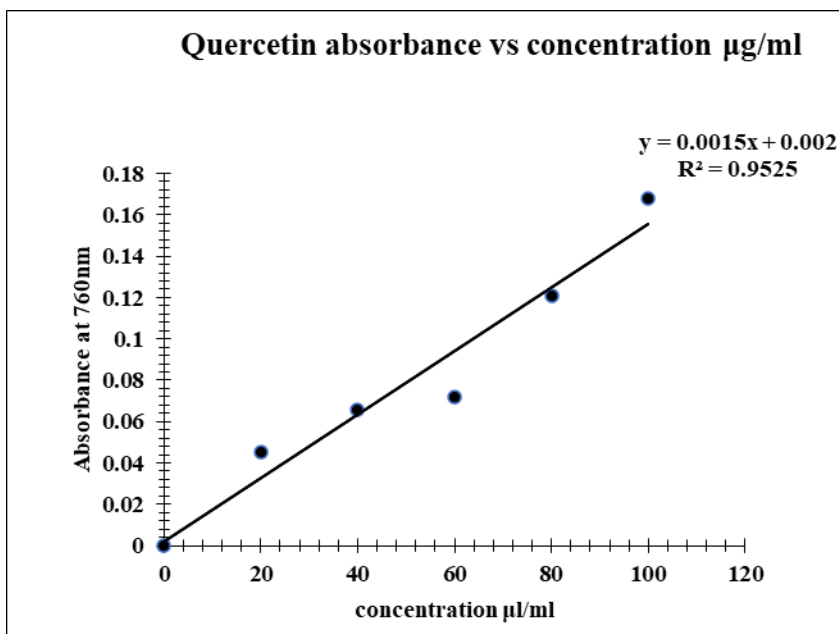


Figure 4.2. Calibration curve for Total Flavonoid content

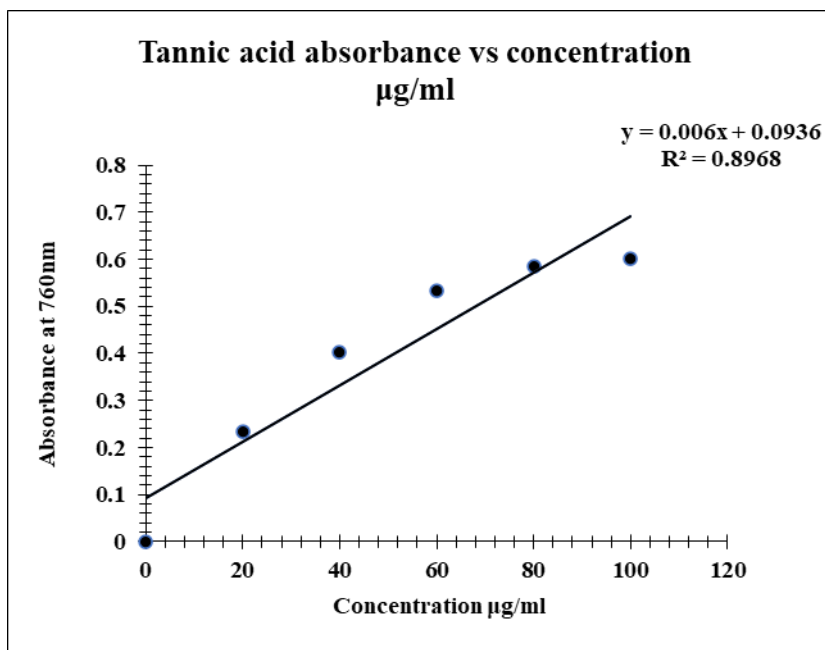


Figure 4.3. Calibration curve for Total Tannin content

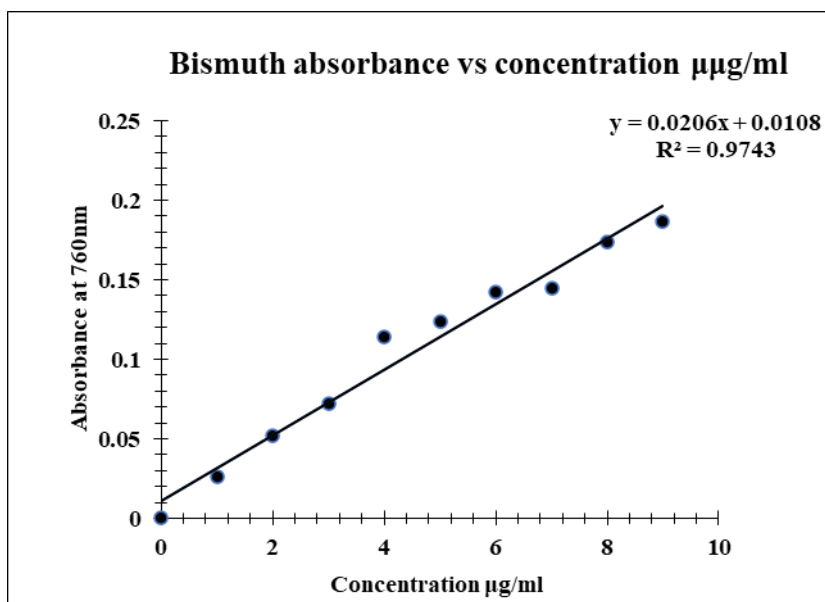


Figure 4.4. Calibration curve for Total Alkaloids content

Table 4.6. Total phenolic content (TPC), Total Flavonoids content (TFC), Total Tannins content (TTC) and Total Alkaloid content of (TAC) *Trema orientalis* Leaf extract and Bark extract.

Sr no.	Sample	TPC mg GAE/ g of dry extract	TFC mg QE/g of dry extract	TTC mg TAE/ g of dry extract	TAC mg BiNO ₃ /g of dry extract
1	Leaf extract	1.92±0.005	13±0.01	3.32±0.11	5.8 ±0.002
2	Bark extract	4.132±0.07	35.3±0.01	133±0.18	8.35±0.003

Note: GAE – Gallic acid equivalent, Q- Quercetin, TAE- Tannic acid equivalent, BiNO₃ – Bismuth nitrate

us. It is been observed that the bark contains good amount of total phenol, tannins, flavonoids, and alkaloids in comparison to leaf extract (**Table 4.6**). The graphical representation of calibration curves is seen in **Figure 4.1, Figure 4.2, Figure 4.3, and Figure 4.4**.

4.3. Bio-fabrication of silver nanoparticles from the aqueous extract of *Trema orientalis* using silver nitrate as precursor salt.

The green synthesis of silver nanoparticles was initiated using 5 mM silver nitrate salt. The initial synthesis of silver nanoparticle synthesis was confirmed by development of yellowish-brown colour with leaf extract (**Plate 4.10**) and brownish colour with bark extract (**Plate 4.11**) during incubation period of 4 hour which was due to excitation of the Surface Plasmon Resonance (SPR), typical of silver nanoparticles (Banerjee 2010). The isolated powdered silver nanoparticles (**Plate 4.12**) were further utilized for characterisation.

4.4. Characterisation of silver nanoparticles using UV-vis spectroscopy, FTIR, XRD, FESEM-EDS, and DLS and Zeta potential analysis

4.4.1. UV-vis spectroscopy

UV-Visible spectroscopy analysis depends on the generation of the colour in the reaction mixture due to the excitation of the Surface Plasmon Resonance (SPR) band, The typical absorbance peak values for silver nanoparticles are in range 420nm to 430nm (Mulvaney *et al.*, 1996). Larger silver nanoparticles have redshift (absorb at longer wavelength) with broad peaks, whereas smaller, spherical silver nanoparticles absorb at about 400 nm and have narrow peaks. It is also indicative of the stability of silver nanoparticles because, as the particles aggregate, the peaks begin to expand and reduce intensity as secondary peaks with higher wavelengths form (Dawadi *et al.*, 2021). Likewise, the dispersion of silver nanoparticles can be inferred from the peak broadening. Broad peaks

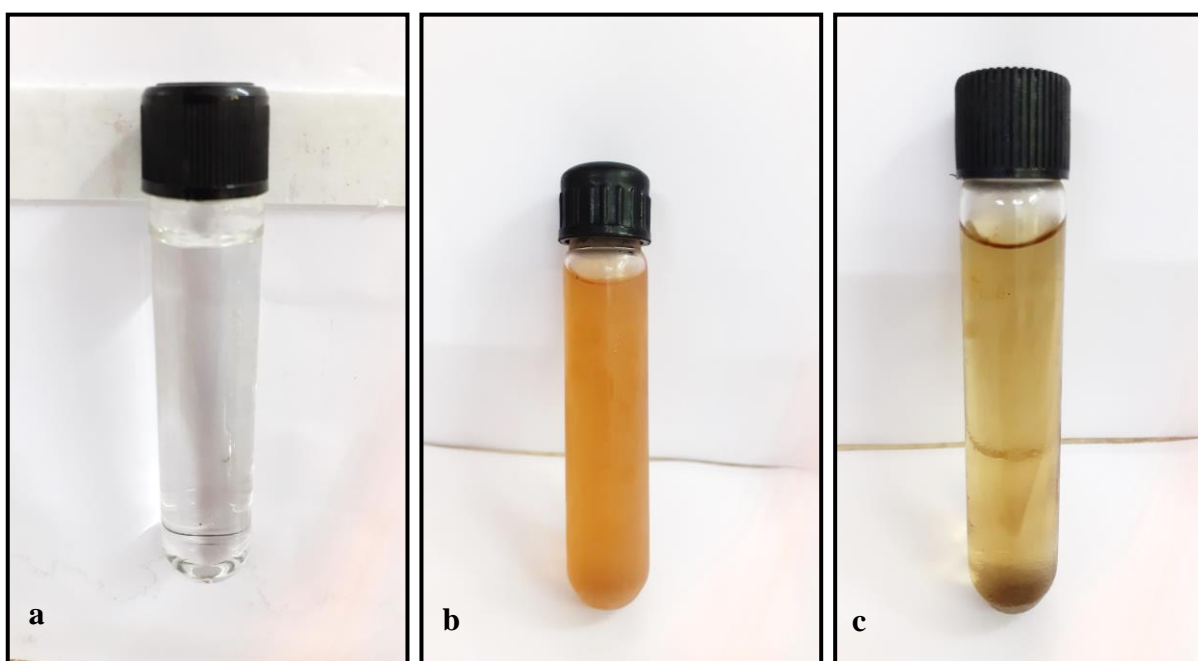


Plate 4.9. a) Silver nitrate solution b) *Trema orientalis* Leaf extract c) *Trema orientalis* Bark extract.

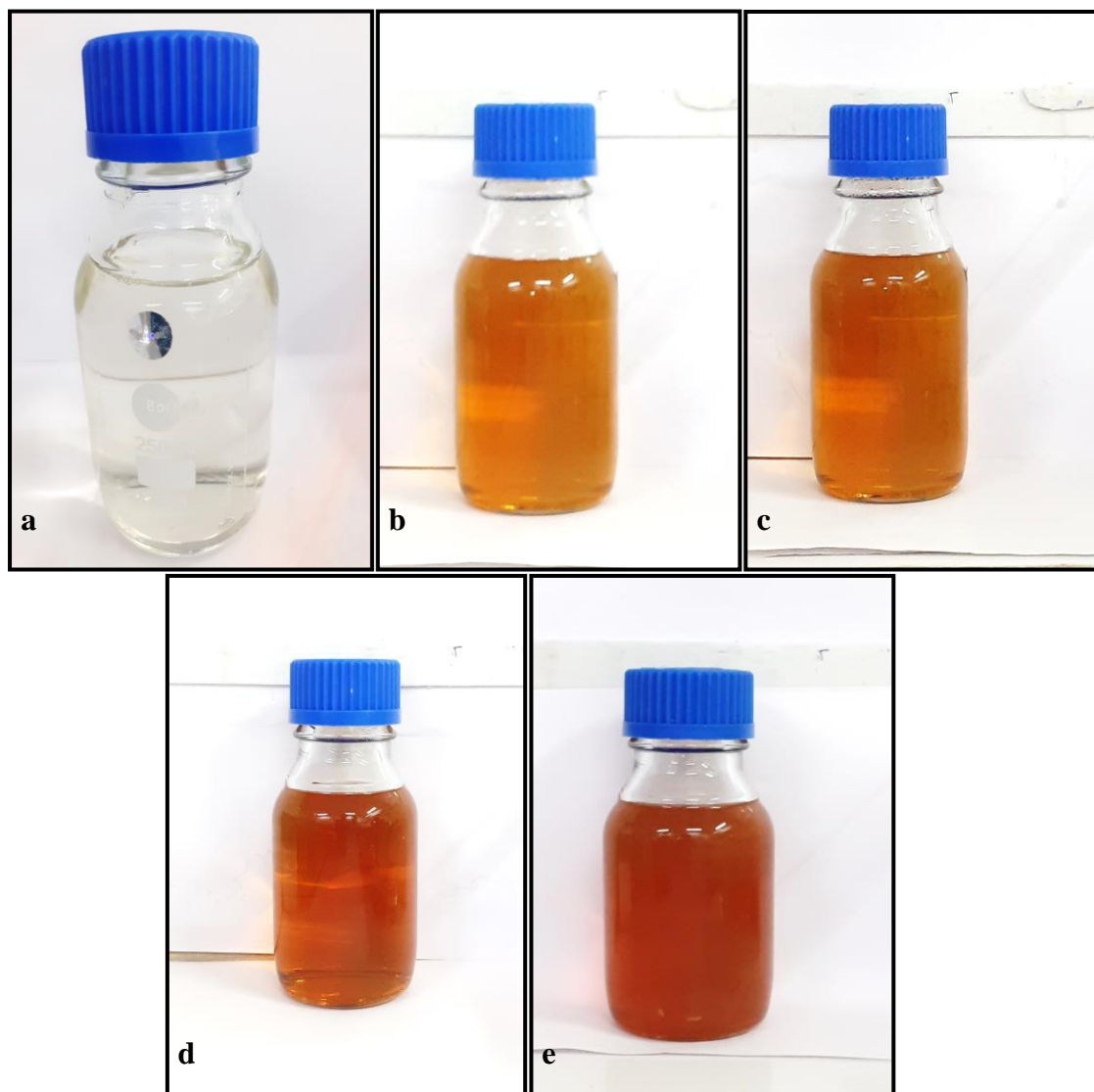


Plate 4.10. Represents the colour change during the silver nanoparticles synthesis from *Trema orientalis* leaf extract: a) Before incubation b) 1 hour incubation c) 2 hours of incubation d) 3 hours of incubation e) 4 hours of incubation.

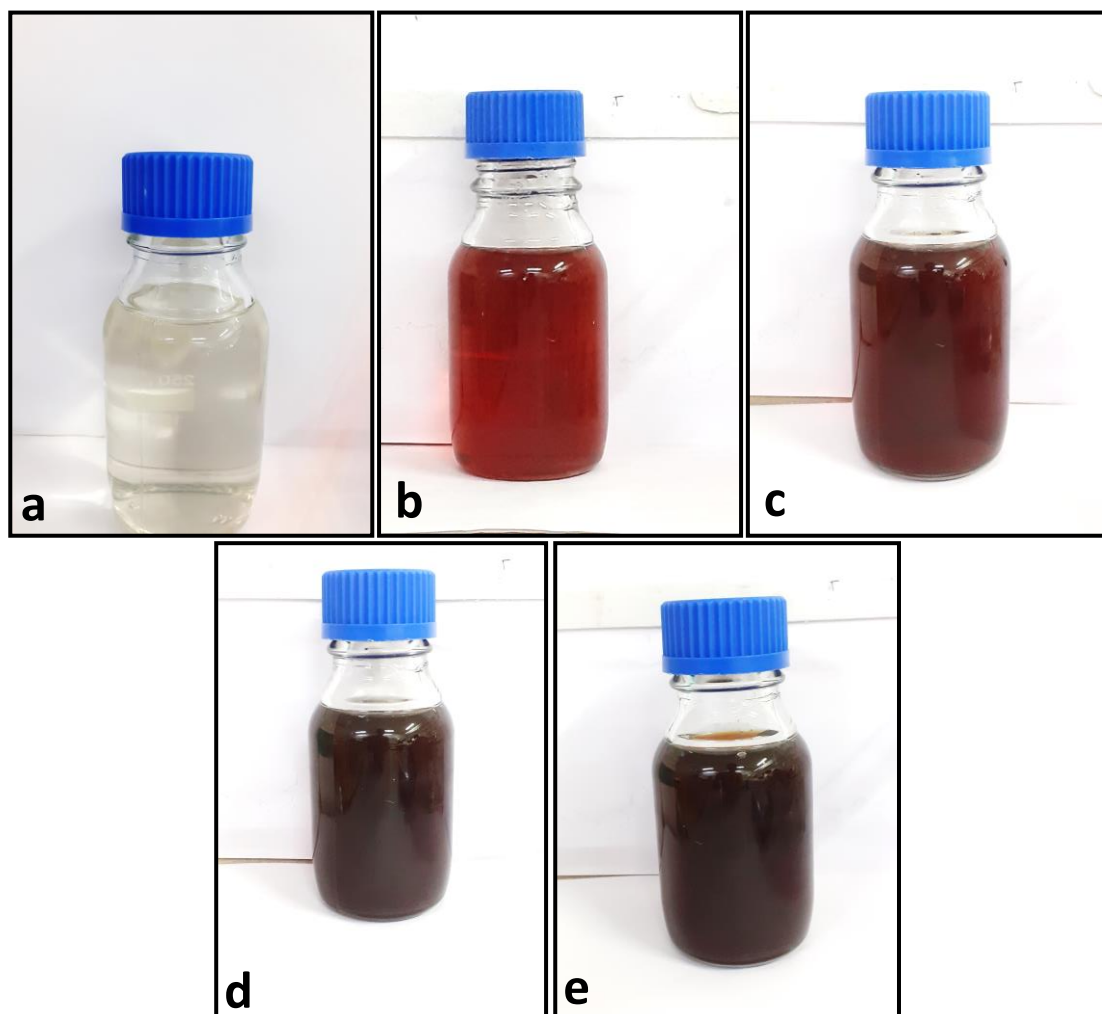


Plate 4.11. Represents the colour change during the silver nanoparticles synthesis from *Trema orientalis* bark extract: a) Before incubation b) 1 hour incubation c) 2 hours of incubation d) 3 hours of incubation e) 4 hours of incubation.

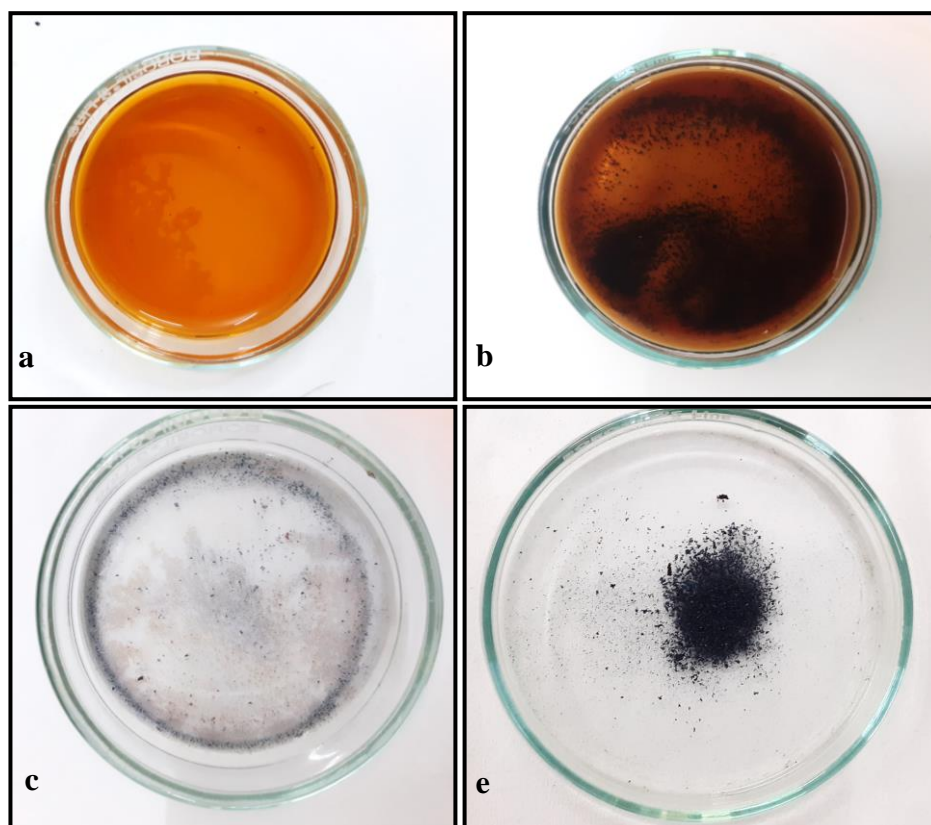


Plate 4.12. a) Synthesised silver nanoparticles from *Trema orientalis* leaf extract before drying b) Synthesised silver nanoparticles from *Trema orientalis* bark extract before drying c) Synthesised silver nanoparticles from *Trema orientalis* leaf extract after drying d) Synthesised silver nanoparticles from *Trema orientalis* bark extract after drying.

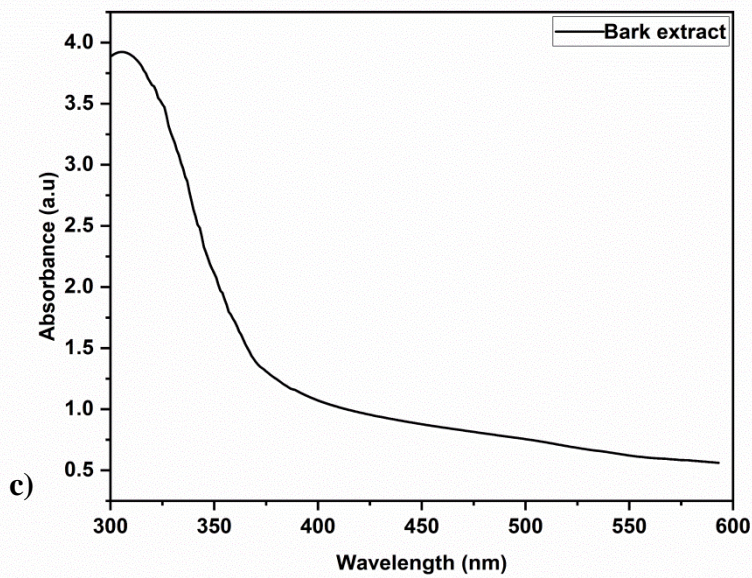
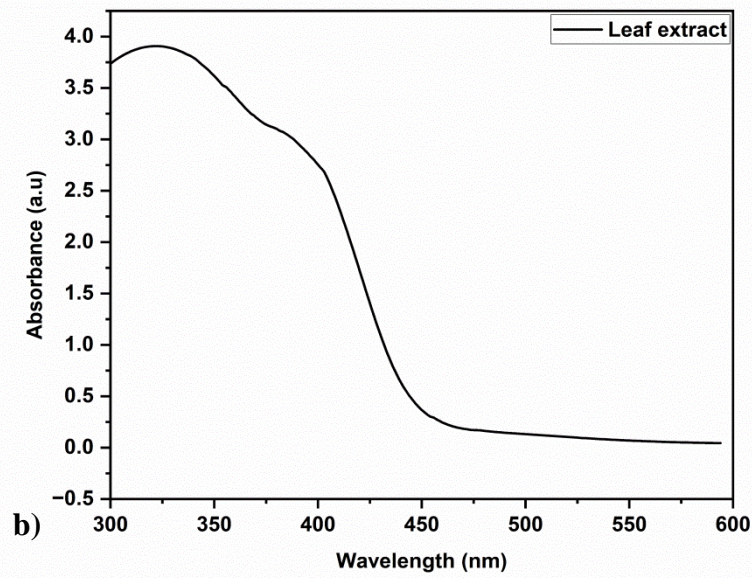
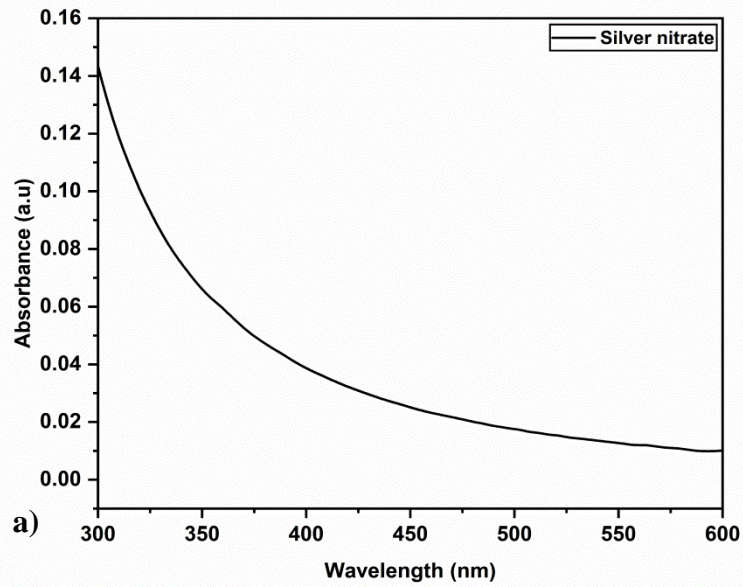


Figure 4.5. UV-visible absorption spectrum for a) Silver nitrate b) *Trema orientalis* leaf extract and c) *Trema orientalis* bark extract.

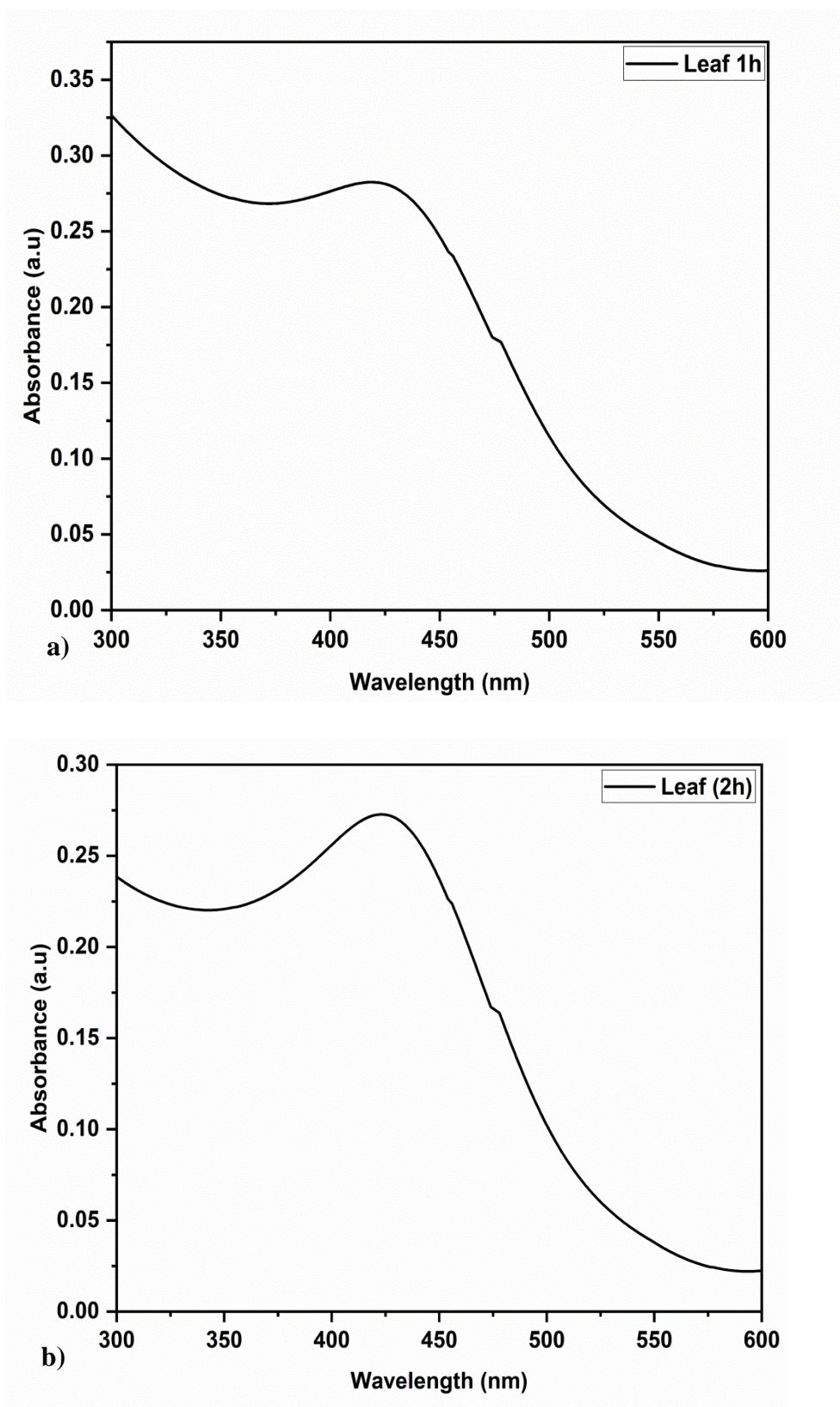


Figure 4.6. UV-Visible Spectrum for Silver nanoparticles synthesized from leaf extract of *Trema orientalis* a) 1 hour of incubation b) 2 hours of incubation.

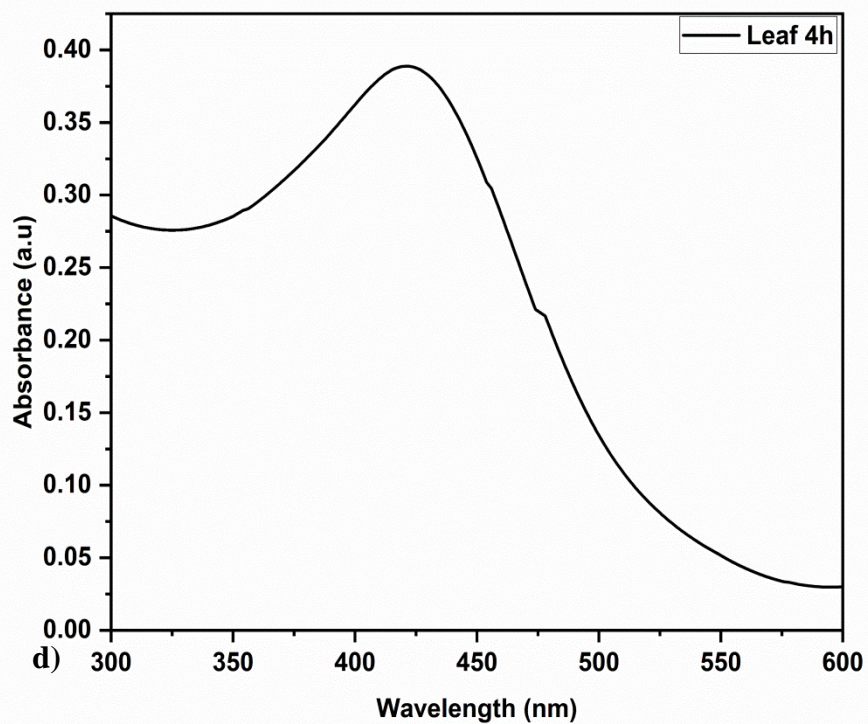
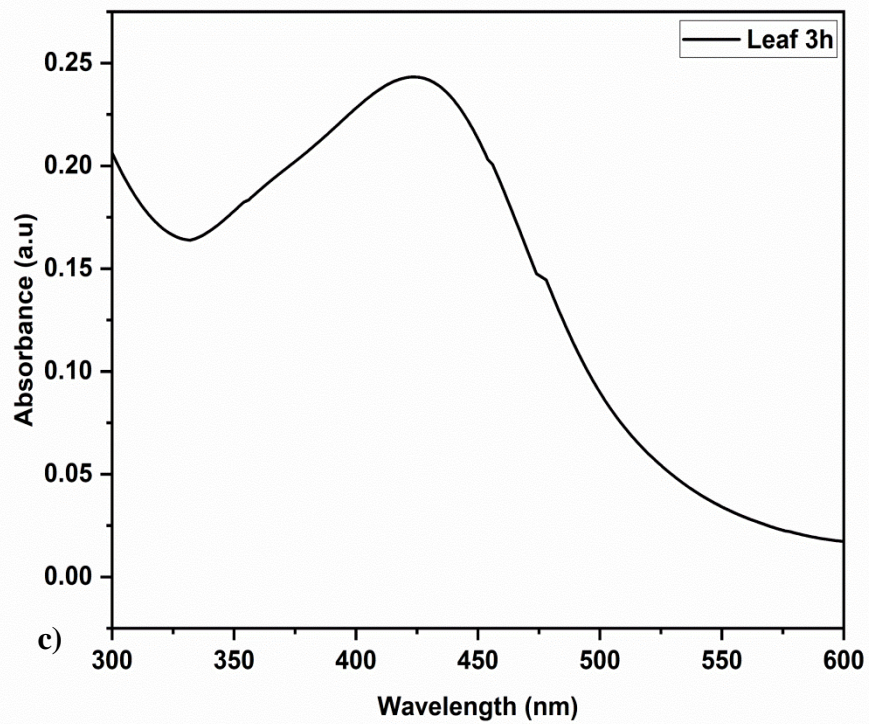


Figure 4.7. UV-visible spectrum for Silver nanoparticles synthesised from leaf extract of *Trema orientalis* c) 3 hours of incubation d) 4 hours of incubation.

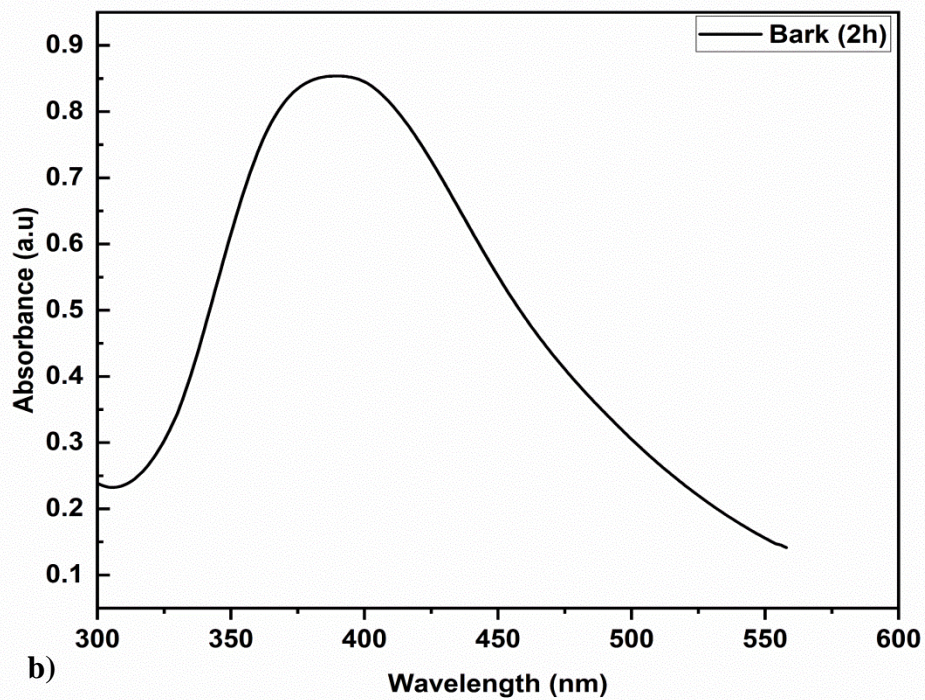
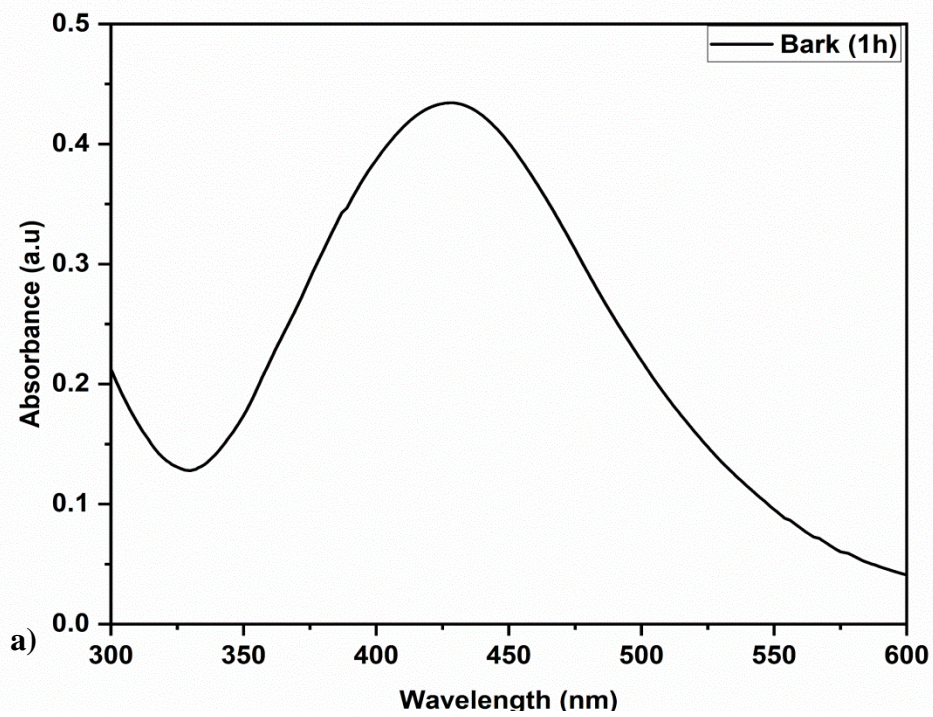


Figure 4.8. UV-visible Spectrum for Silver nanoparticles synthesized from Bark extract of *Trema orientalis* a) 1 hour of incubation b) 2 hours of incubation.

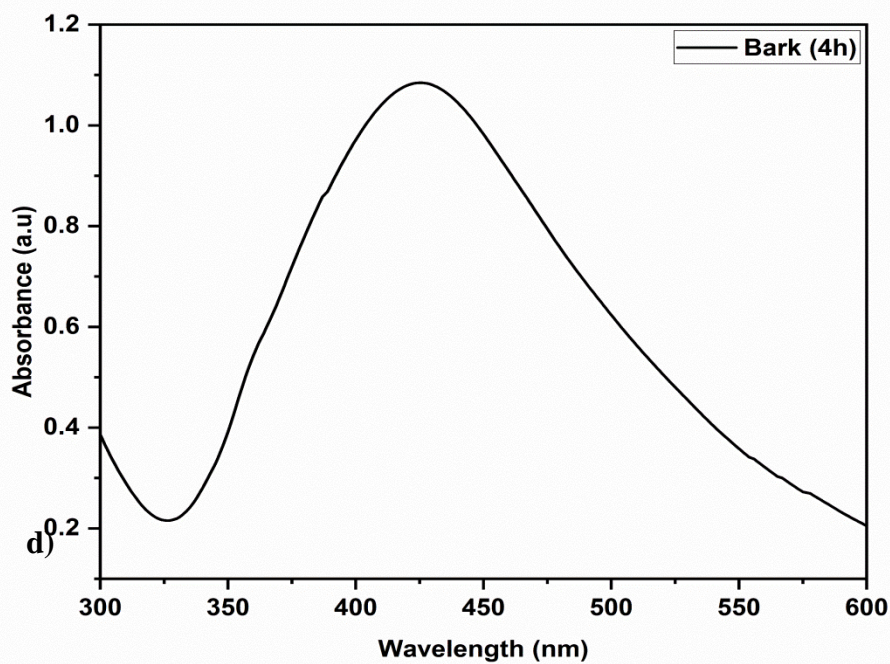
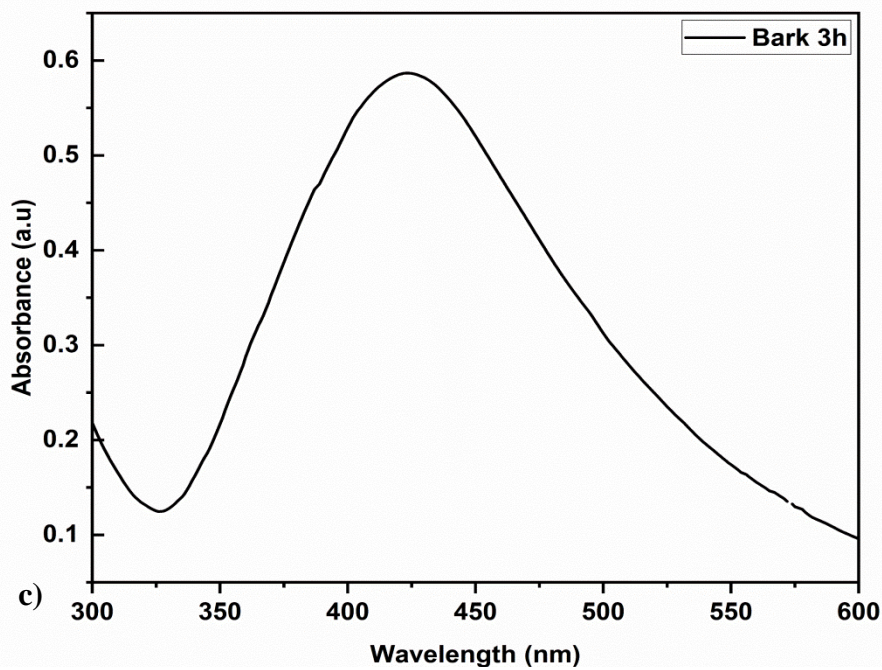


Figure 4.9. UV-visible spectrum for Silver nanoparticles synthesised from Bark extract of *Trema orientalis* c) 3 hours of incubation d) 4 hours of incubation.

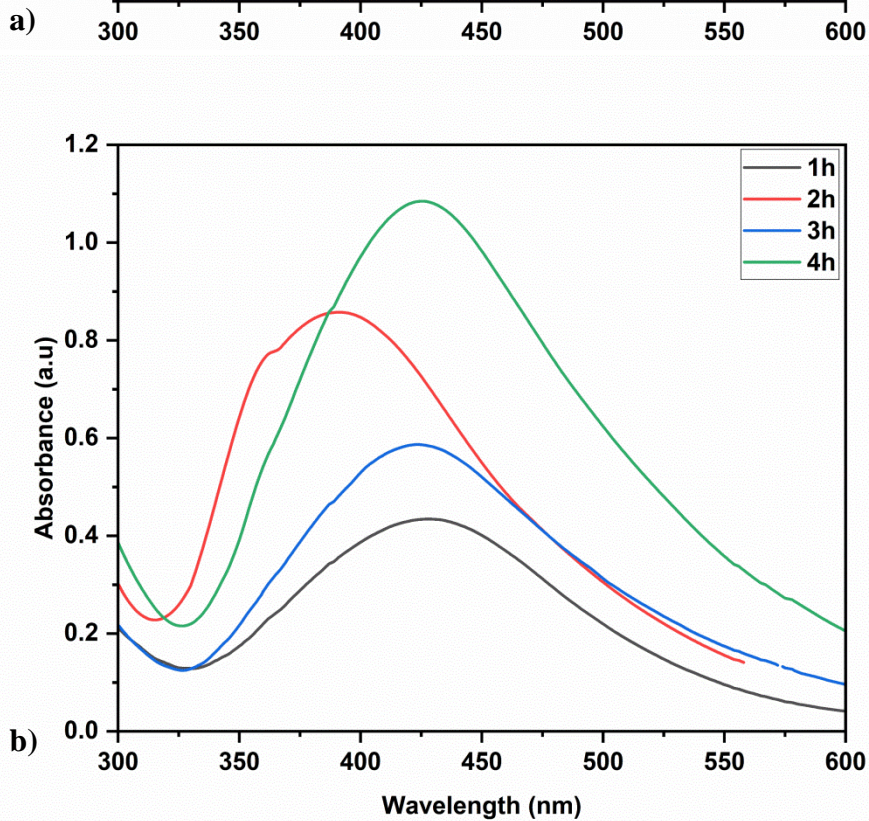
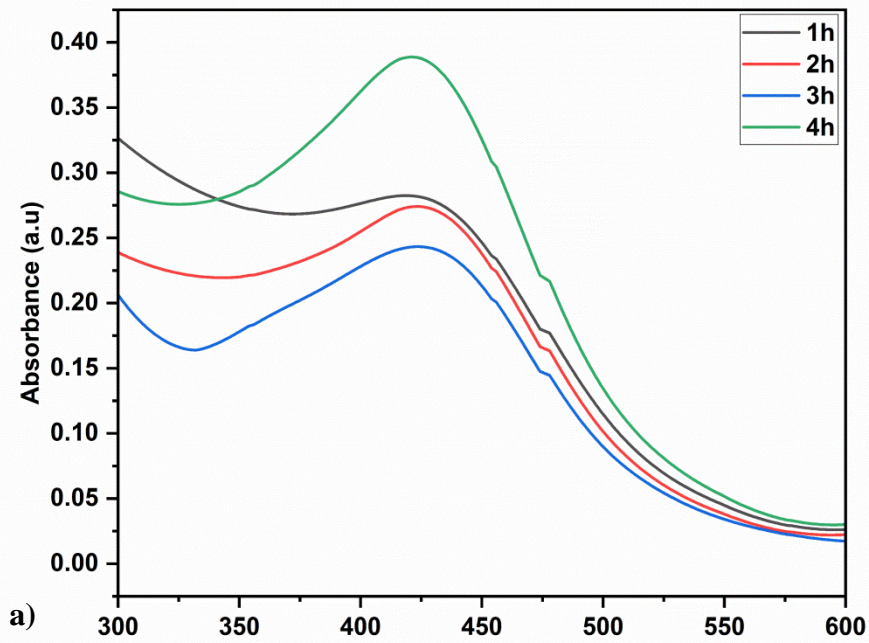


Figure 4.10. UV-visible spectrum for Silver nanoparticles at different hours of incubation (1 hour to 4 hours) a) From *Trema orientalis* Leaf extract and b) *Trema orientalis* Bark extract.

typically signify the development of a wide dispersity, or broader size range distribution, of silver nanoparticles in the solution. The size and shape of the solution are indicative of the colloidal silver nanoparticles' optical properties; hence, the solution's unique colour can be used to observe and monitor the synthesis reaction's development (Gupta *et al.*, 2017; Meva *et al.*, 2019).

For the current study the colour of the mixture was recorded at 1 hr, 2 hr, 3hr and 4 hr duration for both leaf and bark sample. The intensity of the peaks in both cases increased when the samples were treated at increasing time duration. After each hour the SPR was recorded using UV-Visible spectrophotometer at the range from 300nm to 600nm. There was no SPR peaks recorded for silver nitrate and both the extracts which indicates there is no silver nanoparticles present in the solution (**Figure 4.5**).

The SPR peak values for duration 1 hr, 2 hr, 3 hr, 4 hr duration of silver nanoparticles synthesis using leaf extract was found to be 422 nm, 425nm, 424nm and 425 nm respectively, indicating the synthesis of silver nanoparticles (**Figure 4.6** and **Figure 4.7**). The SPR peak values for duration 1 hr, 2 hr, 3 hr, 4 hr duration of silver nanoparticles synthesis using bark extract was found to be 427nm, 425nm, 423nm and 426 nm respectively, indicating the synthesis of silver nanoparticles (**Figure 4.8** and **Figure 4.9**). In a study conducted by Ahmed (2015) the silver nanoparticles were synthesised using *Azadirachta indica* leaf water extract yellowish to colloidal brown colour during incubation period indicated the silver nanoparticles synthesises which is like the study conducted by us.

4.4.2. Fourier Transform Infrared Spectroscopy (FTIR) Analysis

With the use of Fourier Transform Infrared Spectroscopy (FTIR), which combines infrared radiation with bonding in molecules to produce stretching and bending vibrations (in the 4000-400cm⁻¹ region), one can characterise the role of chemicals, metabolites involved in reducing and capping silver nanoparticles, and the presence of chemical residue on the

surface of silver nanoparticles (Mourdikoudis *et al.*, 2018). The FTIR analysis confirmed the dual role of the plant extract as a reducing and capping agent and presence of some functional group on silver nanoparticles. For leaf extract (**Table 4.7**) peak at 3566 cm^{-3} corresponds to -OH alcoholic group, 2354 corresponds to C=N bonding and 1508 corresponds to C=C aromatic strong bonding. For silver nanoparticles extracted from leaf extract (**Table 4.8**), peak at 3567 cm^{-3} corresponds to -OH alcoholic group, the peak at 1844 cm^{-3} corresponds to strong C=O anhydride stretch also the peak at 1734 cm^{-3} indicates the presence of C=O strong ester stretch, the peak at 1506 cm^{-3} indicates the C=C strong aromatic group. For bark extract (**Table 4.9**) peak at 3620 cm^{-3} corresponds to -OH alcoholic group, 2326 corresponds to C=N bond, peak at 1735 corresponds to C=O ketone group peak at 1677 corresponds to strong C=O amide stretch, peak at 1529 indicates C=C bonding and peak at 1492 corresponds to N=O bonding. For silver nanoparticles extracted from bark extract (**Table 4.10**), peak at 3620 cm^{-3} corresponds to -OH alcoholic group, the peak at 1675 cm^{-3} corresponds to strong C=O amide stretch and peak 1522 cm^{-3} indicates the C=C strong aromatic group.

The presence of several vibrations in the FTIR chromatograph proves the participation of phytochemicals as reducing agents in the biosynthesis of nanoparticles. The **Figure 4.11** and **Figure 4.12** demonstrates the FTIR peaks for each sample.

In a study conducted by Ahmed (2015) the silver nanoparticles were synthesised using *Azadirachta indica* leaf water extract the FTIR analysis revealed the responsible functional group for silver nanoparticles synthesis are N-H, O-H, Amide group, alkylene group and C-O bonds, which is also like our observations.

Table 4.7. FTIR data showing wave number at characteristic functional group for *Trema orientalis* leaf extract.

Sr. No	Wave number cm^{-1}	Characteristics
1	3566	-OH Alcoholic
2	2354	C=N group
3	1508	C=C aromatic group

Table 4.8. FTIR data showing wave number at characteristic functional group for *Trema orientalis* leaf extract synthesized silver nanoparticles.

Sr. No	Wave number cm^{-1}	Characteristics
1	3620	O-H alcoholic group
2	1684	C=C Amide group
3	1675	C=C Amide group
4	1522	C=C Aromatic group

Table 4.9. FTIR data showing wave number at characteristic functional group for *Trema orientalis* bark water extract.

Serial No	Wave number cm^{-1}	Characteristics
1	3620	O-H alcoholic group
2	2326	C-N bonding
3	1735	C=O ketone group
4	1677	C=O ester group
5	1529	C=C aromatic group

Table 4.10. FTIR data showing wave number at characteristic functional group for *Trema orientalis* bark water extract synthesized silver nanoparticles.

Serial No	Wave number cm^{-1}	Characteristics
1	3567	O-H Alcoholic Group
2	1844	C=O Anhydride
3	1734	C=O Ester
4	1717	C=O Ketone
5	1506	C=C Aromatic group
6	1458	C-H ₂ Alkene group

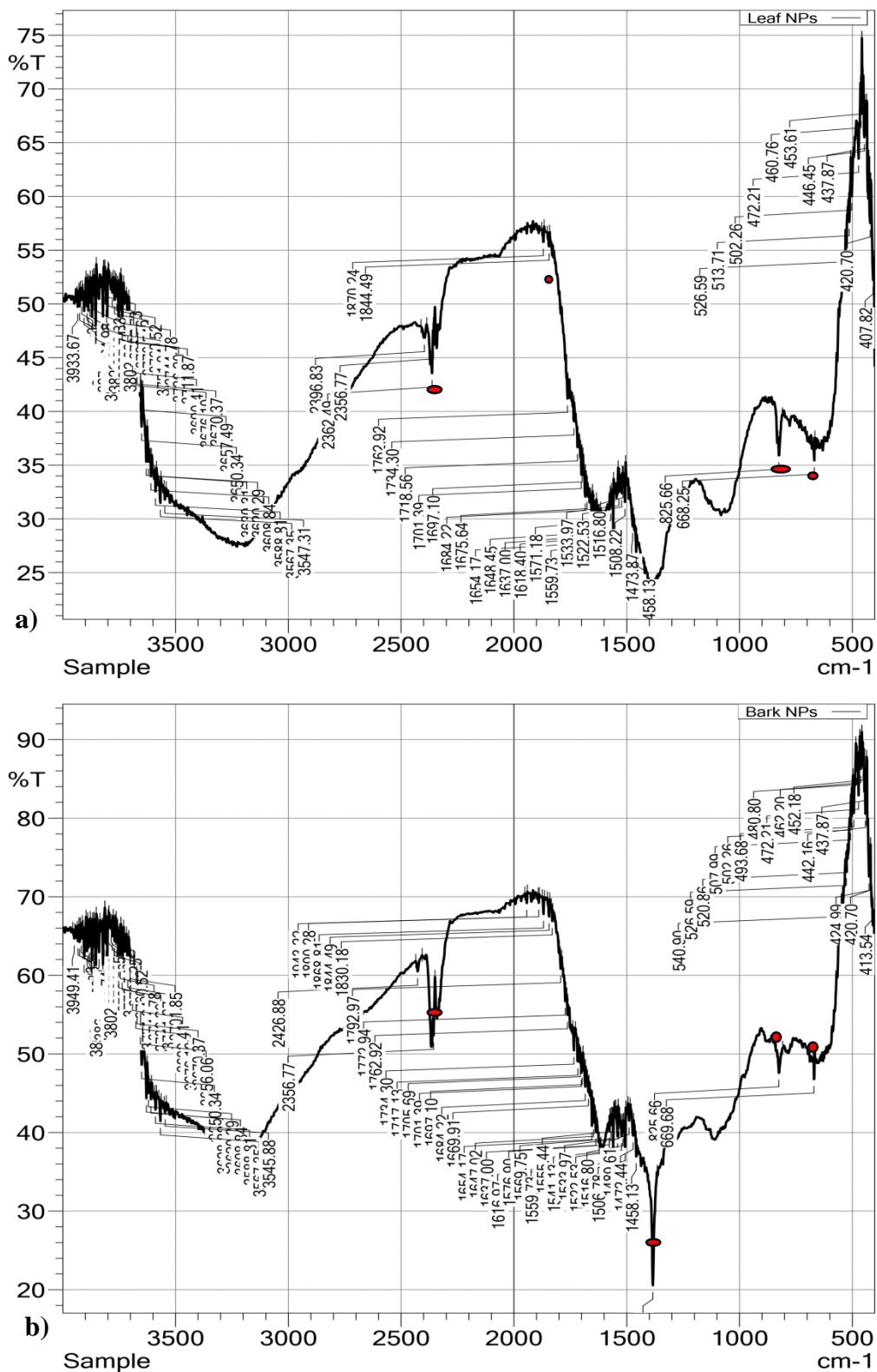


Figure 4.12. FTIR graph for Silver nanoparticles synthesized from *Trema orientalis* a) Leaf extract b) Bark extract.

4.4.3. Field Emission Scanning Electron microscopy (FE-SEM) and Energy dispersive x-ray spectrophotometry (EDS)

Field Emission Scanning Electron microscopy (FE-SEM) is used to determine the surface shape, size, aggregation, and dispersion of nanoparticles using electron beams as imaging probes (Gupta *et al.*, 2019). It produces high-resolution images at the nanoscale scale, demonstrates the involvement of biomatrix or encapsulation of Ag NPs, and can be utilised to evaluate nanoparticle size (Dawadi *et al.*, 2021).

The FE-SEM images of silver nanoparticles synthesised from leaf extract (**Plate 4.13**) and bark extract (**Plate 4.14**) and their mean size distribution histogram are shown in **Figure 4.13**. The silver nanoparticles synthesised from both the extracts exhibited spherical shape. The average size of silver nanoparticles synthesised from leaf and bark water extract was found to be 22.31nm and 22.37nm respectively.

Energy-dispersive X-ray spectroscopy (EDS) is used to determine the elemental composition, relative abundance, and impurities of nanoparticles by X-ray interaction with the material. The presence of emission peaks at 3keV indicates the presence of silver crystallites, and the absence of any other peaks confirms the impurity-free silver nanoparticles, whereas the presence of other peaks such as carbon and oxygen could indicate the interaction of metabolites with silver nanoparticles on the surface or the oxidation of silver nanoparticles (Dawadi *et al.*, 2021).

The sample of leaf extract synthesised nanoparticles showed the presence of Ag (56.2%), Cl (3.2%), C (8.6%) and O (32%) in which Ag (silver) was in higher amount, its weight % is found to be 56.2% (**Figure 4.14.a**) The other elements may be present due the composition of leaf extract and other chemical reaction in the mixture. The sample of bark extract synthesised nanoparticles showed the presence of Ag (53.6%), Ca (1.0%), Cl (3.3%), C (9%) and O (33.2%) in which Ag (silver) was in higher amount, its weight % is found to be

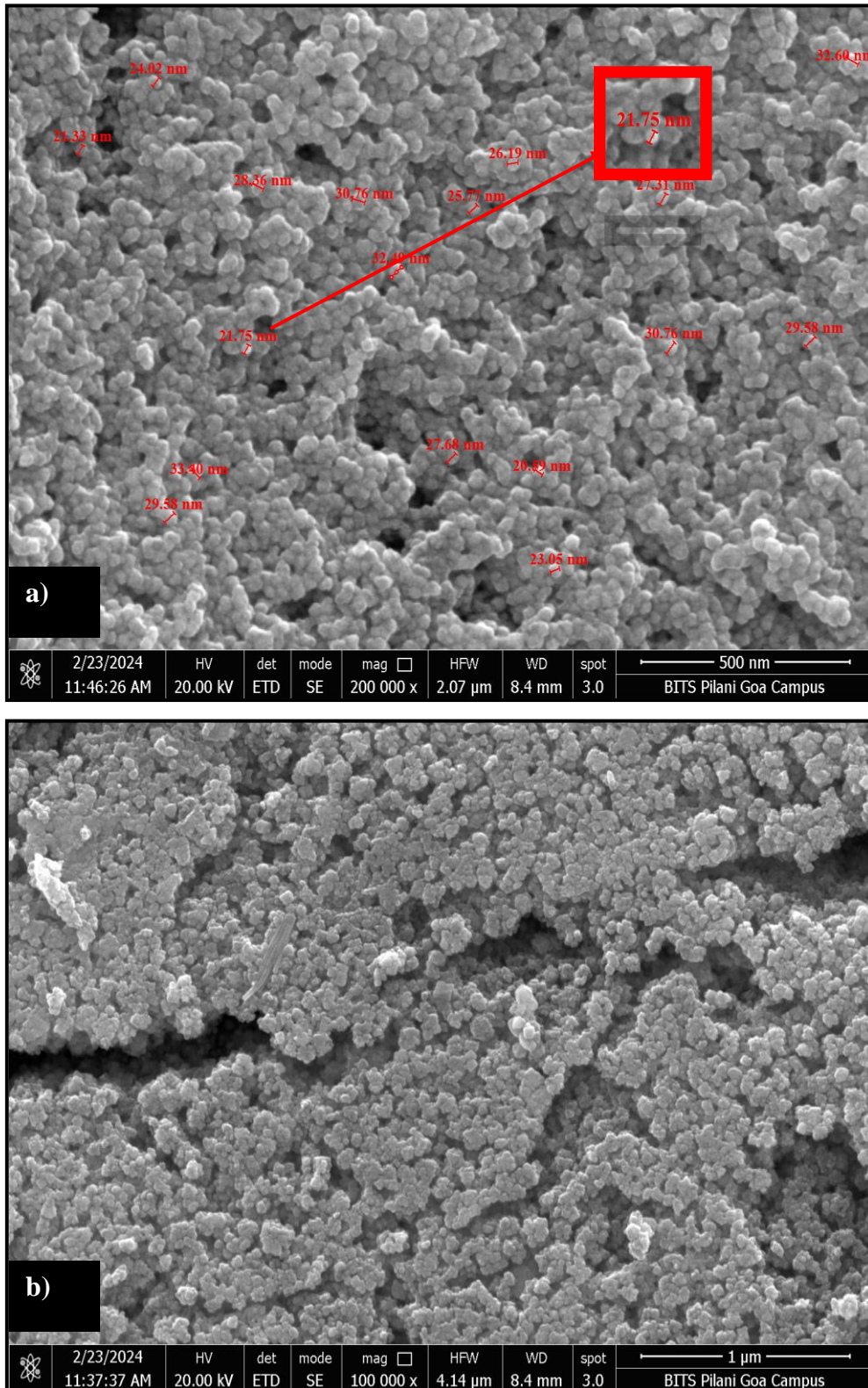


Plate 4.13. FESEM images of Silver nanoparticles synthesised from *Trema orientalis* leaf extract a) at 500 nm scale (inset image enlarge view) b) 1 μm scale.

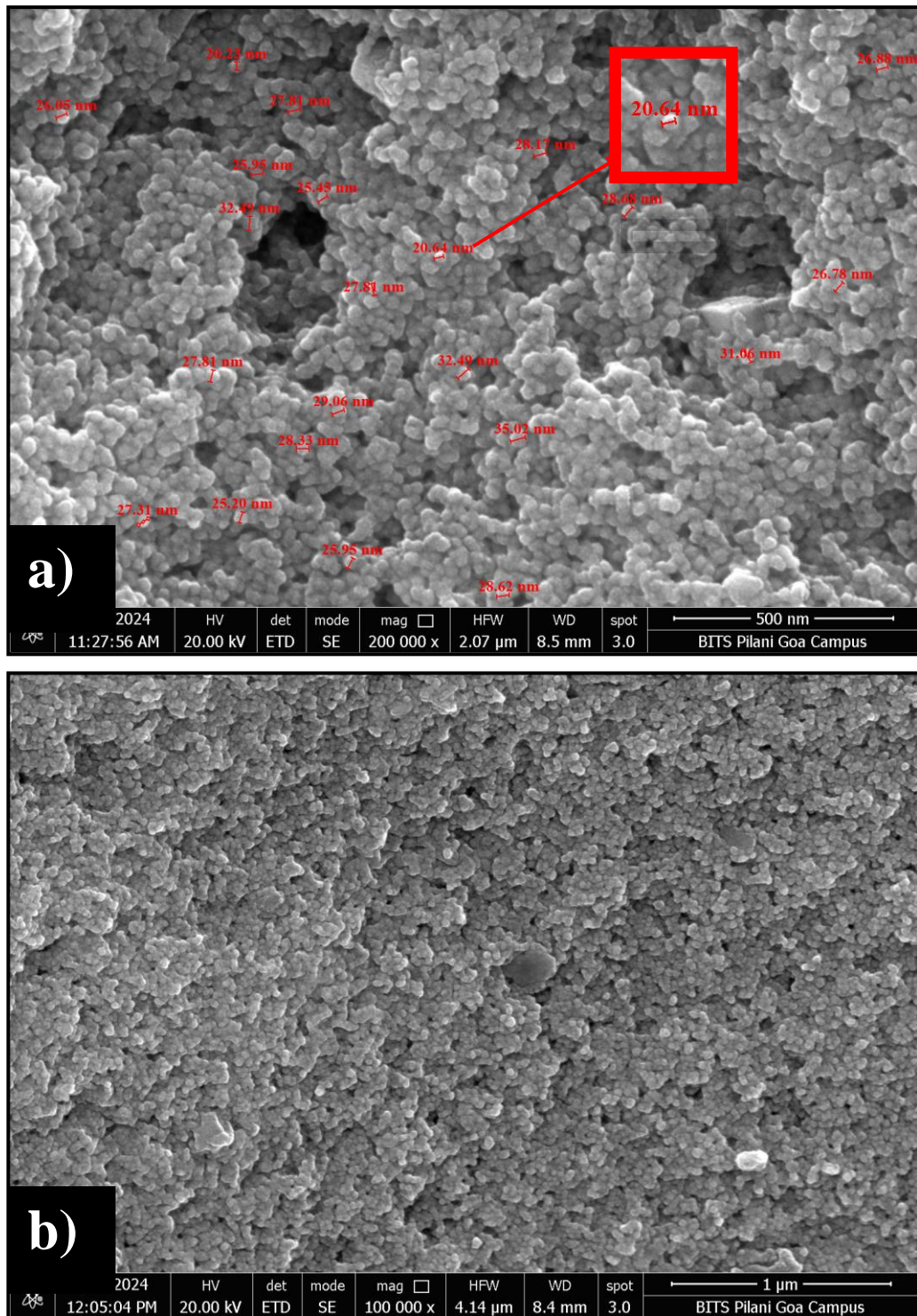


Plate 4.14. FESEM images of Silver nanoparticles synthesised from *Trema orientalis* bark extract a) at 500 nm (inset image) scale b) 1 μm scale.

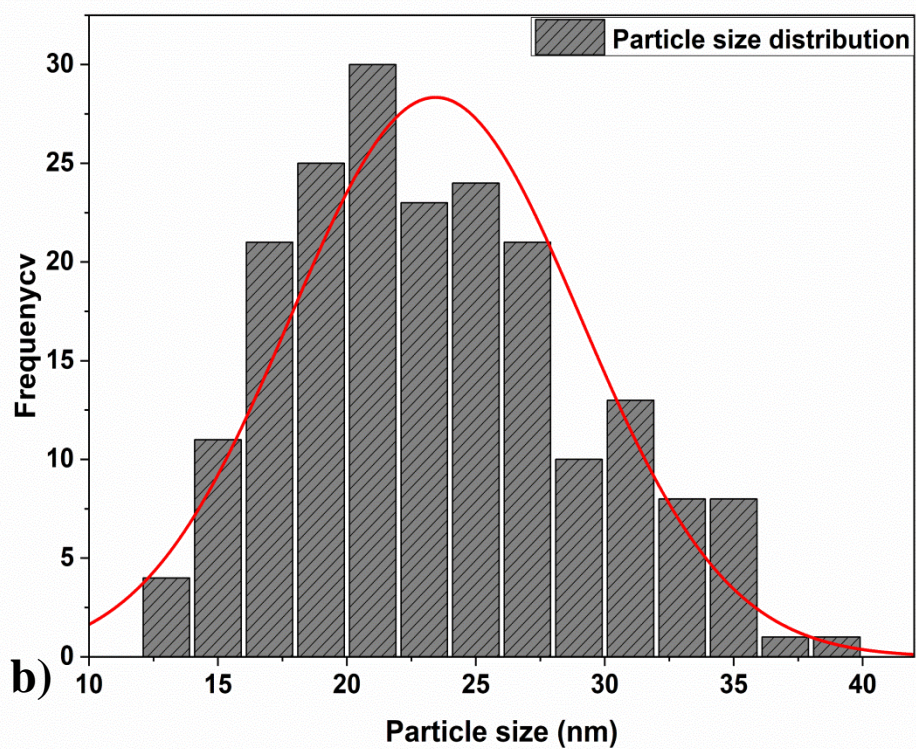
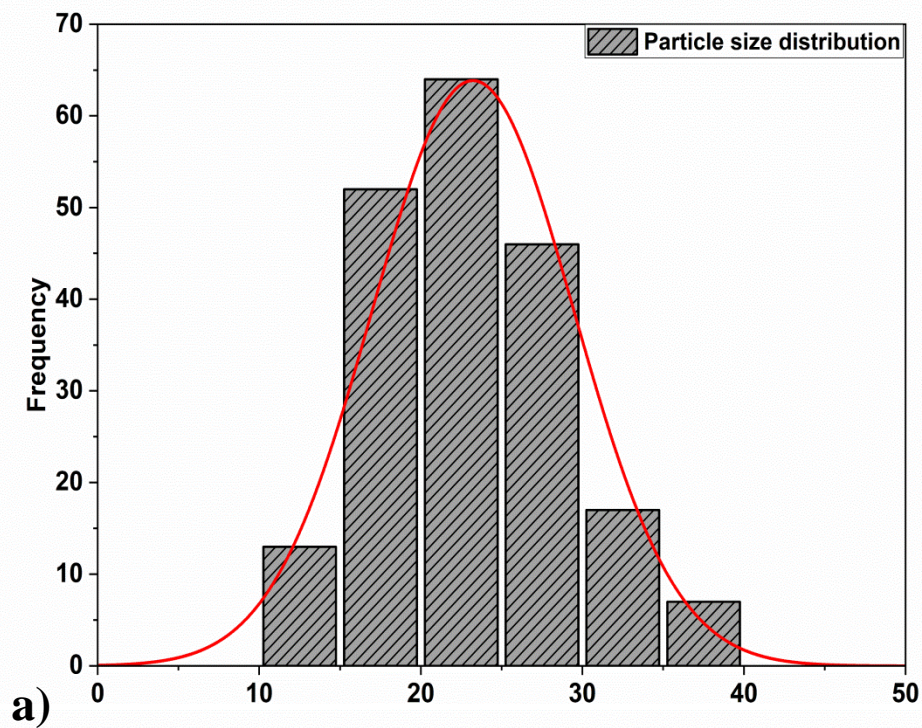


Figure 4.13. Particles size distribution for Silver nanoparticles synthesised from *Trema orientalis* a) Leaf extract b) Bark extract.

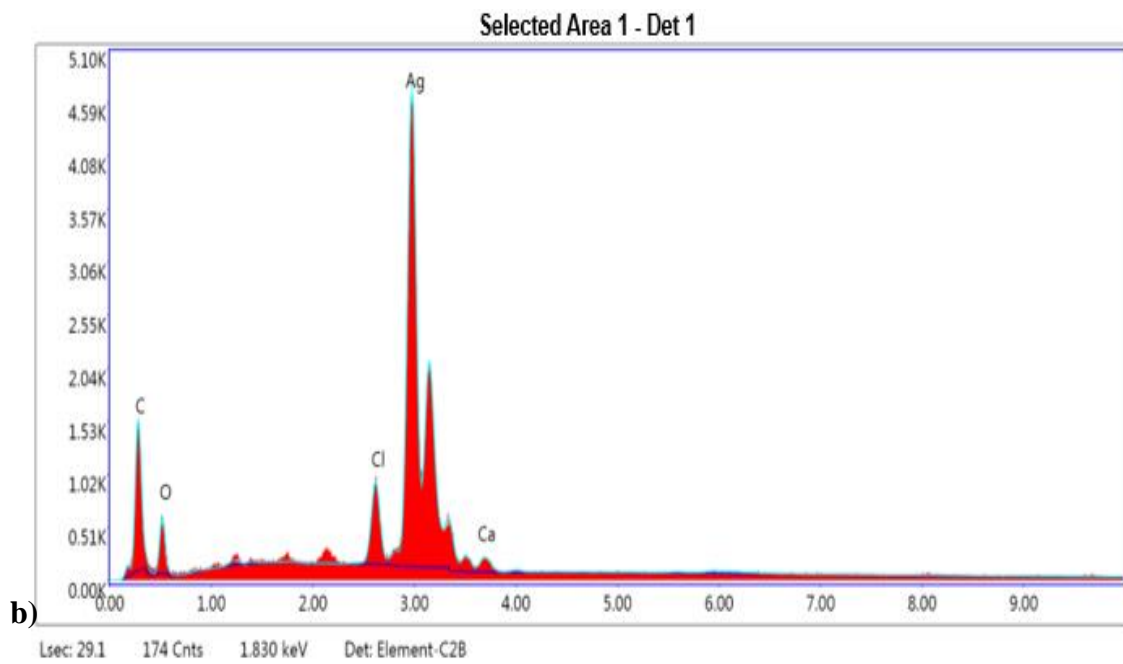
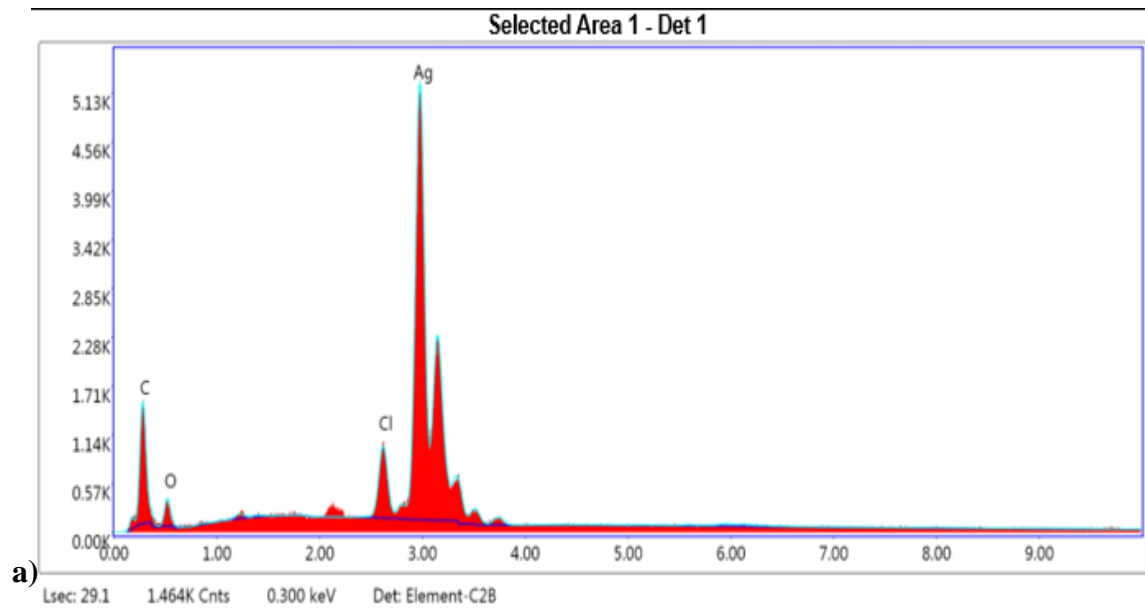


Figure 4.14. EDS data for silver nanoparticles synthesized from *Trema orientalis* a) leaf extract b) Bark extract.

53.6% (**Figure 4.14. b**). The other elements may be present due the composition of leaf extract and other chemical reaction in the mixture.

In a study conducted by Yousaf (2020), the silver nanoparticles synthesised from *Achillea millefolium* leaf water extract the size and shape was found to be spherical the size obtained by SEM analysis was found to be 20.7nm, the size is found to be like the results obtained by us.

4.4.4.X-Ray diffraction (XRD) analysis

In the XRD patterns, diffraction peaks for silver nanoparticles synthesised from leaf extract and bark extract were seen around 38.2°, 44.4°, 64.6° and 76.8° respectively for both the samples of silver nanoparticles. **Table 4.11** and **Table 4.12** indicates the 2-theta value, FWHM and crystallite sizes of nanoparticles extracted from leaf extract and bark extract respectively. The peaks were like the study reported by Rajput (2020) in which the silver nanoparticles were synthesised from leaf water extract of *Atropa acuminata*.

According to the crystallographic lattice planes, the indexed and miller (hkl) for each peak are (111), (200), (220), (311) (**JCPDS file no. 04-0783**) the highly intense peak demonstrates polycrystalline phase composition of the produced silver nanoparticles synthesised from both leaf and bark extract, confirming the synthesis of face centered cubic (FCC) crystalline silver nanoparticles (**Figure 4.15**). The other peaks for silver nanoparticles synthesised from leaf extract are 210, 122, 211, 321, 222 and one's from bark extract are 210, 122, 211, 321, 222 which may be due to the composition from extracts or unreduced silver nitrate (Rajput *et al.*, 2020).The particle size of the prepared sample was determined using Debye-Scherrer formula which was found to be 23.88 nm for leaf based silver nanoparticles and 20.88 nm for silver nanoparticles synthesised from bark extract which is closely similar to the sizes revealed by FE-SEM that is 22.31 from bark extract and 22.37 from leaf extract.

Table 4.11. 2θ value, FWHM and Crystalline size of silver nanoparticles synthesized from *Trema orientalis* leaf water extract.

Sr. No	2θ (Degrees)	FWHM	Crystalline size in (nm)
1	27.91007	0.29351	26.26764
2	29.55148	0.13709	56.03314
3	31.03596	0.1422	53.83047
4	32.32228	0.29874	25.54178
5	38.24451	1.30268	5.761919
6	46.31515	0.41371	17.65534
7	54.91058	0.3387	20.81349
8	57.56356	0.36354	19.15291
9	64.6192	0.7203	9.321523
10	77.18835	1.38205	4.492694

Table 4.12. 2θ value, FWHM and Crystalline size of silver nanoparticles synthesized from *Trema orientalis* bark water extract.

Sr. No	2θ (Degrees)	FWHM	Crystalline size in (nm)
1	27.92679	0.1846	97.41454
2	32.34274	0.19113	43.2772
3	38.23781	0.95959	7.822184
4	40.87992	9.86642	-0.40228
5	46.34313	0.23832	30.64547
6	54.93004	0.23506	58.82049
7	57.59592	0.30378	6.537245
8	64.63166	1.38203	-0.65247
9	67.56249	0.353	0.205324
10	77.43939	1.62666	3.810419
11	81.49743	1.54259	3.901511
12	90.17668	8.73421	-0.76021

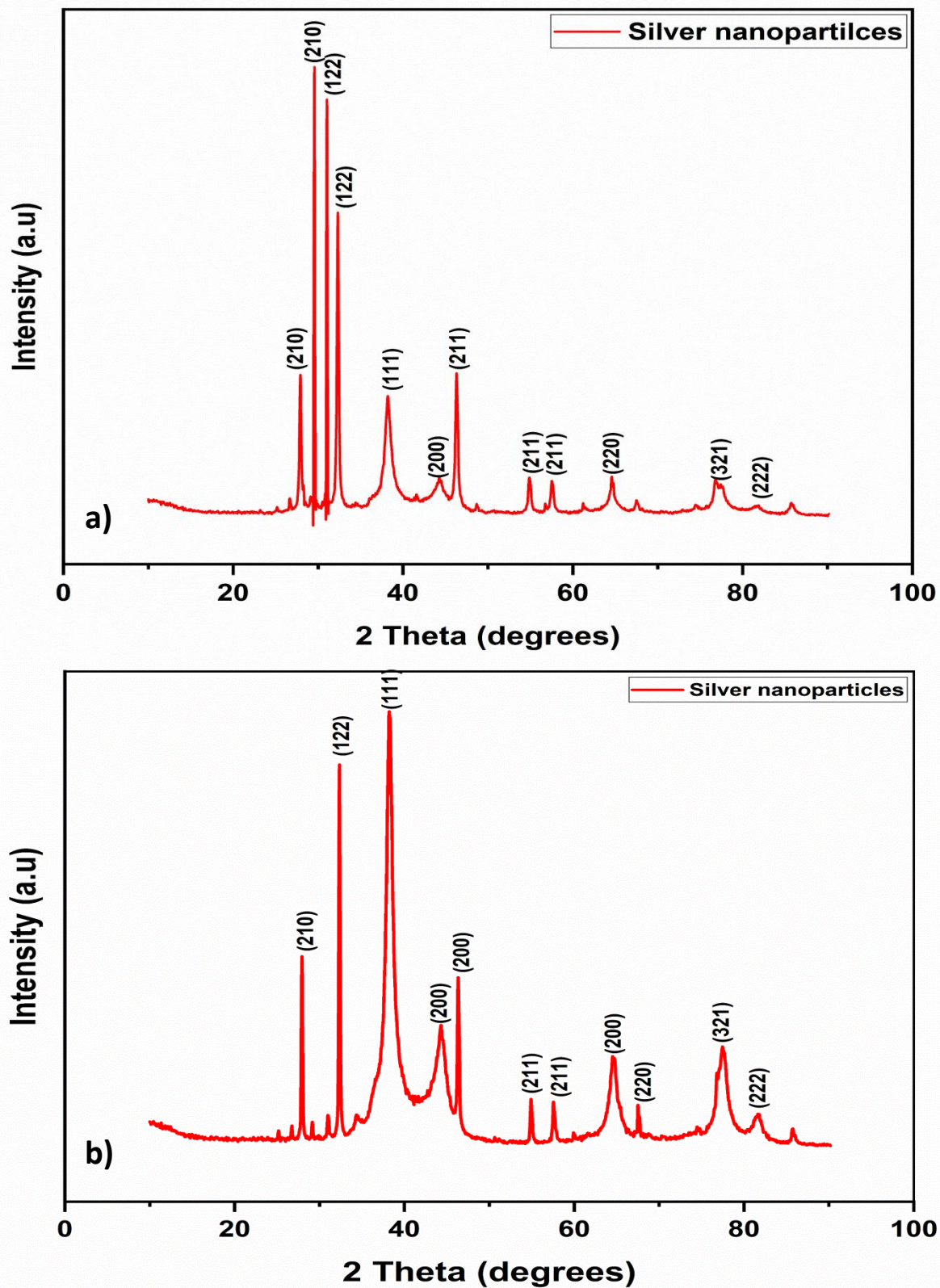


Figure 4.15. XRD Graph for Silver nanoparticles synthesized from *Trema orientalis* a) Leaf extract b) Bark extract.

4.4.5. DLS (DYNAMIC LIGHT SCATTERING) and ZETA Potential value

Dynamic light scattering (DLS) is a quick, simple, and non-destructive method for measuring particle size at the micrometre and nanometre regimes. A laser, which is a monochromatic light source, is passed through a suspension of nanoparticles, which scatter light at different intensities because of Brownian motion. The size of the particles is subsequently determined using the Stokes-Einstein relationship (Dawadi *et al.*, 2021). It evaluates the hydrodynamic diameter of the nanoparticles that are affected by the capping agents, stabilisers, and surfactants as well as if an electrical double layer is adsorbed on the surface of the particles. It functions best with monodisperse nanoparticles (Zahran *et al.*, 2020).

Thus, the nanoparticle's measured size is somewhat larger than the actual size measured from XRD and FE-SEM. The DLS also measures the zeta potential of silver nanoparticles where the large magnitude value indicates the electrostatically stabilized nanoparticles i.e., no aggregation. In DLS analysis if the polydispersity index is less than 0.5 than the particles are monodisperse and if its greater than 0.5 than it is considered as polydisperse. DLS for silver nanoparticles synthesised from leaf extract shows polydispersity index 0.282 which indicates particles are monodispersed in a solution (**Figure 4.16.a**). Similarly, for silver nanoparticles synthesised from bark extract the polydispersity index was 0.234 (**Figure 4.16. b**). The average size showed for silver nanoparticles synthesised from leaf and bark extract are 1727 nm and 1036 nm respectively which is usually not considered. The DLS is used usually to understand only the polydispersity of particle in a colloidal solution.

The zeta potential implies the electrostatic attraction or repulsion between the nanoparticles in solution. nanoparticles having zeta potential values less than -30 mV or greater than +30 mV indicates high degree of stability in the colloidal solution (Khorrami *et*

al., 2018). The zeta potential for silver nanoparticles synthesised from leaf and bark extract was -23mV and -18 mV (**Figure 4.17**) respectively indicating that the particles are negatively charged and are stable. In the study conducted by Rajput (2019) in which the silver nanoparticles were synthesised from leaf water extract of *Atropa acuminata* the zeta potential value was found to be -33.5 mV which is highly stable in but the zeta potential of our studied particles is found to be moderately stable.

From the characterization techniques we can conclude that the characteristics of both leaf and bark extract-based silver nanoparticles are spherical, crystalline, monodispersed, with a size range of 20 to 23nm, with a negatively charged surface having moderate stability, making them suitable for biological applications.

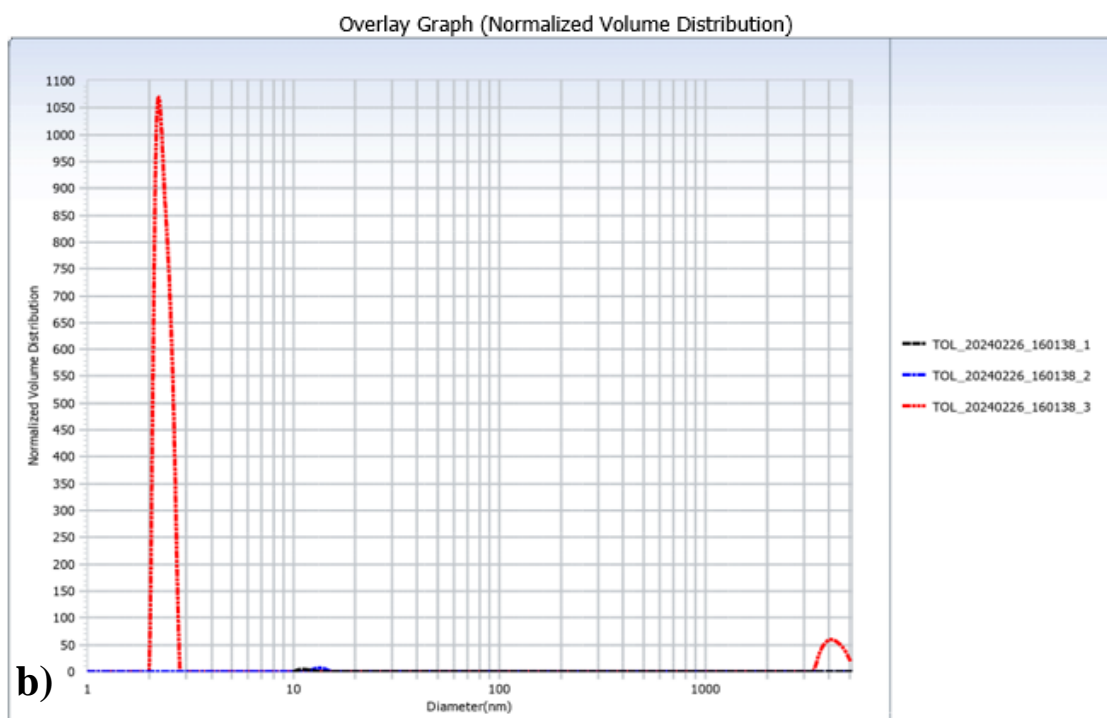
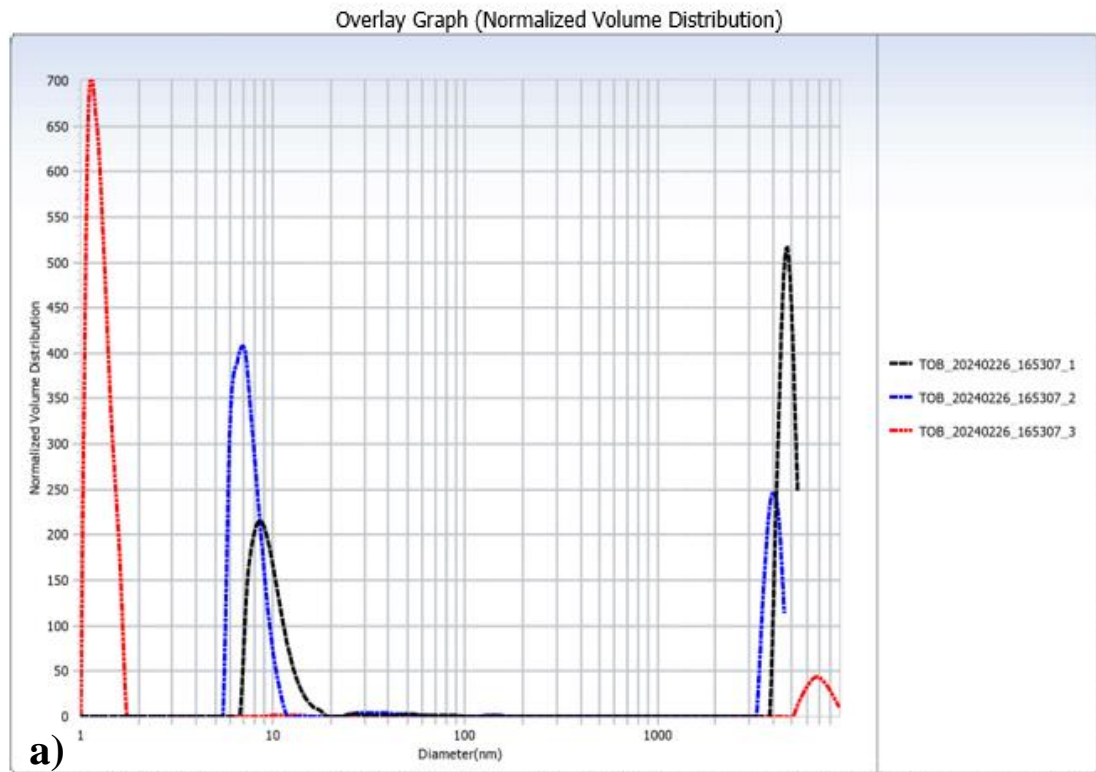


Figure 4.16. DLS data for silver nanoparticles synthesised from *Trema orientalis*
a) Leaf extract and b) Bark extract

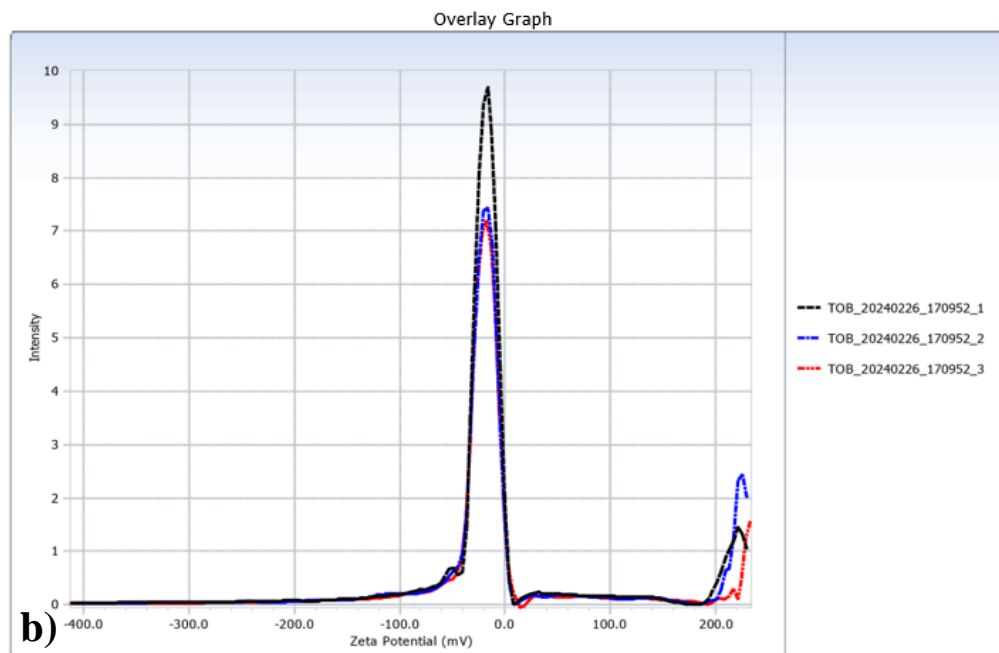
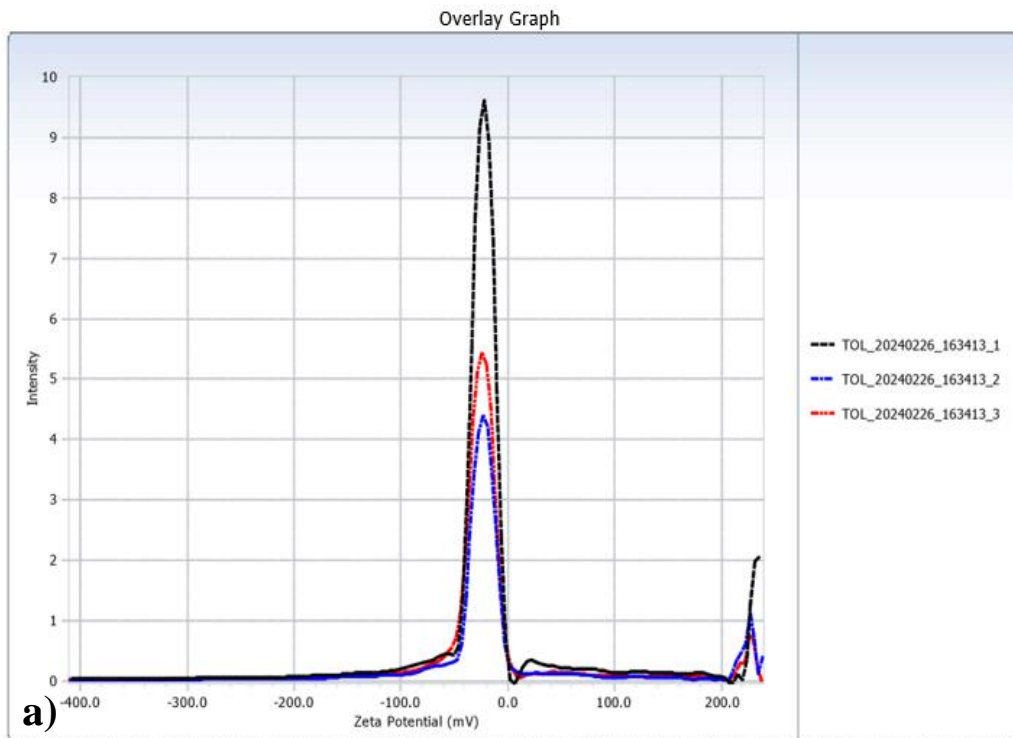


Figure 4.17. Zeta potential data for Silver nanoparticles synthesized from *Trema orientalis* a) Leaf extract , b) Bark extract

4.5. Evaluation of the bio-fabricated silver nanoparticles for biological activities such as antioxidant, antidiabetic, and anti-inflammatory activities.

4.5.1. Antioxidant studies

The DPPH is a free radical which upon accepting an electron becomes a stable molecule (Rajput *et al.*, 2019). In the DPPH free radicle activity, the scavenging activity increases as the concentration of standard and plant extract increases as shown in **Table 4.13**.

There was no significant colour change was observed in the reaction (**Plate 4.15**, **Plate 4.16**) but the scavenging percentage of both extract and nanoparticles was increasing as the concentration increases. The graphical results are presented in **Figure 4.18** and **Figure 4.19**. The IC₅₀ value (**Table 4.14**) of the Ascorbic acid was found to be 47.9 ±0.19µg/ml., The IC₅₀ value for leaf extract and bark extract is found to be 436±0.005 µg/ml and 423.2±0.1 µg/ml respectively.

In the study conducted by Trono (2016), reported the IC₅₀ value of water extract of *Trema orientalis* leaf to be 55.69µg/ml and with methanolic leaf extract it was 48µg/ml. Also, Uddin (2009), reported the IC₅₀ value for methanolic extract to be 110µg/ml. The IC₅₀ value obtained by us were very high but the percentage inhibition was increasing as the concentration increases indicating the potential antioxidant activity of the extract.

The IC₅₀ value for silver nanoparticles synthesised from leaf extract is found to be 1212.07±0.008µg/ml and for silver nanoparticles synthesised from bark extract is found to be 522±0.002 µg/ml. The earlier study conducted by Kharat (2016) reported the IC₅₀ value for DPPH activity of silver nanoparticles as 126.6±0.06 µg/ml.

The results revealed that the antioxidant property of plant extract is better than silver nanoparticles which may be due to the synergetic effect of all the phytochemicals like phenols, flavonoids, tannins, glycosides, which is responsible for better scavenging of free radicle is comparison to spherical silver nanoparticles alone.

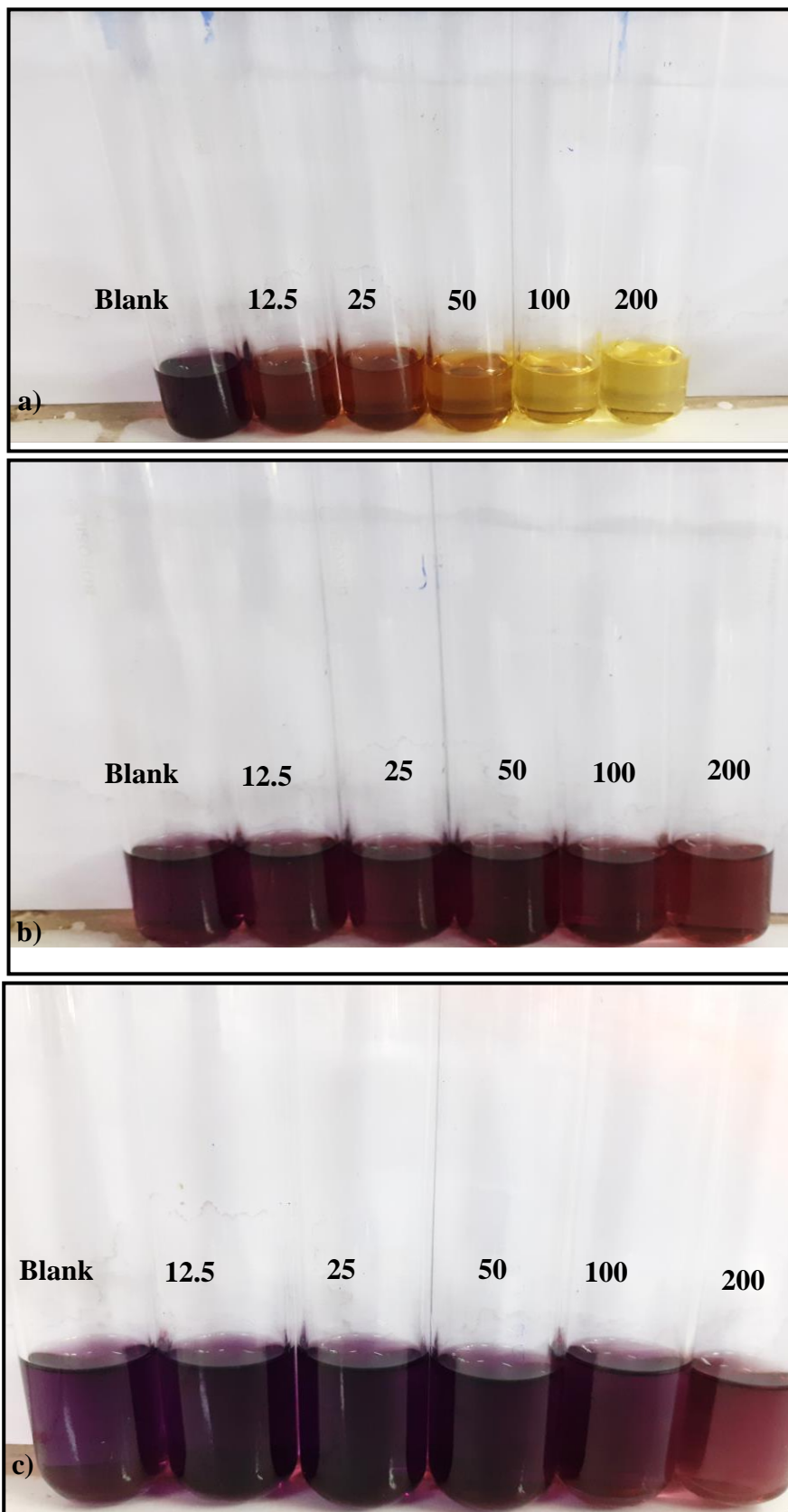


Plate 4.15. DPPH Scavenging activity by a) Ascorbic acid, b) *Trema orientalis* leaf extract c) *Trema orientalis* Bark extract.

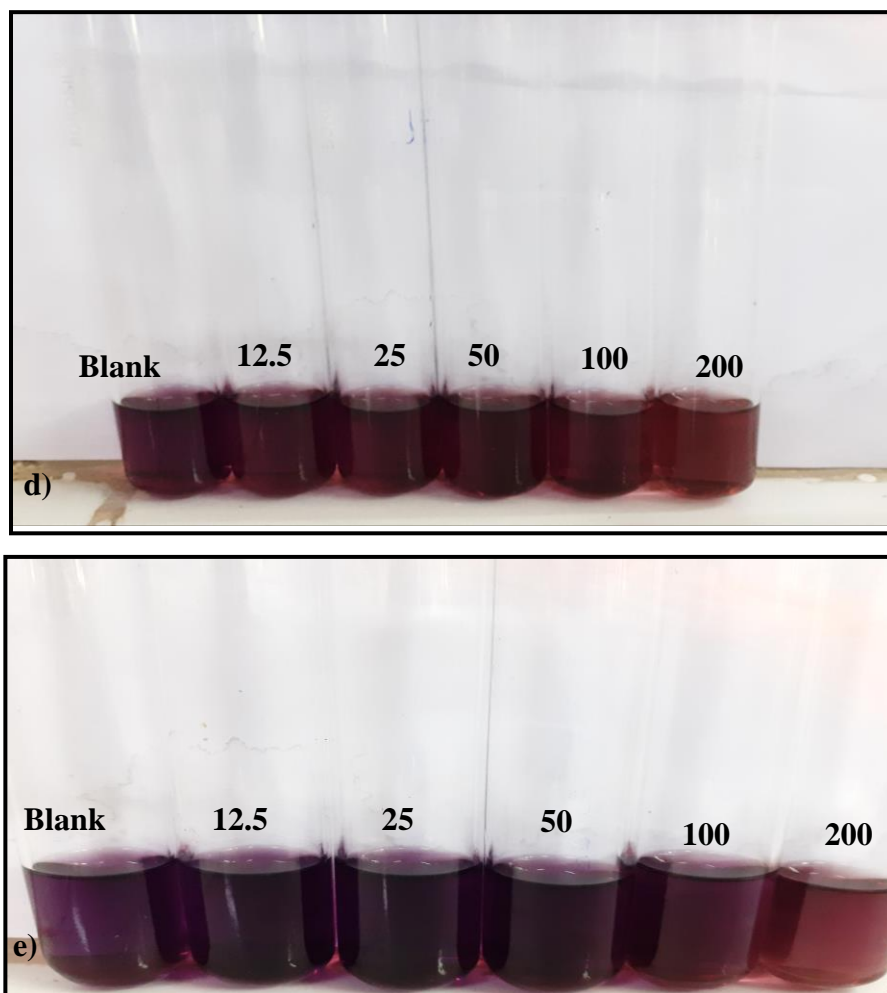


Plate 4.16. DPPH Scavenging activity by d) Silver nanoparticles synthesised from *Trema orientalis* leaf extract e) Silver nanoparticles synthesised from *Trema orientalis* Bark extract.

Table 4.13. DPPH free radical scavenging assay: % scavenging activity of DPPH by Ascorbic acid and water extract of leaf and bark of *Trema orientalis* and silver nanoparticles synthesized from respective extracts.

Sr no.	Concentration mg/ml	L-ascorbic acid	Leaf extract	Bark extract	NP from Leaf extract	NP from Bark extract
1	12.5	30±0.42	2.3±0.003	1.8±0.003	2.3±0.002	0.18±0.001
2	25	48±0.26	8.7±0.001	8.3±0.001	8.7±0.002	2.5±0.003
3	50	55±0.0.05	9±0.01	8.5±0.007	9±0.008	6.2±0.006
4	100	71±0.0.05	14.4±0.003	17.3±0.04	14.4±0.009	12.2±0.001
5	200	82±0.01	24.5±0.002	24.1±0.002	24.5±0.007	18.3±0.001

Note: ±Standard deviation, NP (Nanoparticles)

Table 4.14. IC₅₀ values for DPPH free radical scavenging activity.

Sr no.	Sample	IC ₅₀ µg/ml
1	Ascorbic acid	47.9±0.19
2	Leaf extract	436±0.005
3	Bark extract	423±0.1
4	Silver nanoparticles synthesised from leaf extract	1212±0.008
5	Silver nanoparticles synthesised from bark extract	522±0.002

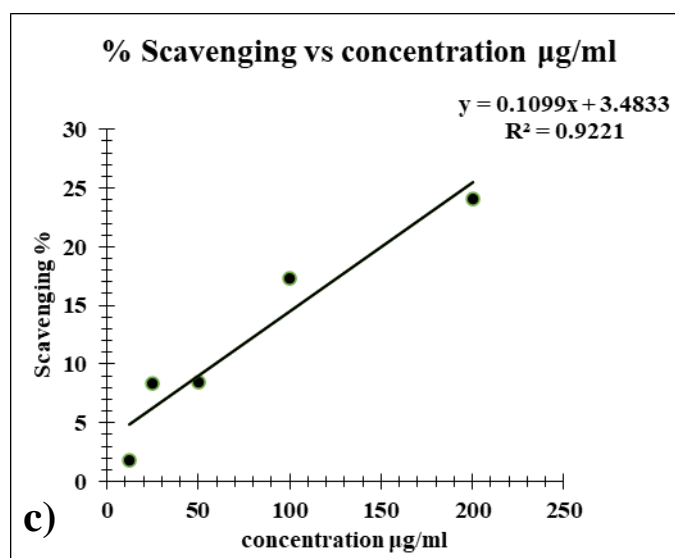
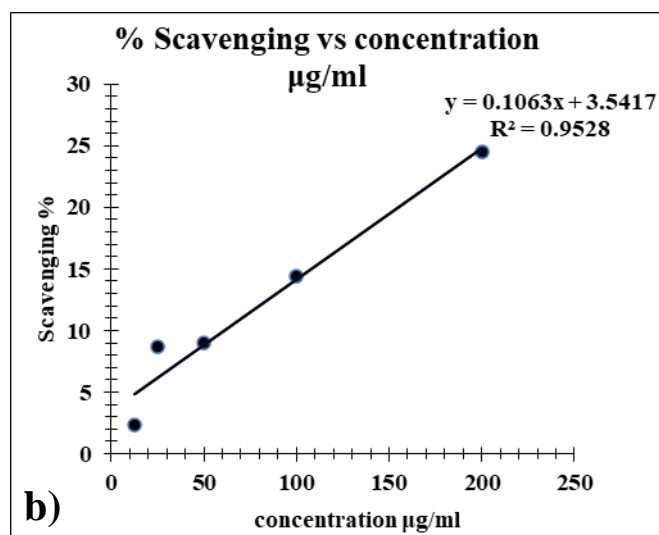
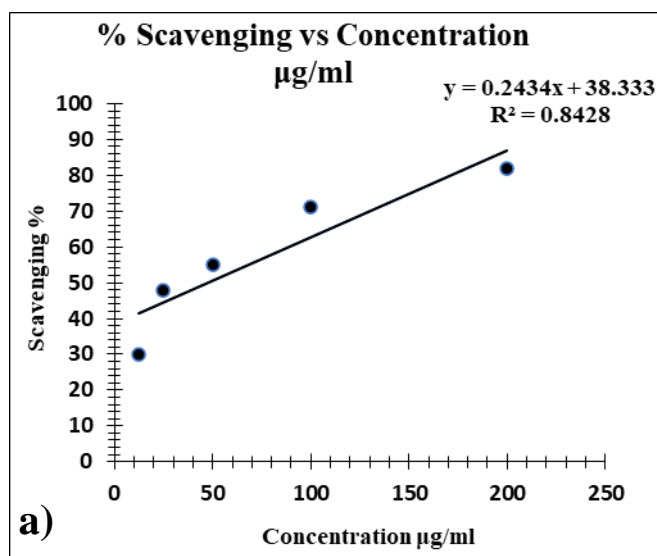


Figure 4.18. Antioxidant activity: DPPH radical scavenging activity by a) Ascorbic acid b) *Trema orientalis* Leaf extract c) *Trema orientalis* Bark extract.

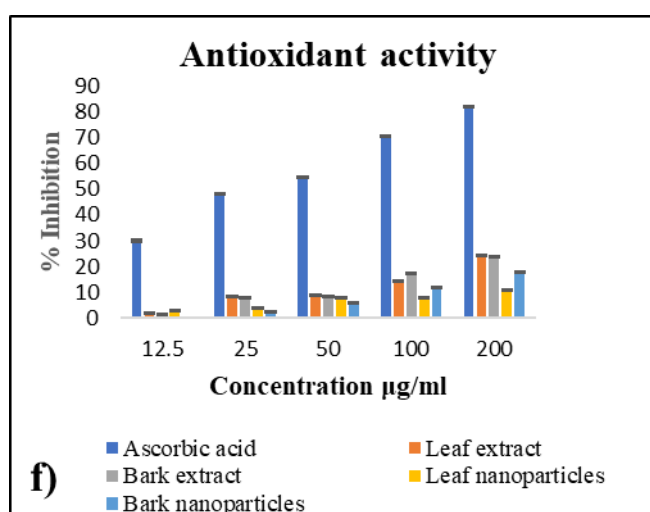
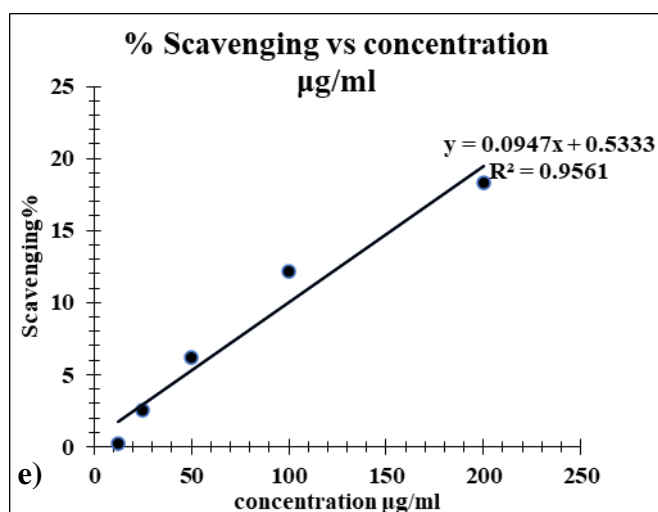
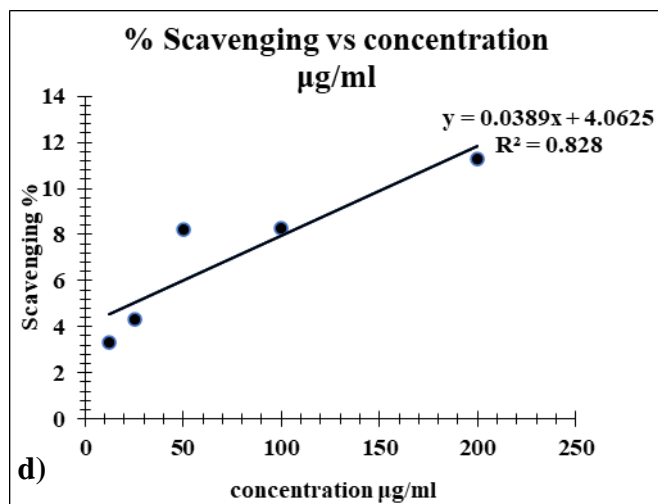


Figure 4.19. Antioxidant activity: DPPH radical scavenging activity by Silver nanoparticles synthesized from *Trema orientalis* d) Leaf extract e) Bark extract f) Comparative graph.

4.5.2 Antidiabetic assay

For starch iodine colour test (**Plate 4.17**, **Plate 4.18**) at each concentration the amount of starch was noted, as the series concentration of standard and plant extract increases the absorbance also increases at highest concentration as the starch breakdown by α -amylase gets inhibited (**Figure 4.20** and **Figure 4.21**).

For Acarbose (**Table 4.15**) that is the standard the absorbance at 20 μ l/ml is found to be 0.412nm and it was found to be increased with concentration and at the highest concentration which 100 μ g/ml the absorbance is found to be 0.865nm. The absorbance value for leaf extract (**Table 4.16**) at 20 μ g/ml was 0.682 nm and as the concentration increases the absorbance increased, at 100 μ g/ml the absorbance was 0.777 nm.

For silver nanoparticles synthesised from leaf extract (**Table 4.17**) the absorbance value 20 μ g/ml was 0.415 nm and as the concentration increases the absorbance increased, at 100 μ g/ml the absorbance was 0.614 nm. For bark extract (**Table 4.18**) the absorbance value 20 μ g/ml was 0.781 nm and as the concentration increases the absorbance increased, at 100 μ g/ml the absorbance was 0.825nm

For silver nanoparticles synthesised from bark extract (**Table 4.19**) the absorbance value 20 μ g/ml was 0.451 nm and as the concentration increases the absorbance increased, at 100 μ g/ml the absorbance was 0.712nm. The result revealed the potential antidiabetic activity of silver nanoparticles, which is like the study conducted by Balan (2016) which reported the potential antidiabetic activity of silver nanoparticles synthesised from *Lonicera japonica* leaf extract. The α -amylase inhibition assay was performed using the DNSA method.

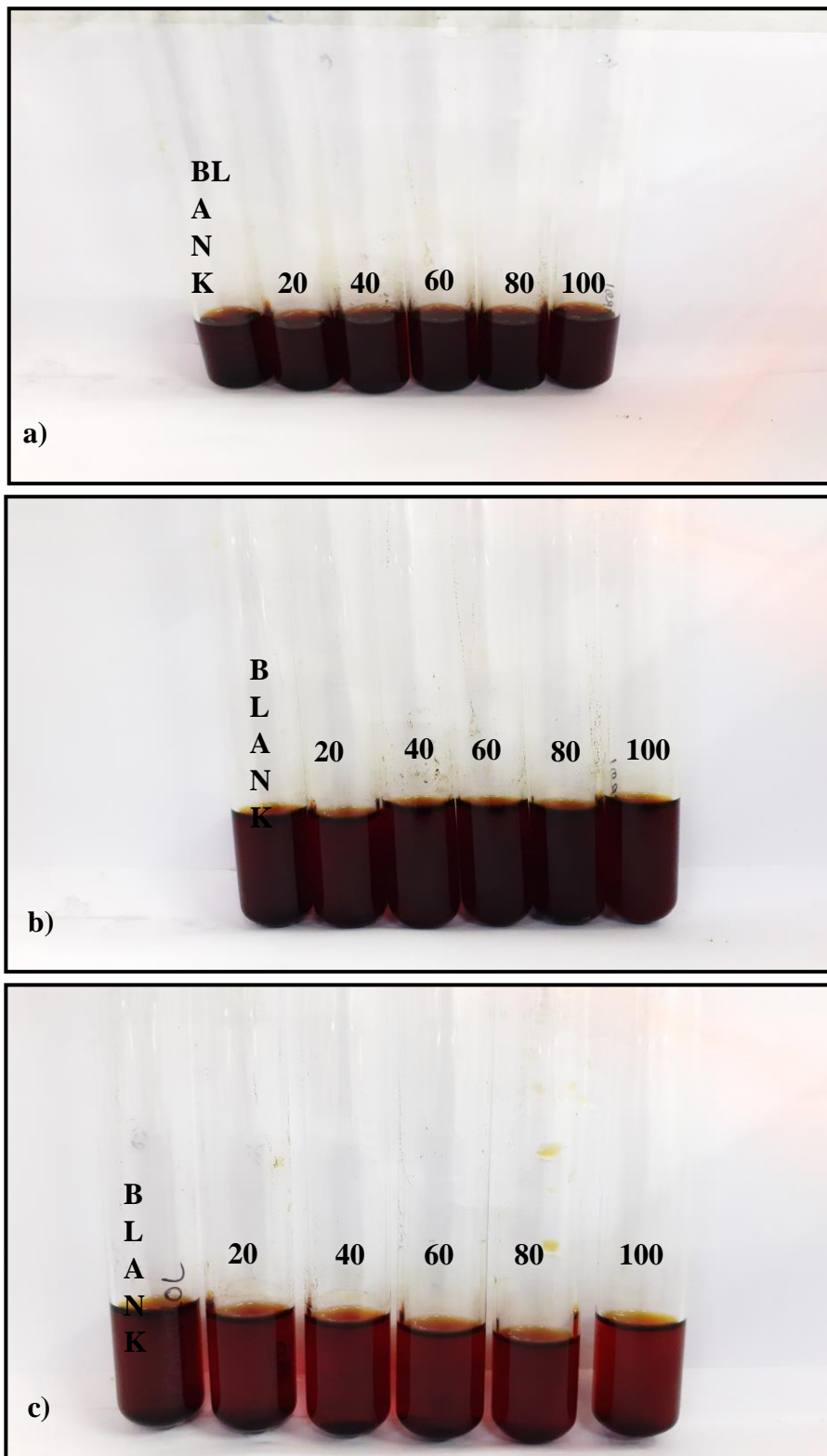


Plate 4.17. Antidiabetic activity by a) by Acarbose b) by *Trema orientalis* Leaf extract c) by *Trema orientalis* Bark extract.

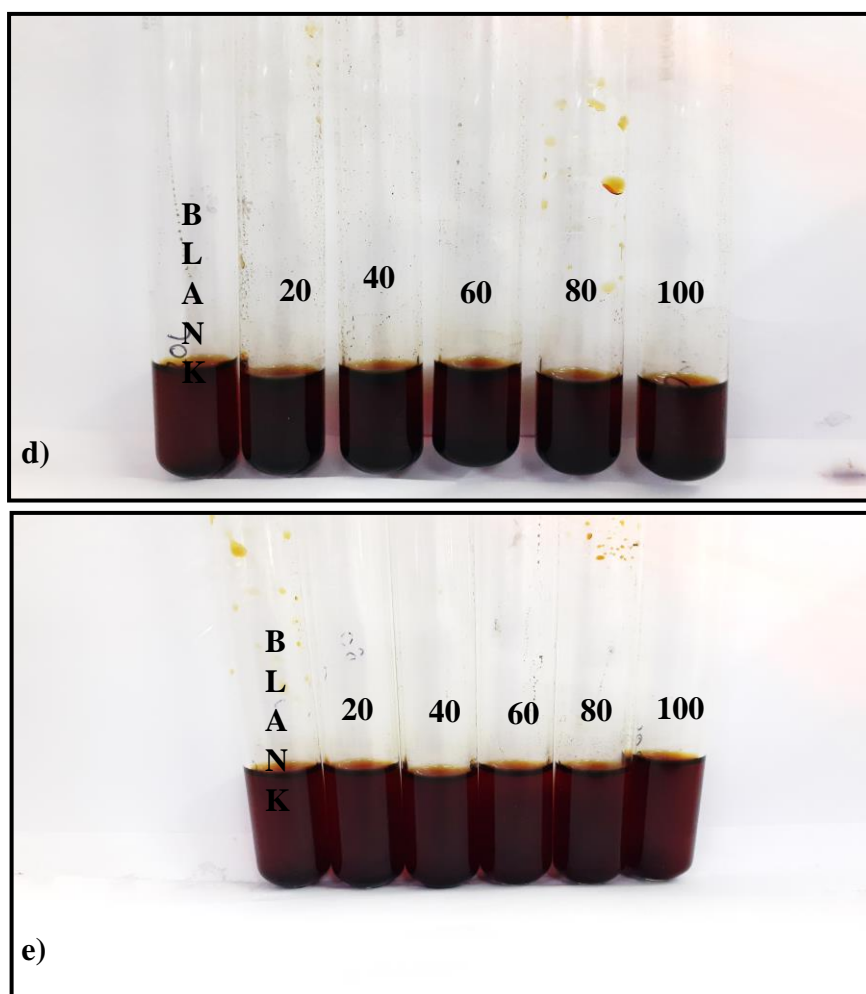


Plate 4.18. Antidiabetic activity by d) Silver nanoparticles synthesised from *Trema orientalis* leaf extract e) Silver nanoparticles synthesised from *Trema orientalis* bark extract.

Table 4.15. Starch-iodine assay for Acarbose.

Concentration µg/ml	Absorbance at 620nm			Mean Absorbance
	R ₁	R ₂	R ₃	
Control	0.415	0.412	0.411	0.412±0.002
20	0.436	0.434	0.434	0.437±0.001
40	0.538	0.537	0.538	0.538±0.005
60	0.611	0.61	0.613	0.611±0.001
80	0.768	0.767	0.769	0.768±0.08
100	0.865	0.864	0.867	0.865±0.001

Note: ± Standard deviation

Table 4.16. Starch-iodine assay for *Trema orientalis* Leaf extract.

Concentration µg/ml	Absorbance at 620nm			Mean Absorbance
	R ₁	R ₂	R ₃	
Control	0.697	0.685	0.6886	0.690±0.006
20	0.687	0.68	0.679	0.682±0.004
40	0.705	0.702	0.7	0.702±0.002
60	0.71	0.689	0.699	0.699±0.010
80	0.752	0.75	0.753	0.751±0.001
100	0.779	0.775	0.778	0.777±0.002

Note: ± Standard deviation

Table 4.17. Starch-iodine assay for silver nanoparticles synthesized from *Trema orientalis* leaf extract.

Concentration $\mu\text{g/ml}$	Absorbance at 620nm			Mean Absorbance
	R ₁	R ₂	R ₃	
Control	0.635	0.632	0.629	0.632 \pm 0.003
20	0.41	0.415	0.421	0.415 \pm 0.005
40	0.438	0.429	0.439	0.435 \pm 0.005
60	0.552	0.553	0.549	0.551 \pm 0.002
80	0.596	0.599	0.595	0.596 \pm 0.002
100	0.618	0.615	0.61	0.614 \pm 0.004

Note: \pm Standard deviation

Table 4.18. Starch-iodine assay for *Trema orientalis* bark extract.

Concentration $\mu\text{g/ml}$	Absorption at 620nm			Mean OD
	R ₁	R ₂	R ₃	
Control	0.726	0.728	0.725	0.726 \pm 0.001
20	0.78	0.786	0.779	0.781 \pm 0.003
40	0.789	0.79	0.788	0.789 \pm 0.001
60	0.79	0.798	0.789	0.792 \pm 0.004
80	0.819	0.812	0.816	0.815 \pm 0.002
100	0.828	0.82	0.829	0.825 \pm 0.004

Note: \pm Standard deviation

Table 4.19. Starch-iodine assay for silver nanoparticles synthesized from *Trema orientalis* bark extract.

Concentration µg/ml	Absorbance at 620nm			Mean OD
	R ₁	R ₂	R ₃	
Control	0.631	0.429	0.63	0.563±0.11
20	0.429	0.468	0.464	0.453±0.021
40	0.448	0.451	0.45	0.449±0.001
60	0.565	0.556	0.554	0.558±0.005
80	0.632	0.63	0.629	0.63±0.001
100	0.711	0.715	0.71	0.712±0.02

Note: ± Standard deviation

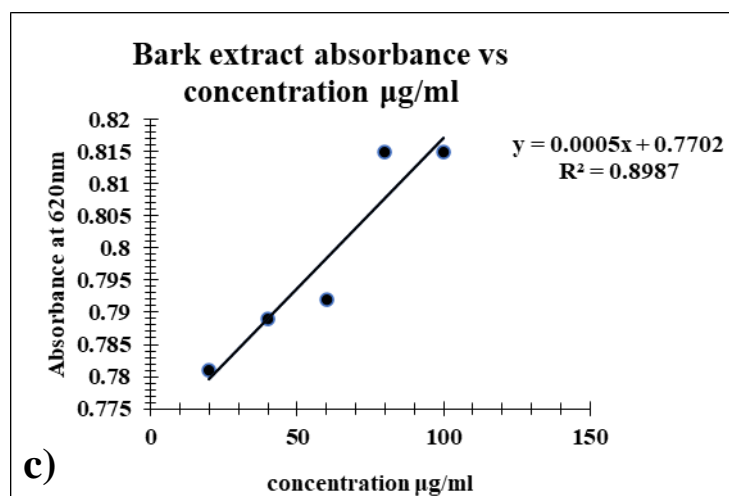
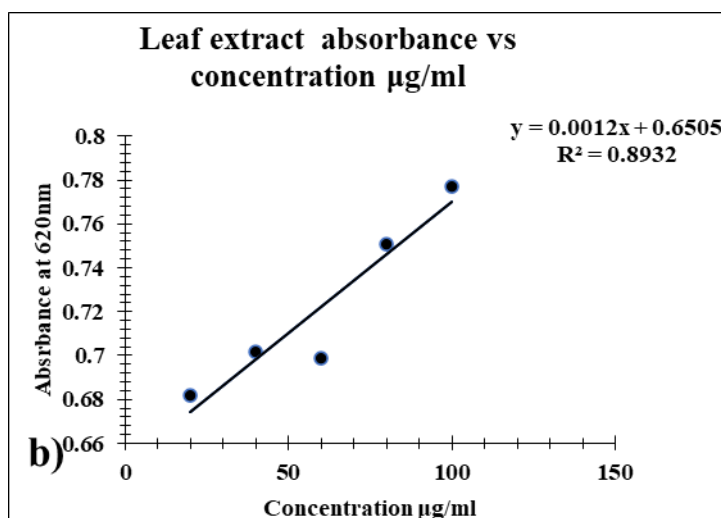
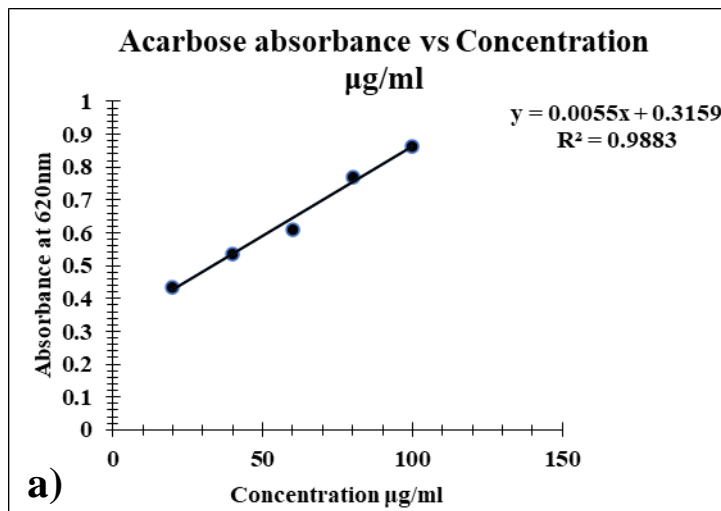


Figure 4.20. Antidiabetic activity: Starch iodine assay for a) Acarbose b) *Trema orientalis* Leaf extract and c) *Trema orientalis* Bark extract

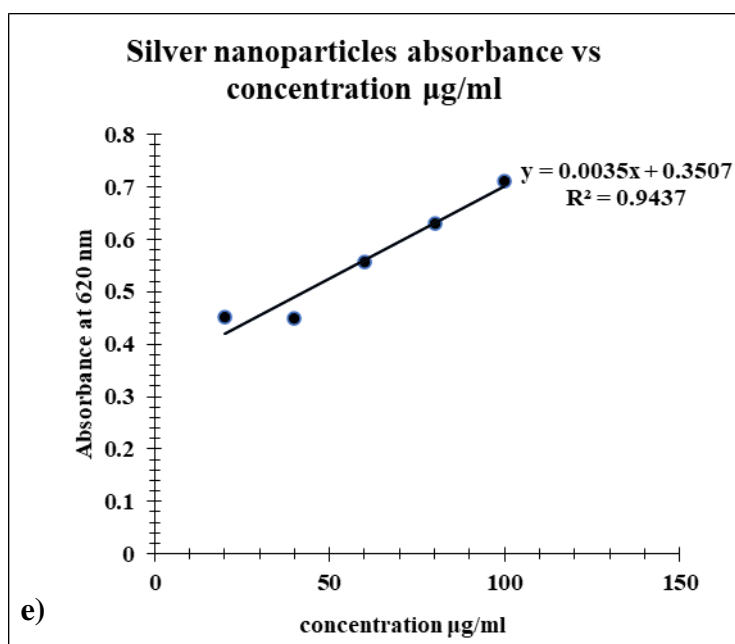
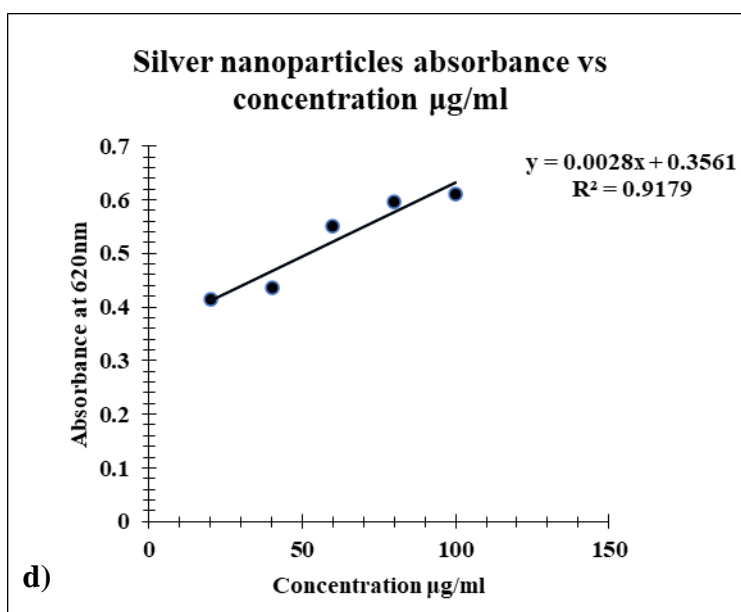


Figure 4.21. Antidiabetic activity: Starch iodine assay for Silver nanoparticles synthesized from *Trema orientalis* d) Leaf extract and e) Bark extract.

4.5.3. Anti-inflammatory assay

Protein denaturation is the well-known potential cause for inflammation responses. When proteins are denaturated, autoantigens are produced, which lead to severe inflammation in rheumatoid disorders (Das *et al.*, 2019). For protein denaturation assay using egg albumin the percentage inhibition was calculated, the percentage inhibition increased as the concentration of standard drug, plant extract and silver nanoparticles increased (**Plate 4.19**, **Plate 4.20**), as shown in **Table 4.20**. The graphical results are presented in **Figure 4.22** and **Figure 4.23**.

The IC_{50} value (**Table 4.21**) for Diclofenac sodium which is the standard drug was found to be $53 \pm 0.01 \mu\text{g/ml}$. The IC_{50} value for leaf extract was found to be $130 \pm 0.003 \mu\text{g/ml}$ and the IC_{50} value for bark extract was found to be $129 \pm 0.001 \mu\text{g/ml}$. The IC_{50} value for silver nanoparticles synthesised from leaf extract was found to be $106 \pm 0.06 \mu\text{g/ml}$ and for silver nanoparticles synthesised from bark extract was found to be $57.6 \pm 0.01 \mu\text{g/ml}$. The silver nanoparticles exhibited better anti-inflammatory activity than plant extracts. From which bark nanoparticles exhibited strong inhibition activity.

It was seen that the silver nanoparticles have better anti-inflammatory activity in comparison to plant extract, it can be stated that synthesised nanoparticles can control the production of auto antigens which cause denaturation of proteins during inflammation. The above results were like the study conducted by Rajput (2019), in which the study reported that IC_{50} value for silver nanoparticle synthesised from *Atropa acuminata* leaf extract was $12.98 \mu\text{g/ml}$ and the anti-inflammatory activity was better than its respective plant extract from which silver nanoparticles were synthesised.

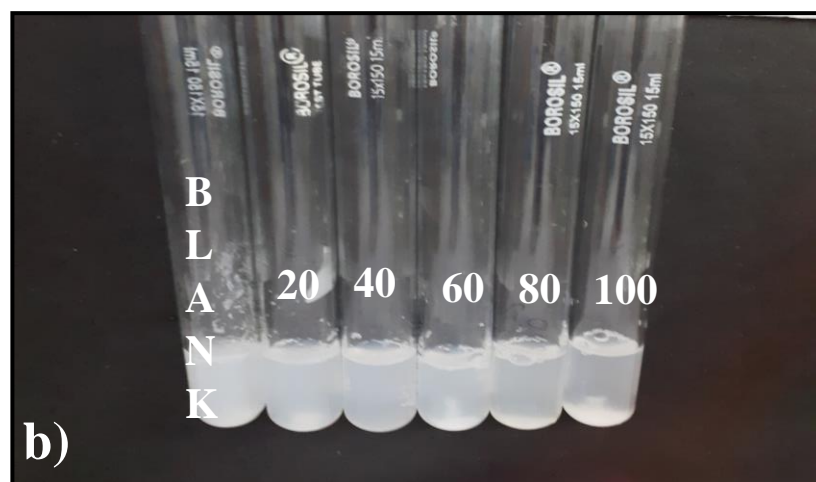
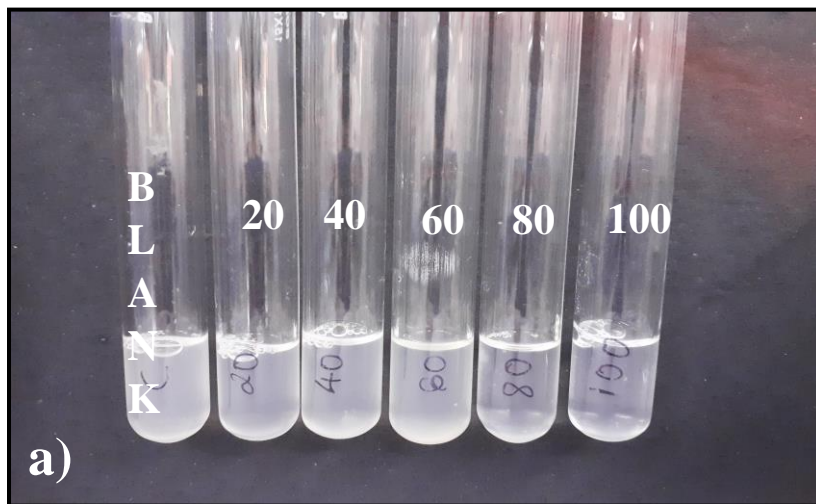


Plate 4.19. Anti-inflammatory activity by a) Diclofenac sodium b) *Trema orientalis* Leaf extract b) *Trema orientalis* Bark extract.

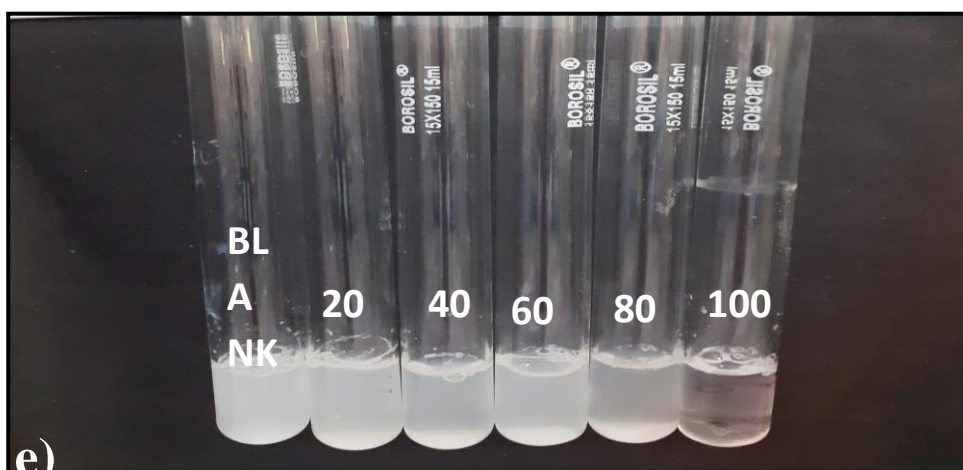
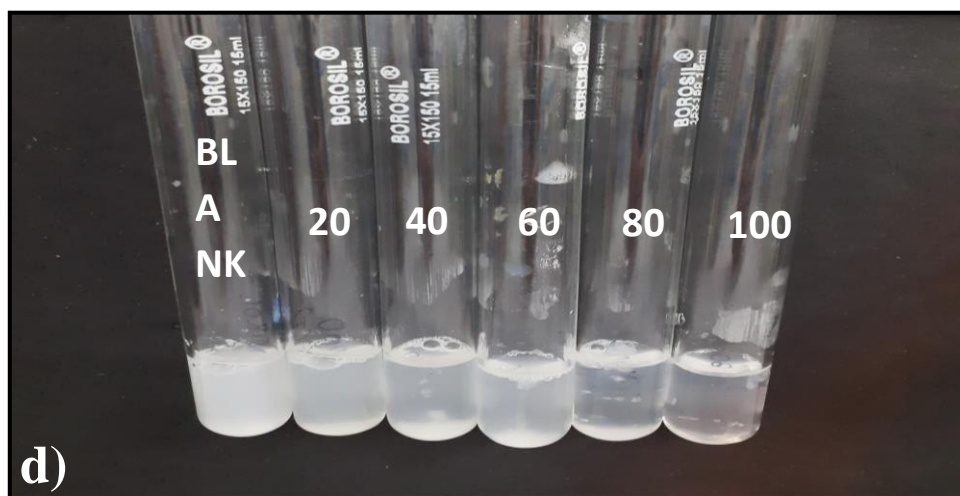


Plate 4.20. Anti-inflammatory activity by d) Silver nanoparticles synthesised from *Trema orientalis* leaf extract e) Silver nanoparticles synthesised from *Trema orientalis* bark extract.

Table 4.20. Protein Denaturation assay using egg albumin: % inhibition of egg albumin denaturation by Diclofenac sodium, *T. orientalis* leaf and bark extract and silver nanoparticles extracted from respective extracts.

Sr no.	Concentration $\mu\text{g/ml}$	Diclofenac sodium	Leaf extract	Bark extract	NP from Leaf extract	NP from Bark extract
1	20	8.2 \pm 0.004	21.5 \pm 0.003	21.8 \pm 0.009	27.2 \pm 0.04	29.5 \pm 0.001
2	40	56 \pm 0.301	33.5 \pm 0.002	33.76 \pm 0.001	28.1 \pm 0.05	31.3 \pm 0.04
3	60	66 \pm 0.131	34.5 \pm 0.001	34.7 \pm 0.001	33 \pm 0.15	47.5 \pm 0.004
4	80	68 \pm 0.065	39.9 \pm 0.0	40.2 \pm 0.004	43.07 \pm 0.06	70.6 \pm 0.001
5	100	74 \pm 0.027	40.9 \pm 0.009	41.1 \pm 0.007	49.53 \pm 0.06	79.4 \pm 0.001

Note: \pm Standard deviation, NP-Nanoparticles

Table 4.21. IC₅₀ values for Anti-inflammatory assay.

Sr no.	Sample	IC ₅₀ $\mu\text{g/ml}$
1	Diclofenac sodium	53 \pm 0.01
2	Leaf extract	130 \pm 0.003
3	Bark extract	129 \pm 0.001
4	Silver nanoparticles synthesised from leaf extract	106 \pm 0.06
5	Silver nanoparticles synthesised from bark extract	57.6 \pm 0.01

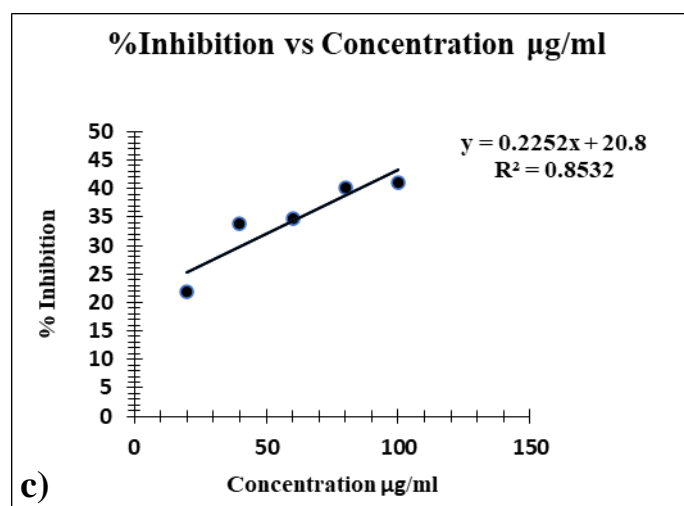
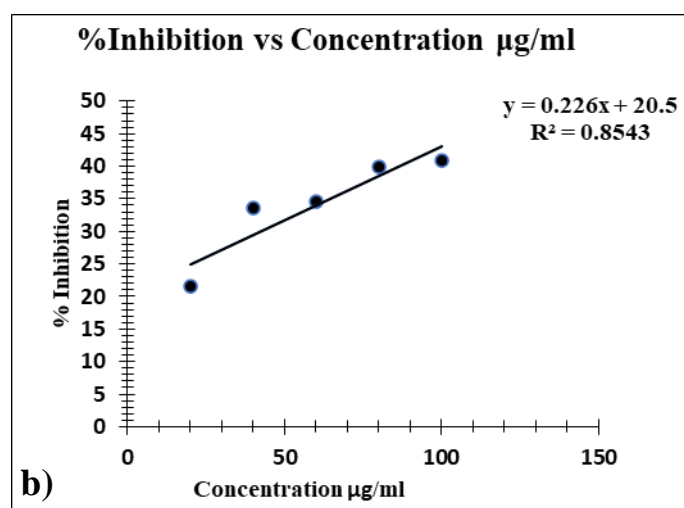
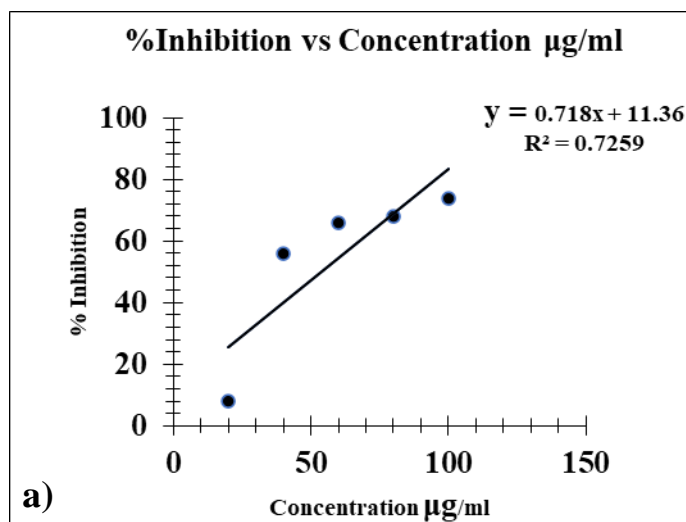


Figure 4.22. Anti-inflammatory activity: Protein denaturation inhibition activity by a) Diclofenac sodium b) *Trema orientalis* Leaf extract c) *Trema orientalis* Bark extract.

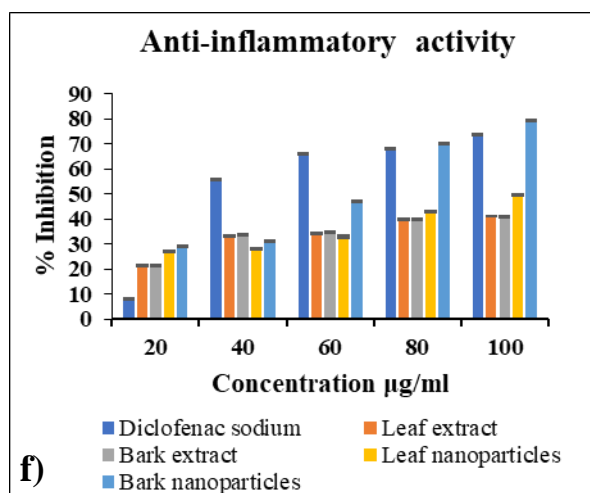
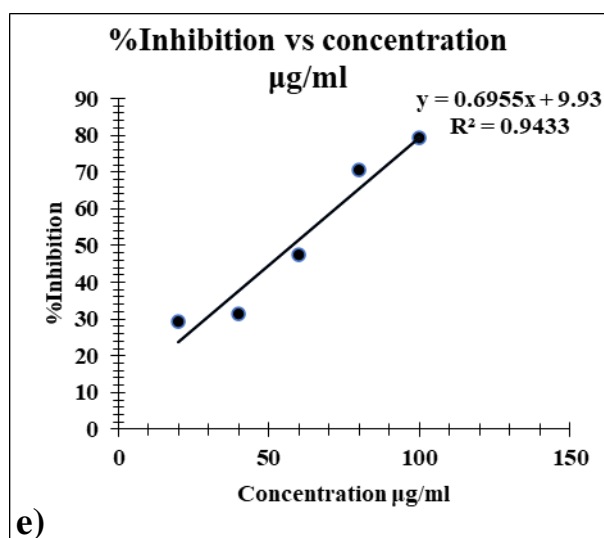
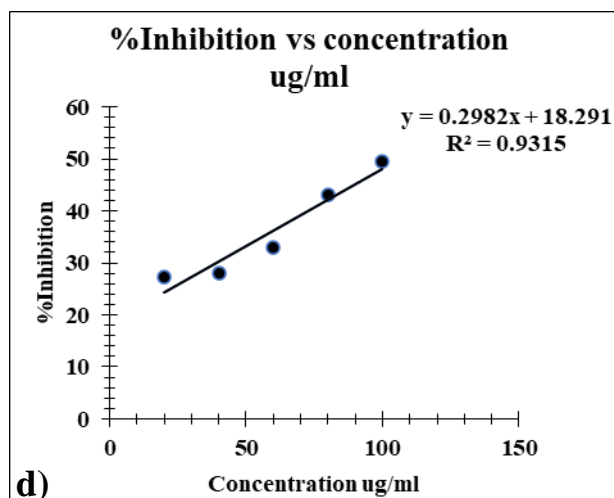


Figure 4.23. Anti-inflammamatory activity: Protein denaturation inhibition activity by Silver nanoparticles extracted from *Trema orientalis* d) Leaf extract and e) Bark extract f) Comparative graph.

CHAPTER 5: CONCLUSIONS

5.CONCLUSIONS

From the study, we can conclude that *Trema orientalis* leaf and bark can be used for the green synthesis of silver nanoparticles. The phytochemical analysis revealed the presence of alkaloids, carbohydrates, glycosides, phenols, saponins, gums, and mucilage in the leaf and bark water extract.

For the leaf water extract, the amounts of the total phenol content were 1.92 ± 0.005 mg GAE/g of dry extract, the total tannins content was 3.23 ± 0.11 mg TAE/g of dry extract, the total flavonoids content was 13 ± 0.01 mg QE/g of dry extract, and the total alkaloid content was 5.8 ± 0.002 mg BiNO₃E/g of dry extract.

In the bark water extract, the total phenols content was 4.132 ± 0.007 mg GAE/g of dry extract, total tannin content was 133 ± 0.18 mg TAE/g of dry extract, the total flavonoid content was 35.3 ± 0.01 mg QE/g of dry extract, and total alkaloid content was 8.35 ± 0.003 mg BiNO₃E/g of dry extract.

The synthesised silver nanoparticles were characterised using UV-visible spectroscopy, FTIR analysis, XRD analysis, FE-SEM, EDS, DLS, and ZETA potential techniques. These analyses showed that the particles had a spherical morphology and ranged in size from 20 to 23 nm. The functional groups on their surface were identified as O-H and amide. Additionally, the particles were found to be monodispersed and negatively charged, indicating their moderate stability.

When silver nanoparticles were evaluated for various biological activities, the results showed that plant extract had better antioxidant properties than silver nanoparticles. This could be because all phytochemicals, such as phenols, flavonoids, tannins, and glycosides, work synergistically to better scavenge free radicals when compared to spherical silver nanoparticles alone.

The study was conducted to evaluate antidiabetic activity of silver nanoparticles in comparison to the plant extract, the starch iodine colour test was conducted which revealed that as the concentration of the plant extract and silver nanoparticle increased the absorbance also increased indicating that the starch is not breaking down as the alpha amylase is inhibited by the extract and nanoparticles, the results were compared in accordance to the standard antidiabetic drug which is acarbose.

It was seen that the silver nanoparticles have better anti-inflammatory activity as compared to the plant extract, it can be stated that synthesised nanoparticles can control the production of auto-antigens which cause denaturation of proteins during inflammation. The silver nanoparticles showcased its potential use in antioxidant, antidiabetic, and anti-inflammatory activities.

The limited studies reported in the phytochemical and biosynthesis of nanoparticles using *Trema orientalis* extracts have led to the opportunity to work on this aspect. The rich repository of secondary metabolites of the selected plant identified in the study showcases its usage in the ethnomedicinal aspects. The capacity to produce silver nanoparticles holds significant promise, aiding in the mitigation of challenges associated with the production of nanoparticles through physical and chemical methods. Green synthesis of nanoparticles stands out as a secure, environmentally friendly, and cost-effective approach. Silver nanoparticles are known to have excellent antimicrobial activity as per studies, and have less side effects hence useful in drug delivery and anti-cancer medicines.

Synthesising silver nanoparticles from *Trema oreintalis* and its subsequent evaluation for antioxidant, antidiabetic and anti-inflammatory potentials helped in understanding its potential in the pharmacology and biomedical field.

CHAPTER 6: REFERENCES

6.REFERENCES

- A. S., & Mani, N. (2019). Anti-inflammatory activity of silver nanoparticles synthesized from *Eichhornia crassipes*: An in vitro study. *Journal of Pharmacognosy and Phytochemistry*, 8(4), 2556-2558.
- Abbasi, E., Milani, M., Fekri Aval, S., Kouhi, M., Akbarzadeh, A., Tayefi Nasrabadi, H., ... & Samiei, M. (2016). Silver nanoparticles: synthesis methods, bio-applications and properties. *Critical reviews in microbiology*, 42(2), 173-180.
- Abou El-Nour, K. M., Eftaiha, A. A., Al-Warthan, A., & Ammar, R. A. (2010). Synthesis and applications of silver nanoparticles. *Arabian journal of chemistry*, 3(3), 135-140.
- Adil, S. F., Assal, M. E., Khan, M., Al-Warthan, A., Siddiqui, M. R. H., & Liz-Marzán, L. M. (2015). Biogenic synthesis of metallic nanoparticles and prospects toward green chemistry. *Dalton Transactions*, 44(21), 9709–9717.
- Adinortey, M. B., Galyuon, I. K., & Asamoah, N. O. (2013). *Trema orientalis* Linn. Blume: A potential for prospecting for drugs for various uses. *Pharmacognosy reviews*, 7(13), 67–72.
- Ahmad, A., Mukherjee, P., Senapati, S., Mandal, D., Khan, M. I., Kumar, R., & Sastry, M. (2003). Extracellular biosynthesis of silver nanoparticles using the fungus *Fusarium oxysporum*. *Colloids and surfaces B: Biointerfaces*, 28(4), 313-318.
- Ahmad, S., Ullah, F., Sadiq, A., Ayaz, M., Imran, M., Ali, I., ... & Shah, M. R. (2016). Chemical composition, antioxidant and anticholinesterase potentials of essential oil of *Rumex hastatus* D. Don collected from the North West of Pakistan. *BMC complementary and alternative medicine*, 16, 1-11.

- Ahmed, S., Ahmad, M., Swami, B. L., & Ikram, S. (2016). A review on plants extracts mediated synthesis of silver nanoparticles for antimicrobial applications: a green expertise. *Journal of advanced research*, 7(1), 17-28.
- Alam, M. N., Bristi, N. J., & Rafiquzzaman, M. (2013). Review on in vivo and in vitro methods evaluation of antioxidant activity. *Saudi pharmaceutical journal*, 21(2), 143-152.
- Al-Robai, S. A., Zabin, S. A., Ahmed, A. A., Mohamed, H. A., Alghamdi, A. A., & Ahmed, A. A. (2022). Phenolic contents, anticancer, antioxidant, and antimicrobial capacities of MeOH extract from the aerial parts of *Trema orientalis* plant. *Open Chemistry*, 20(1), 666-678.
- Amorim, E. L., Nascimento, J. E., Monteiro, J. M., Peixoto Sobrinho, T. J. S., Araújo, T. A., & Albuquerque, U. P. (2008). A simple and accurate procedure for the determination of tannin and flavonoid levels and some applications in ethnobotany and ethnopharmacology. *Functional Ecosystems and Communities*, 2(1), 88-94.
- Angasa, E., Ningsih, S., Manaf, S., Murni, S. A., & Umbara, F. (2011). Iron chelating and antiradical activity of kayu manik leaves (*Trema orientalis*). *Indonesian Journal of Chemistry*, 11(2), 196-199.
- Baillie, J. K., Thompson, A. A. R., Irving, J. B., Bates, M. G. D., Sutherland, A. I., Macnee, W., & Webb, D. J. (2009). Oral antioxidant supplementation does not prevent acute mountain sickness: double blind, randomized placebo-controlled trial. *QJM: An International Journal of Medicine*, 102(5), 341-348.
- Balan, K., Qing, W., Wang, Y., Liu, X., Palvannan, T., Wang, Y., ... & Zhang, Y. (2016). Antidiabetic activity of silver nanoparticles from green synthesis using *Lonicera japonica* leaf extract. *Rsc Advances*, 6(46), 40162-40168.

- Barbera, R., Trovato, A., Rapisarda, A., & Ragusa, S. (1992). Analgesic and antiinflammatory activity in acute and chronic conditions of *Trema guineense* (Schum. et Thonn.) Ficalho and *Trema micrantha* Blume extracts in rodents. *Phytotherapy Research*, 6(3), 146-148
- Bhushan, B. (Ed.). (2017). *Springer handbook of nanotechnology*. Springer.
- Blois, M. S. (1958). Antioxidant determinations by the use of a stable free radical. *Nature*, 181(4617), 1199-1200.
- Burduşel, A. C., Gherasim, O., Grumezescu, A. M., Mogoantă, L., Fikai, A., & Andronescu, E. (2018). Biomedical applications of silver nanoparticles: an up-to-date overview. *Nanomaterials*, 8(9), 681.
- Castro-Longoria, E., Vilchis-Nestor, A. R., & Avalos-Borja, M. (2011). Biosynthesis of silver, gold and bimetallic nanoparticles using the filamentous fungus *Neurospora crassa*. *Colloids and surfaces B: Biointerfaces*, 83(1), 42-48.
- Chang, C. C., Yang, M. H., Wen, H. M., & Chern, J. C. (2002). Estimation of total flavonoid content in propolis by two complementary colorimetric methods. *Journal of food and drug analysis*, 10(3).
- Choi, J. Y., Thapa, R. K., Yong, C. S., & Kim, J. O. (2016). Nanoparticle-based combination drug delivery systems for synergistic cancer treatment. *Journal of Pharmaceutical Investigation*, 46, 325-339.
- Das, P., Ghosal, K., Jana, N. K., Mukherjee, A., & Basak, P. (2019). Green synthesis and characterization of silver nanoparticles using belladonna mother tincture and its efficacy as a potential antibacterial and anti-inflammatory agent. *Materials Chemistry and Physics*, 228, 310-317.

- Dawadi, S., Katuwal, S., Gupta, A., Lamichhane, U., Thapa, R., Jaisi, S., ... & Parajuli, N. (2021). Current research on silver nanoparticles: Synthesis, characterization, and applications. *Journal of nanomaterials*, 2021, 1-23.
- DeFronzo, R. A., Ferrannini, E., Groop, L., Henry, R. R., Herman, W. H., Holst, J. J., ... & Weiss, R. (2015). Type 2 diabetes mellitus. *Nature reviews Disease primers*, 1(1), 1-22.
- Dharmadeva, S., Galgamuwa, L. S., Prasadinie, C., & Kumarasinghe, N. (2018). In vitro anti-inflammatory activity of *Ficus racemosa* L. bark using albumin denaturation method. *AYU (An international quarterly journal of research in Ayurveda)*, 39(4), 239-242.
- Dimo, T., Ngueguim, F. T., Kamtchoung, P., Dongo, E., & Tan, P. V. (2006). Glucose lowering efficacy of the aqueous stem bark extract of *Trema orientalis* (Linn) Blume in normal and streptozotocin diabetic rats. *Die Pharmazie-An International Journal of Pharmaceutical Sciences*, 61(3), 233-236.
- El-Naggar, N. E. A., Hussein, M. H., & El-Sawah, A. A. (2017). Bio-fabrication of silver nanoparticles by phycocyanin, characterization, in vitro anticancer activity against breast cancer cell line and in vivo cytotoxicity. *Scientific reports*, 7(1), 10844.
- File, P. D. (1967). Joint committee on powder diffraction standards. *ASTM, Philadelphia, Pa*, 9-185.
- Gomathi, A. C., Rajarathinam, S. X., Sadiq, A. M., & Rajeshkumar, S. (2020). Anticancer activity of silver nanoparticles synthesized using aqueous fruit shell extract of *Tamarindus indica* on MCF-7 human breast cancer cell line. *Journal of drug delivery science and technology*, 55, 101376.
- Gupta, A., Koirala, A. R., Gupta, B., & Parajuli, N. (2019). Improved method for separation of silver nanoparticles synthesized using the *Nyctanthes arbor-tristis* shrub. *Acta Chemica Malaysia*, 3(1), 35-42.

- Gupta, A., Koirala, A. R., Joshi, B., Khanal, S., Gupta, B., & Parajuli, N. (2017). Synthesis of silver nanoparticles using leaves of *Taraxacum officinale* and their antimicrobial activities. *Advanced Science, Engineering and Medicine*, 9(3), 221-228.
- Haley, R. M., & von Recum, H. A. (2019). Localized and targeted delivery of NSAIDs for treatment of inflammation: A review. *Experimental Biology and Medicine*, 244(6), 433-444.
- Harman, D. (1992). Free radical theory of aging. *Mutation Research/DNAging*, 275(3-6), 257-266.
- Hasan, S. (2015). A review on nanoparticles: their synthesis and types. *Res. J. Recent Sci*, 2277, 2502.
- Hemlata, Meena, P. R., Singh, A. P., & Tejavath, K. K. (2020). Biosynthesis of silver nanoparticles using *Cucumis prophetarum* aqueous leaf extract and their antibacterial and antiproliferative activity against cancer cell lines. *ACS omega*, 5(10), 5520-5528.
- Hernández-Arteaga, A., de Jesús Zermeño Nava, J., Kolosovas-Machuca, E. S., Velázquez-Salazar, J. J., Vinogradova, E., José-Yacamán, M., & Navarro-Contreras, H. R. (2017). Diagnosis of breast cancer by analysis of sialic acid concentrations in human saliva by surface-enhanced Raman spectroscopy of silver nanoparticles. *Nano Research*, 10, 3662-3670.
- Hu, J., Odom, T. W., & Lieber, C. M. (1999). Chemistry and physics in one dimension: synthesis and properties of nanowires and nanotubes. *Accounts of chemical research*, 32(5), 435-445.
- Huang, W. J., Zhang, X. I. A., & Chen, W. W. (2016). Role of oxidative stress in Alzheimer's disease. *Biomedical reports*, 4(5), 519-522.
- Hussein, R. A., & El-Anssary, A. A. (2019). Plants secondary metabolites: the key drivers of the pharmacological actions of medicinal plants. *Herbal medicine*, 1(3), 11-30.

- Ijaz, I., Gilani, E., Nazir, A., & Bukhari, A. (2020). Detail review on chemical, physical and green synthesis, classification, characterizations and applications of nanoparticles. *Green Chemistry Letters and Reviews*, 13(3), 223-245
- Iravani, S., Korbekandi, H., Mirmohammadi, S. V., & Zolfaghari, B. (2014). Synthesis of silver nanoparticles: chemical, physical and biological methods. *Research in pharmaceutical sciences*, 9(6), 385-406.
- Ivanova, N., Gugleva, V., Dobрева, M., Pehlivanov, I., Stefanov, S., & Andonova, V. (2018). *Silver nanoparticles as multi-functional drug delivery systems* (pp. 71-91). London, UK: IntechOpen.
- Jadhav, K., Deore, S., Dhamecha, D., Hr, R., Jagwani, S., Jalalpure, S., & Bohara, R. (2018). Phytosynthesis of silver nanoparticles: characterization, biocompatibility studies, and anticancer activity. *ACS Biomaterials Science & Engineering*, 4(3), 892-899.
- Jancova, P., Anzenbacher, P., & Anzenbacherova, E. (2010). Phase II drug metabolizing enzymes. *Biomed Pap Med Fac Univ Palacky Olomouc Czech Repub*, 154(2), 103-116.
- Jeevanandam, J., Barhoum, A., Chan, Y. S., Dufresne, A., & Danquah, M. K. (2018). Review on nanoparticles and nanostructured materials: history, sources, toxicity and regulations. *Beilstein journal of nanotechnology*, 9(1), 1050-1074.
- Jibowu, T. (2016). The formation of doxorubicin loaded targeted nanoparticles using nanoprecipitation, double emulsion and single emulsion for cancer treatment. *J Nanomed Nanotechnol*, 7(379), 2.
- Jouyban, A., & Rahimpour, E. (2020). Optical sensors based on silver nanoparticles for determination of pharmaceuticals: An overview of advances in the last decade. *Talanta*, 217, 121071.

- Khalil, M. M., Ismail, E. H., El-Baghdady, K. Z., & Mohamed, D. (2014). Green synthesis of silver nanoparticles using olive leaf extract and its antibacterial activity. *Arabian Journal of chemistry*, 7(6), 1131-1139.
- Kharat, S. N., & Mendhulkar, V. D. (2016). Synthesis, characterization and studies on antioxidant activity of silver nanoparticles using Elephantopus scaber leaf extract. *Materials Science and Engineering: C*, 62, 719-724.
- Khorrami, S., Zarrabi, A., Khaleghi, M., Danaei, M., & Mozafari, M. R. (2018). Selective cytotoxicity of green synthesized silver nanoparticles against the MCF-7 tumor cell line and their enhanced antioxidant and antimicrobial properties. *International journal of nanomedicine*, 8013-8024.
- Kim, S. H., Lee, H. S., Ryu, D. S., Choi, S. J., & Lee, D. S. (2011). Antibacterial activity of silver-nanoparticles against Staphylococcus aureus and Escherichia coli. *Korean J. Microbiol. Biotechnol*, 39(1), 77-85.
- Komolafe, O. O. (2003). Antibiotic resistance in bacteria-an emerging public health problem. *Malawi medical journal*, 15(2), 63-67.
- Kulkarni, N., & Muddapur, U.M. (2014). Biosynthesis of Metal Nanoparticles: A Review. *Journal of Nanotechnology*, 1-8.
- Logeswari, P., Silambarasan, S., & Abraham, J. (2015). Synthesis of silver nanoparticles using plants extract and analysis of their antimicrobial property. *Journal of Saudi Chemical Society*, 19(3), 311-317.
- Madhu, S. E., Sreeja, H., & Priya, J. S. (2020). A preliminary study on phytochemical, antioxidant and cytotoxic activity of leaves of Naregamia alata Wight & Arn. *Materials Today: Proceedings*, 25, 343-348.
- Manosalva, N., Tortella, G., Cristina Diez, M., Schalchli, H., Seabra, A. B., Durán, N., & Rubilar, O. (2019). Green synthesis of silver nanoparticles: effect of synthesis reaction

- parameters on antimicrobial activity. *World journal of microbiology & biotechnology*, 35(6), 88.
- Mao, B. H., Chen, Z. Y., Wang, Y. J., & Yan, S. J. (2018). Silver nanoparticles have lethal and sublethal adverse effects on development and longevity by inducing ROS-mediated stress responses. *Scientific reports*, 8(1), 2445.
- Mathur, P., Jha, S., Ramteke, S., & Jain, N. K. (2018). Pharmaceutical aspects of silver nanoparticles. *Artificial cells, nanomedicine, and biotechnology*, 46(sup1), 115-126.
- Mehta, B. K., Chhajlani, M., & Shrivastava, B. D. (2017, April). Green synthesis of silver nanoparticles and their characterization by XRD. In *Journal of physics: conference series* (Vol. 836, No. 1, p. 012050). IOP Publishing.
- Meulenkamp, E. A. (1998). Synthesis and growth of ZnO nanoparticles. *The journal of physical chemistry B*, 102(29), 5566-5572.
- Meva, F. E. A., Ntomba, A. A., Kedi, P. B. E., Tchoumbi, E., Schmitz, A., Schmolke, L., ... & Janiak, C. (2019). Silver and palladium nanoparticles produced using a plant extract as reducing agent, stabilized with an ionic liquid: sizing by X-ray powder diffraction and dynamic light scattering. *Journal of Materials Research and Technology*, 8(2), 1991-2000.
- Modak, D., Paul, S., & Bhattacharjee, S. (2017). Anti-inflammatory activity of acmella uliginosa (sw.) cass. flower methanolic extract on membrane stabilization and protein denaturation: an in-vitro evaluation. *NBU J Anim Sc*, 11, 61-69.
- Mourdikoudis, S., Pallares, R. M., & Thanh, N. T. (2018). Characterization techniques for nanoparticles: comparison and complementarity upon studying nanoparticle properties. *Nanoscale*, 10(27), 12871-12934.
- Mulvaney, P. (1996). Surface plasmon spectroscopy of nanosized metal particles. *Langmuir*, 12(3), 788-800.

- Nadaroglu, H., GÜNGÖR, A. A., & Selvi, İ. N. C. E. (2017). Synthesis of nanoparticles by green synthesis method. *International Journal of Innovative Research and Reviews*, 1(1), 6-9.
- Nasrollahzadeh, M., Sajadi, S. M., Sajjadi, M., & Issaabadi, Z. (2019). An introduction to nanotechnology. In *Interface science and technology* (Vol. 28, pp. 1-27). Elsevier.
- Njoya, E. M. (2021). Medicinal plants, antioxidant potential, and cancer. In *Cancer* (pp. 349-357). Academic Press.
- Nunes, C. D. R., Barreto Arantes, M., Menezes de Faria Pereira, S., Leandro da Cruz, L., de Souza Passos, M., Pereira de Moraes, L., & Barros de Oliveira, D. (2020). Plants as sources of anti-inflammatory agents. *Molecules*, 25(16), 3726.
- Nwauzoma, A. B., & Dappa, M. S. (2013). Ethnobotanical studies of port Harcourt metropolis, Nigeria. *International Scholarly Research Notices*, 2013.
- O. S. Oluwafemi, J. L. Anyik, N. E. Zikalala, and E. H. M. Sakho (2019). "Biosynthesis of silver nanoparticles from water hyacinth plant leaves extract for colorimetric sensing of heavy metals," *Nano-Structures & Nano-Objects*, vol. 20, p. 100387.
- Ononamadu, C. J., Ezeigwe, O. C., Owolarafe, T. A., Ihegboro, G. O., Lawal, T. A., Salawu, K., ... & Aminu, I. (2020). Starch-iodine assay method underestimates alpha-amylase inhibitory potential of antioxidative compounds and extracts. *BioTechnologia. Journal of Biotechnology Computational Biology and Bionanotechnology*, 101(1), 45-54.
- Parveen, K., Banse, V., & Ledwani, L. (2016). Green synthesis of nanoparticles: Their advantages and disadvantages. In *AIP conference proceedings* (Vol. 1724, No. 1). AIP Publishing.
- Parvez, A., Azad, M. A., Islam, M. Z., Munna, M. M. R., Shaheen, S. M., Rahman, M. M., & Azad, A. K. (2019). A phytochemical and pharmacological review on *Trema orientalis*: a potential medicinal plant. *Pharmacology Online*, 3, 103-119.

- Patra, J. K., Das, G., Fraceto, L. F., Campos, E. V. R., Rodriguez-Torres, M. D. P., Acosta-Torres, L. S., ... & Shin, H. S. (2018). Nano based drug delivery systems: recent developments and future prospects. *Journal of nanobiotechnology*, *16*, 1-33.
- Purkait, P., Bhattacharyya, A., Roy, S., Maitra, S., Das, G. C., & Ghosh Chaudhuri, M. (2023). Green synthesis of ZnO nanoparticle using *Trema orientalis* (L) leaf: an efficient photocatalyst for degradation of zoxamide fungicide in aqueous organic media under UV light irradiation. *International Journal of Environmental Analytical Chemistry*, *103*(2), 307-325.
- Purkait, P., Bhattacharyya, A., Roy, S., Maitra, S., Das, G., & Ghosh Chaudhuri, M. (2020). Green synthesis of TiO₂ nanoparticle: its characterization and potential application in Zoxamide photodegradation. *Journal of Water and Environmental Nanotechnology*, *5*(3), 191-203.
- Raffi, M., Hussain, F., Bhatti, T. M., Akhter, J. I., Hameed, A., & Hasan, M. M. (2008). Antibacterial characterization of silver nanoparticles against *E. coli* ATCC-15224. *Journal of materials science and technology*, *24*(2), 192-196.
- Rajeshkumar, S., Malarkodi, C., Vanaja, M., & Annadurai, G. (2016). Anticancer and enhanced antimicrobial activity of biosynthesized silver nanoparticles against clinical pathogens. *Journal of molecular structure*, *1116*, 165-173.
- Rajput, S., Kumar, D., & Agrawal, V. (2020). Green synthesis of silver nanoparticles using Indian Belladonna extract and their potential antioxidant, anti-inflammatory, anticancer and larvicidal activities. *Plant cell reports*, *39*, 921-939.
- Raliya, R., Saran, R., Choudhary, K., & Tarafdar, J. C. (2013). Biosynthesis and characterization of nanoparticles. current trends in advancement of scientific research and opinion in applied research and opinion in applied microbiology and biotechnology, 6.

- Reverberi, A.P., Kuznetsov, N.T., Meshalkin, V., Salerno, M., & Fabiano, B. (2016). Systematical analysis of chemical methods in metal nanoparticles synthesis. *Theoretical Foundations of Chemical Engineering*, 50, 59-66.
- Robert, D. (2007). Photosensitization of TiO₂ by MxOy and MxSy nanoparticles for heterogeneous photocatalysis applications. *Catalysis Today*, 122(1-2), 20-26.
- Sahayaraj, K., Rajesh, S., & Rathi, J. M. (2012). Silver nanoparticles biosynthesis using marine alga padina pavonica (linn.) and its microbicidal activity. *Digest Journal of Nanomaterials & Biostructures (DJNB)*, 7(4).
- Saleh, A., Zainal-Arifin, S. M., Yahaya, S. F., & Khaleel, A. G. (2020). Antioxidant activities and estimation of phenol and flavonoid contents in the extracts of *Trema orientalis* Linn Blume. *Nigerian Veterinary Journal*, 41(2), 73-84.
- Samaraweera, T., Samaraweera, T., Senadeera, N. N., & Ranaweera, C. B. (2023). In vitro Anti-Inflammatory Activity of Leaves of *Jeffreykia zeylanica* Using the Egg Albumin Denaturation Method and Human Red Blood Cell Stabilization Method. *Asian Plant Research Journal*, 11(6), 56-64.
- Seigler, D. S. (2012). *Plant secondary metabolism*. Springer Science & Business Media.
- Silva, G. A. (2004). Introduction to nanotechnology and its applications to medicine. *Surgical neurology*, 61(3), 216-220.
- Sondi, I., & Salopek-Sondi, B. (2004). Silver nanoparticles as antimicrobial agent: a case study on *E. coli* as a model for Gram-negative bacteria. *Journal of colloid and interface science*, 275(1), 177-182.
- Sreevidya, N., & Mehrotra, S. (2003). Spectrophotometric method for estimation of alkaloids precipitable with Dragendorff's reagent in plant materials. *Journal of AOAC international*, 86(6), 1124-1127.

- Tavarini, S., Degl'Innocenti, E., Remorini, D., Massai, R., & Guidi, L. (2008). Antioxidant capacity, ascorbic acid, total phenols, and carotenoids changes during harvest and after storage of Hayward kiwifruit. *Food chemistry*, *107*(1), 282-288.
- Uddin, S. N. (2008). Antioxidant and antibacterial activities of *Trema orientalis* Linn: an indigenous medicinal plant of Indian subcontinent. *Advances in Traditional Medicine*, *8*(4), 395-399.
- Vonkeman, H. E., & van de Laar, M. A. (2010,). Nonsteroidal anti-inflammatory drugs: adverse effects and their prevention. In *Seminars in arthritis and rheumatism* (Vol. 39, No. 4, pp. 294-312). WB Saunders.
- Wickens, A. P. (2001). Ageing and the free radical theory. *Respiration physiology*, *128*(3), 379-391
- Xiao, Z., Storms, R., & Tsang, A. (2006). A quantitative starch Iodine method for measuring alpha-amylase and glucoamylase activities. *Analytical biochemistry*, *351*(1), 146-148.
- Xu, L., Wang, Y. Y., Huang, J., Chen, C. Y., Wang, Z. X., & Xie, H. (2020). Silver nanoparticles: Synthesis, medical applications, and biosafety. *Theranostics*, *10*(20), 8996.
- Yatoo, M., Gopalakrishnan, A., Saxena, A., Parray, O. R., Tufani, N. A., Chakraborty, S., ... & Iqbal, H. (2018). Anti-inflammatory drugs and herbs with special emphasis on herbal medicines for countering inflammatory diseases and disorders-a review. *Recent patents on inflammation & allergy drug discovery*, *12*(1), 39-58.
- Ying, S., Guan, Z., Ofoegbu, P. C., Clubb, P., Rico, C., He, F., & Hong, J. (2022). Green synthesis of nanoparticles: Current developments and limitations. *Environmental Technology & Innovation*, *26*, 102336.

- Yousaf, H., Mehmood, A., Ahmad, K. S., & Raffi, M. (2020). Green synthesis of silver nanoparticles and their applications as an alternative antibacterial and antioxidant agent. *Materials Science and Engineering: C*, *112*, 110901.
- Zahran, M., Khalifa, Z., Zahran, M. A. H., & Abdel Azzem, M. (2020). Dissolved organic matter-capped silver nanoparticles for electrochemical aggregation sensing of atrazine in aqueous systems. *ACS Applied Nano Materials*, *3*(4), 3868-3875.
- Zinjarde, S. S., Bhargava, S. Y., & Kumar, A. R. (2011). Potent α -amylase inhibitory activity of Indian Ayurvedic medicinal plants. *BMC complementary and alternative medicine*, *11*(1), 1-10.